JANUARY 2018

M.Sc. in Optical Engineering

MEHMET ADIYAMAN

UNIVERSITY OF GAZİANTEP

GRADUATE SCHOOL OF

NATURAL & APPLIED SCIENCES

DESIGN AND PRODUCTION OF A FREE FORM LENS FOR LONG-RANGE ILLUMINATION

M.Sc. THESIS

IN

OPTICAL ENGINEERING

BY

MEHMET ADIYAMAN

JANUARY 2018

Design and Production of a Free Form Lens for Long-Range Illumination

M.Sc. Thesis
in
Optical Engineering
University of Gaziantep

Supervisor
Assoc. Prof. Dr. Ahmet BİNGÜL

By
Mehmet ADIYAMAN

January 2018

REPUBLIC OF TURKEY
GAZİANTEP UNIVERSITY
GRADUATE SCHOOL OF
NATURAL AND APPLIED SCIENCES
OPTICAL ENGINEERING

Name of the Thesis	:	Design and Production of a Free Form Lens for Long-Range Illumination
Name of the Student	:	Mehmet ADIYAMAN
Exam Date	:	26.01.2018

Approval of the Graduate School of Natural and Applied Sciences.

Prof. Dr. Ahmet Necmeddin YAZICI
Director

I certify that this thesis satisfies all the requirements as a thesis for the degree of Master of Science.

Assoc. Prof. Dr. Ahmet BİNGÜL
Head of Department

This is to certify that we have read this thesis and that in our opinion it is fully adequate, in scope and quality, as a thesis for the degree of Master of Science.

Assoc. Prof. Dr. Ahmet BİNGÜL
Supervisor

Examining Committee Members:	Signature
Prof. Dr. Ahmet Necmeddin YAZICI	....
Assoc. Prof. Dr. Koray KÖKSAL	....
Assoc. Prof. Dr. Ahmet BİNGÜL	....

I hereby declare that all information in this document has been obtained and presented in accordance with academic rules and ethical conduct. I also declare that, as required by these rules and conduct, I have fully cited and referenced all material and results that are not original to this work.

Mehmet ADIYAMAN

ABSTRACT

DESIGN AND PRODUCTION OF A FREE FORM LENS FOR LONG-RANGE ILLUMINATION

ADIYAMAN, Mehmet

M.Sc. in Optical Engineering

Supervisor: Assoc. Prof. Dr. Ahmet BİNGÜL

January 2018, 99 pages

In this study, we design and manufacture new prototype of a LED Projector containing Free Form Lenses to cover both visible and infrared regions for the long-range illumination. The geometrical form of the lens is obtained by minimizing the optical path length for the light rays emitted from LED. The lens is produced by the plastic injection method using PMMA material whose transmittance for the concerned optical region is greater than 90%. The optical measurements of the lens is compared with the simulation based on ZEMAX 2009. It is found that, although there are some production errors and LED alignment problems, the optical measurements of the lens are close to the predicted values in the design.

Key words: free form lens, pmma, molding, plastic injection, optical simulation.

ÖZET

UZUN MESAFELİ AYDINLATMA İÇİN ÖZGÜR BİÇİMLİ MERCEK TASARIMI VE ÜRETİMİ

ADIYAMAN, Mehmet
Yüksek Lisans Tezi, Optik Mühendisliği Bölümü
Tez Yöneticisi: Doç. Dr. Ahmet BİNGÜL
Ocak 2018, 99 sayfa

Bu çalışmada, hem görünür hem de kızılötesi bölgeleri kapsayan, uzun mesafeli aydınlatma için özgür biçimli merceklerden oluşan yeni bir tip LED projektörün tasarım ve üretimini yaptık. Merceğin geometrik biçimi, LED üzerinden yayılan ışığın optik yolunun minimize edilmesi ile elde edilmiştir. Mercek, plastik enjeksiyon yöntemi ile, ilgilendiğimiz optik bölgede geçirgenliği %90'ın üzerinde olan PMMA malzemelesi kullanılarak üretilmiştir. Merceğin optik ölçümleri, ZEMAX 2009 uygulamasında yapılan benzetimlerle kıyaslanmıştır. Bazı üretim hatalarına ve LED hizalama problemlerine rağmen, optik ölçümler, tasarımdaki öngörülen değerlere yakın sonuçlar vermiştir.

Anahtar kelimeler: özgür biçimli mercek, pmma, kalıp, plastik enjeksiyon, optik benzetim.

To my family .....

ACKNOWLEDGEMENTS

I am grateful to my supervisor, Assoc. Prof. Dr. Ahmet BİNGÜL, whose expertise, understanding, generous guidance and support made it possible for me to study on a topic that was of great interest to me. It was pleasure working with him. Sir, words can never be enough to thank your kindness.

I would like to express my gratitude to Research Assist. Mustafa KILIN and Uygar ŞAŞMAZ who puts his faith in me and urged me to do better.

I also thank Evrim TANRIVERDİ for letting me use his own license of software ZEMAX 2009.

I would also like to extend my thanks to my friends, K.Kürşad AYIK, Serdar ŞENGÜL, Büşra YAZICI, Gülistan ASLAN, and Betül KONAKLI, who kept me in good spirits during my stay here.

Finally, I would like to thank my parents for their constant encouragement and belief in me during this study.

TABLE OF CONTENTS

Page

LIST OF TABLES

LIST OF FIGURES

LIST OF SYMBOLS

r : Radius

Ω : Steradian

L_e : Radiance

E_e : Irradiance

λ : Wavelength

L_v : Luminance

I_v : Illuminance

lm : Lumen

W : Watt

sr : Steradian

$PMMA$: Poly(methyl methacrylate)

PC : Polycarbonate

PS : Polystyrene

n : Refractive index

h : Planck constant

c : Speed of light

OPL : Optical path length

GPL : Geometric path length

VIS : Visible

IR : Infrared

CHAPTER 1

INTRODUCTION

Admittedly, illumination is one of the main requirements of people. LED (Light Emitting Diode) is an energy-saving light source providing high light efficiency and long life time. Nowadays, many cities across North America, China and Europe start to prefer LED for internal/external/street illumination. In our country, both government politics and companies working many years on the illumination sector foresee that all illumination systems are going to be based on LEDs in the near future.

Despite the high light efficiency, the direct light output of LEDs spreads at obtuse angle. This results in a disadvantage in the use of LEDs when illuminating a surface, being at a large distance from the source, uniformly at an acute angle. This issue, can be improved either by placing a free form lens having a suitable geometric form in front of the LED or by using parabolic reflectors. As a result, LEDs can be used in illumination as projector or used in and optical communication. However, free form lens lenses (being smaller, lighter and cheaper) are more useful compared to the reflectors. Furthermore, lenses used in projectors have different geometry than that of classical lenses. This type of illumination lenses having a flexible geometry is known as Free Form Lens. Firstly, the Free Form Lenses are drawn attention in academic society and then they are used by illumination and optical communication companies.

In the production of lenses, generally, Acrylics (PMMA) whose visible light transmittances are greater than 90% are used as the lens material. Technically, the production of the free form lens lenses can be performed in a few steps. First, optical design of the lens and the mechanical design of the lens mold are implemented by computer software. Then, the lens mold made by steel is manufactured using a CNC machine having high spatial resolution. The free form lens lens material is molten and poured into the lens mold. Finally, the transmittance, the illumination performance and the light distribution of the lens are tested after removing the cold lens from the mold. If every step is fulfilled successfully, lens can be used as a final product.

LED lenses are widely used in both internal/external illumination [1–7] and wireless optical communication systems [8–10]. In the illumination sector in our country, manufacturers prefers mostly reflectors. Although this solution is easy, in general, the reflector geometry is much larger than that of LED and as result the cost of production becomes expensive [3]. On the other hand, many companies preferring lenses in the illumination import lenses and their bodies from the overseas unfortunately. There are 10-20 LED lenses per armature and at least ten armatures are used in a normal illumination project. Therefore, the production of the LED lenses in our country will result in a significant contribution to our economy.

The main targets of this thesis are to design and manufacture the new Prototype LED Projector containing Free Form Lenses and performing in both visible and infrared regions for the long-range illumination, and to minimize the dependence of our country on this issue to the others. By using capabilities in our university in Physics and Optical Engineering Departments, we have studied on a Free Form Lens mentioned. Up to now we are able to design and produce free form lens lenses used to illuminate at acute angle by means of our potentials and Gaziantep Industry. It is found that, despite some production errors and LED alignment problems, the optical measurements of this lens are not very far from the predicted values in the design.

The chapter organization of the thesis is as follows.Chapter 2 describes some theoretical background related to the radiometry and the photometry. Material selection, design and simulation of the optical system are given in Chapter 3. In Chapter 4, production steps and optical tests are presented respectively. Finally, a summary and a conclusion are given in Chapter 5.

CHAPTER 2

BASIC UNITS USED IN ILLUMINATION

In this section, basic quantities and their units used in lighting will be given briefly. In the thesis, the radiometric units are used to describe infrared part of the LED projector. As for visible region, photometric units are preferred as usual.

2.1 Radiometry

Radiometry is the perception and measurement of electromagnetic radiation energy. Optical radiometry is a field that deals with the measurement of ultraviolet(UV), visible(VIS) and infrared(IR) regions of the electromagnetic spectrum [11]. To understand radiometric units, it is necessary to understand what solid angle is.

2.1.1 Solid Angle

Central angle viewing the slice of a circumference of length $2\pi r$ of a circle with radius r, is defined as 1 radian angle and a full circular angle is declared as 2π radian. Figure 2.1 shows the center angle.

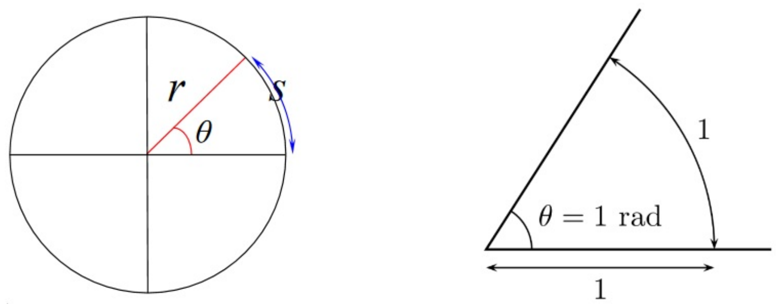

Figure 2.1 Central Angle.

Likewise, central solid angle viewing the area of a surface of area r^2 of a circle with radius r, is defined as 1 steradian angle. Since the surface area of a sphere is $4\pi r^2$, a point in space is known as spherically as 4π steradian(Ω, sr) solid angle. Figure 2.2 shows the solid angle.

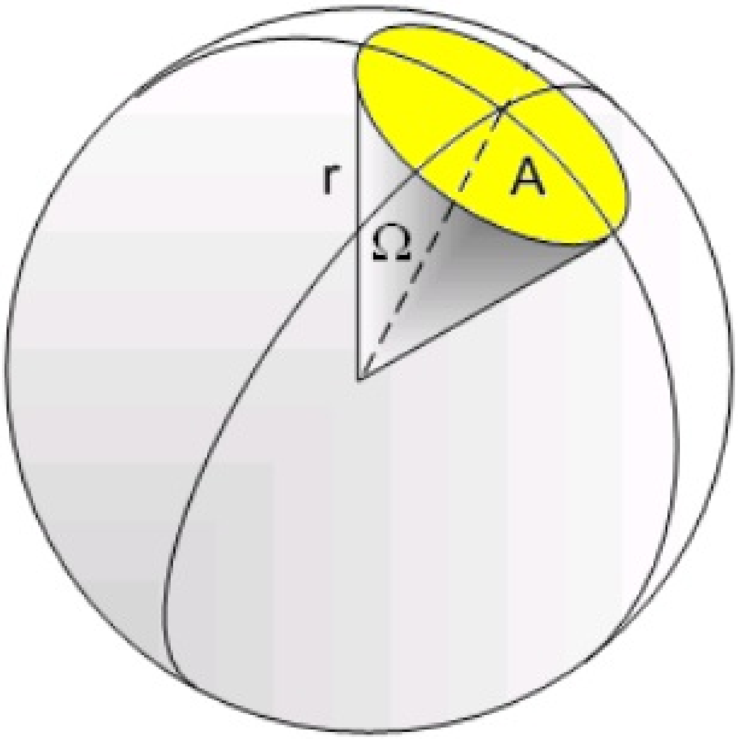

Figure 2.2 Solid Angle.

2.1.2 Radiometric Units

In this section, information about radiometric quantities is given. In Table 2.1, radiometric quantities, symbols and units are shown.

Table 2.1 Radiometric Units.

Radiometric Quantities	Symbol	Unit
Radiant Intensity	I_e	Wsr^{-1}
Radiant Flux	Φ_e	W
Radiant Energy	Q_e	Ws
Radiance	L_e	$Wsr^{-1}m^{-2}$
Irradiance	E_e	Wm^{-2}

- **Radiance :** Radiation flux per solid angle from a surface to the perpendicular unit projection surface. It is indicated by L symbol and unit is $W/m^2 sr$. Radiance is the basic radiometric unit, and the other units are derived from the radiance unit.

- **Radiant Flux :** Unit time is the amount of radiation power that falls or emerges onto a surface. It is indicated by the symbol Φ_E and the unit is W(J/s).

- **Radiant Intensity :** It is the radiation flux per solid angle emitted from a source in a certain direction. It is indicated by the symbol I_E and the unit is W/sr.

- **Irradiance :** Radiation flux density on a surface. It is indicated by the symbol E_E and the unit is W/m^2 [12] .

2.2 Photometry

Photometry investigate the visible region of the electromagnetic spectrum. Photometry is the measurement of electromagnetic radiation, weighted by the reaction of the human eye. According to the wavelength and a measure this response varies from person to person. Therefore internationally recognized standard observer functions are used to provide a consistent measurement system. These are the V(λ) function which is valid for photopic vision i.e. daylight levels and the x function for scotopic vision i.e. low illumination levels. Mesotopic photometry is used to ensure a smooth transition between functions at intermediate light levels, ie, at twilight levels [13].

2.2.1 Luminosity Function

The luminosity function or luminous efficiency function describes the average spectral sensitivity of human visual perception of brightness. It is indicated by the symbol $V(\lambda)$. This function is determined by International Commission on Illumination (CIE) is the international authority on light, illumination, colour, and colour spaces [13].

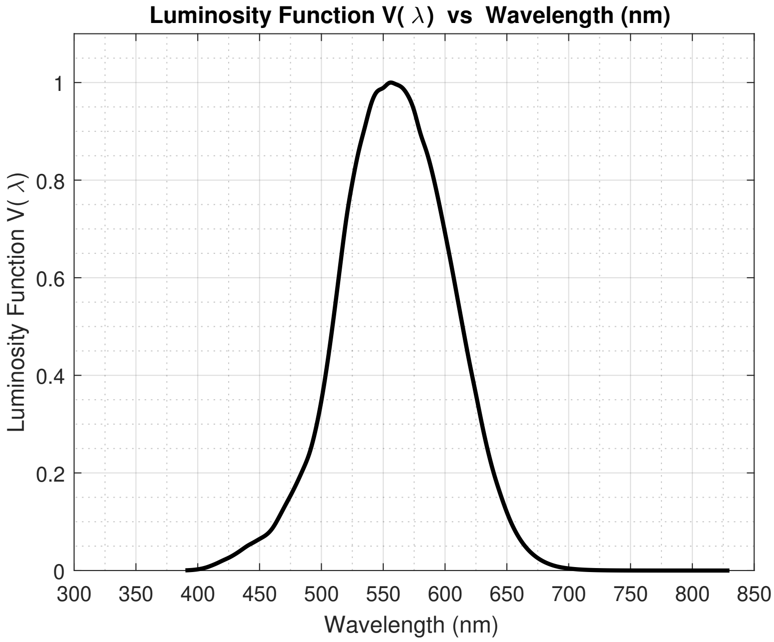

Figure 2.3 The average spectral sensitivity of human visual perception of brightness.

2.2.2 Photometric Units

In this section, information about photometric quantities is given. In Table 2.2, photometric quantities, symbols and units are shown.

Table 2.2 Photometric Units

Photometric Quantities	Symbol	Unit
Luminous Intensity	I_v	cd
Luminous Flux	Φ_v	lm
Luminous Energy	Q_v	cd sr s
Luminance	L_v	cd m^{-2}
Illuminance	E_v	lux(lm m^{-2})

- **Luminous Flux :** Luminous flux called the amount of light emitted from a source per unit of time. The difference between radiant flux and luminous flux is determined by the response of the human eye. The luminous flux is indicated by the symbol Φ_v and the unit is lumen(cd sr).
- **Luminous Intensity :** Light power is a measure of the power per unit solid angle emitted by a light source in a certain direction, depending on

the luminosity function, which is a standardized model of the sensitivity of the human eye. The luminous intensity is indicated by the symbol I_v and the unit is candela.

- **Luminance :** Luminance is the photometric measurement of luminous intensity in the unit area of the light moving in a certain direction. The luminance is indicated by the symbol L_v and the unit is candela per square meter. Luminance is usually used to characterize the emission or reflection from flat, diffuse surfaces.
- **Illuminance :** The illuminance is the total amount of luminous flux per unit area. This is the measure of how much light is illuminated by a surface weighted wavelength. E_v is indicated by the symbol and the unit is lux(lm/m^2) [13, 14].

2.2.3 Radiometry and Photometry Conversion

Each radiometric quantity has a photometric counter weighted by the spectral response of the human eye. In order to be able to convert between radiometric and photometric units, we need to know the photopic spectral luminous efficiency curve $V(\lambda)$. The wavelength at which the human eye is most sensitive is determined to be 555 nm. Thus, as stated in the definition of candela, the power of 1 watt equals 683 lumens in the light of 555 nm wavelength. The following equation 2.1 is used to convert between units.

$$\Phi_v = K_m \int_{\lambda=380nm}^{\lambda=830nm} \Phi_E V(\lambda) d\lambda \tag{2.1}$$

where ;
Φ_v is the luminous flux in lumens
K_m is a scaling factor equal to 683 lm/W
Φ_E is the spectral power in W/nm
$V(\lambda)$ is the photopic spectral luminous efficiency function.

Unit conversions are tabulated below in table 2.3

Table 2.3 Radiometric and Photometric Conversion.

Radiometric Quantities	Unit	Conversion	Unit	Photometric Quantities
Radiant Intensity	$W \cdot sr^{-1}$	$\Phi_v = \frac{cd \cdot sr}{W} \frac{W}{sr \cdot nm} nm$	cd	Luminous Intensity
Radiant Flux	W	$\Phi_v = \frac{cd \cdot sr}{W} \frac{W}{nm} nm = cd \cdot sr$	lm	Luminous Flux
Radiant Energy	W·s	$\Phi_v = \frac{cd \cdot sr}{W} \frac{W \cdot s}{nm} nm = cd \cdot sr \cdot s$	$lm \cdot s$	Luminous Energy
Radiance	$W \cdot sr^{-1} \cdot m^{-2}$	$\Phi_v = \frac{cd \cdot sr}{W} \frac{W}{sr \cdot m^2 \cdot nm} nm$	$\frac{cd}{m^2}$	Luminance
Irradiance	$W \cdot m^{-2}$	$\Phi_v = \frac{cd \cdot sr}{W} \frac{W}{m^2 \cdot nm} nm = \frac{cd \cdot sr}{m^2}$	$\frac{lm}{m^2}$	Illuminance

CHAPTER 3

OPTICAL DESIGN AND SIMULATION

3.1 Introduction

The main objective of this thesis is to build a lens for long range illumination for both visible and near infrared regions. This chapter contains detailed descriptions about the lens material selection, LED selection, the lens design based on optical path length calculations and the simulation performance for the study.

First, three materials which are mostly used in free form lens manufacturing industry are introduced to be used in a lens design. Then, the lens design procedure based on Fermat's Principle is explained. The equations obtained in design are implemented in MATLAB [15] using two dimensional (2D) geometry. Then, to obtain 3D geometry and assign suitable material to the lens, the SolidWorks [16] software is used. Finally, ZEMAX 2009 software [17] used for optical simulation including LED, 3D lens and detector is introduced.

3.2 Lens Material

In this section, three different plastic materials which will be used in the lens are introduced. They are respectively known as PMMA, PC and PS and their dispersion curves (index of refraction vs wavelength plot) are shown in Figure 3.1. Today, manufacturers prefers mostly PMMA since it has lower index of refraction and better optical transparency properties.

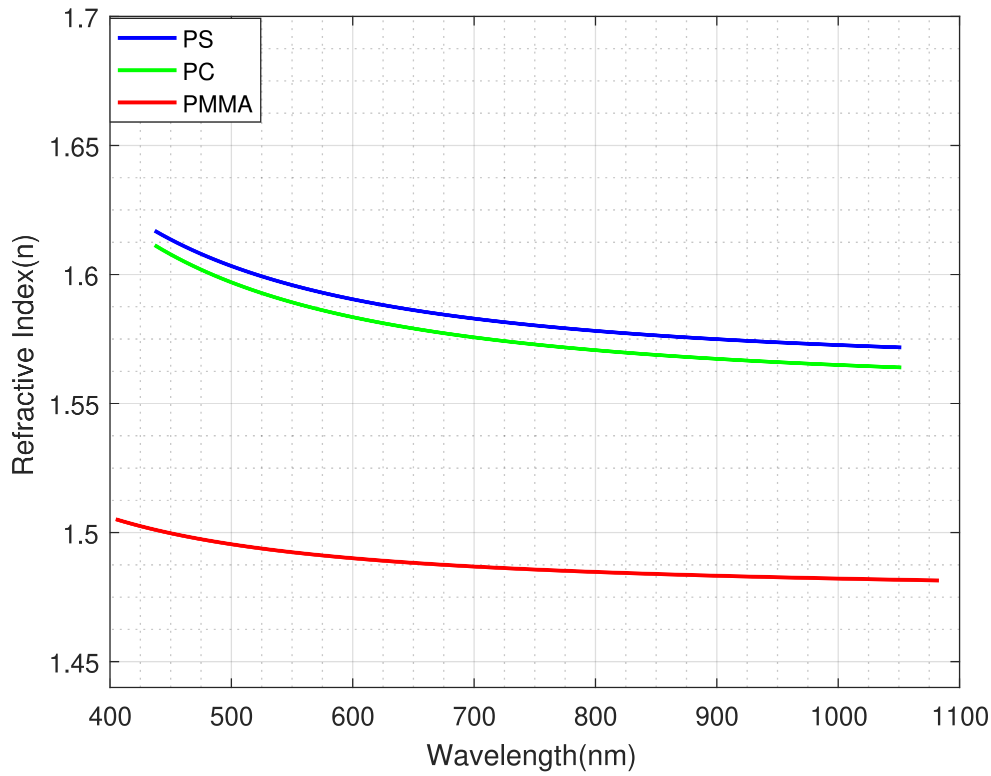

Figure 3.1 Dispersion curves of PMMA, PC and PS [18].

3.2.1 PMMA

PMMA (poly(methyl methacrylate)) is a transparent thermoplastic material. It is also known as acrylic or acrylic glass. This material is used as a layer or in the form of a pellet as a molding material. PMMA can be used instead of glass due to its lightness and resistance to breakage. PMMA is not a type of silica based glass in opposite of those generally known. If this material is to be used in the optics, it may be preferred instead of polycarbonate. Because this material's UV tolerance, transparency and tenacity are better than polycarbonate. Also, its lower cost, ease of processing and smaller index of refraction dominates the reason to choose PMMA [19]. Some physical properties of PMMA are shown in Table 3.1 .

Table 3.1 Properties of PMMA [20].

Optical Properties	**Unit**	**Value**
Transmittance	%	92
Haze		0.5
Refractive Index		1.4859
Other Properties		
Density	$\frac{g}{cm^3}$	1.19
Processing Conditions		
Predrying Temperature	$°C$	80 -90
Predrying Time	h	2-3
Melt Temperature	$°C$	220-260
Mold Temparature	$°C$	60-90
Mechanical Properties		
Tensile Modulus	MPa	3300
Stress at Break	MPa	77
Strain at Break	%	5.5

3.2.2 Polycarbonate

Polycarbonate(PC) is one of the engineering plastics which is transparent, corrosion resistant, self-quenching when it does, with little change dimensions in time and temperature, very low moisture absorption and very good mechanical properties. This material is suitable for both injection molding and extrusion. The light transmittance of the material is over 85% and it has superior UV resistance. Nevertheless it has disadvantages such as yellowing of the material [19]. This material is used in the lighting parts of automobiles, packaging industry, bottles, containers and tableware, household goods, consumer products and electronic devices and so on [21]. In addition, the specifications of the material are also shown in Table 3.2.

Table 3.2 Properties of PC [22]

Optical Properties	**Unit**	**Value**
Transmittance	%	¿85
Haze	¡	1
Refractive Index		1.5848
Other Properties		
Density	$\frac{g}{cm^3}$	1.2
Processing Conditions		
Predrying Temperature	$^{\circ}C$	120
Predrying Time	h	4-6
Melt Temperature	$^{\circ}C$	290-310
Mold Temparature	$^{\circ}C$	60-90
Mechanical Properties		
Tensile Modulus	MPa	2400
Stress at Break	MPa	70
Strain at Break	%	2.2

3.2.3 Polystyrene

Polystyrene (or briefly PS) is a polymer produced by styrene polymerisation. PS is a transparent thermoplastic material. This material is hard, has a high dielectric property, low water absorption and odorless material . The transmittance of this material in the wavelength of the visible region is 90% [19, 23]. Nevertheless, it has disadvantages such as opacity and yellowing of the material. This material is used in packaging industry, electronic devices, automobile headlamps, interior lighting and refrigerator shelves sectors. The specifications of PS are shown in Table 3.3.

Table 3.3 Properties of PS [24]

Optical Properties	**Unit**	**Value**
Transmittance	%	90
Haze		0.5
Refractive Index		1.5916
Other Properties		
Density	$\frac{g}{cm^3}$	1.04
Processing Conditions		
Predrying Temperature	$^{\circ}C$	60 -70
Predrying Time	h	1-3
Melt Temperature	$^{\circ}C$	193-232
Mold Temparature	$^{\circ}C$	38-66
Mechanical Properties		
Tensile Modulus	MPa	1724
Stress at Break	MPa	40
Strain at Break	%	3.5

3.2.4 LED

LED (light emitting diode) is a semiconductor material that emits light when current is passed through it. LED is diode-structured, the current flows in one direction. LEDs are formed by combination of two semiconductor materials which are p-type and n-type. Free electrons on the valance band pass through conduction band when they are excited by the applied forward bias. This increases number of electrons on the conduction band so population inversion occurs. Collected electrons here will fall down valance band to become stable and produce electron-hole pairs. Excess energy of electrons is released by radiating photons. This procedure is known as the production of light. To put it simply, LED is a material that turns electric energy into light. Since the LEDs are made of different semiconductor materials, the band-gap energies are different [25], such as GaAs, InGaN and GaN, etc. In this way, LEDs are produced in different wavelengths. The band-gap energy formula is shown in Equation 3.1.

$$E_g = \frac{hc}{\lambda} \tag{3.1}$$

where h is Planck Constant and has the value $h = 6.626070040(81) \times 10^{-34}$ J.s and c is the speed of light. Its exact value is $c = 299792458$ m/s.

Today, LEDs are more preferred because of their high light efficiency, spreading different colors, size, dimming and long life. The disadvantages are temperature dependency, voltage sensitivity and environmental conditions. In this study, we have used OSRAM brand SFH4715 coded infrared and LUW CVBP coded white LEDs. The reason we choose the LEDs we use is that the light distribution is close to the light distribution of the point light source. The properties and spectral distributions of the LEDs used are shown in the following Table 3.4 and 3.5 and in Figure 3.2.

Table 3.4 Properties of infrared LED (OSRAM SFH4715) [26].

Parameter	Symbol	Values	Unit
Peak Wavelength	λ	860	nm
Centroid Wavelength	λ	850	nm
Spectral Bandwidth	$\triangle\lambda$	30	nm
Rise and Fall Time	tr/tf	7/14	ns
Radiant Intensity	I_e	270	mW/sr
Total Radiant Flux	Φ_e	630	mW
Forward Voltage	V_F	≤ 1.8	V
Power Consumption	P_{tot}	1.8	W
Operation Temperature Range	T_{op}	-40 - 125	$°C$
Junction Temperature	T_j	145	$°C$

Table 3.5 Properties of visible LED (OSRAM LUW CVBP) [27].

Parameter	Symbol	Values	Unit
Luminous Flux	ϕ_V	112 - 180	lm
Viewing Angle	2φ	120	°
Chromaticity coordinates	Cx	0.33	-
	Cy	0.34	-
Forward Voltage	V_F	2.95	V
Forward Current	I_F	10 - 1000	mA
Operation Temperature Range	T_{op}	-40 - 125	$°C$
Junction Temperature	T_j	150	$°C$

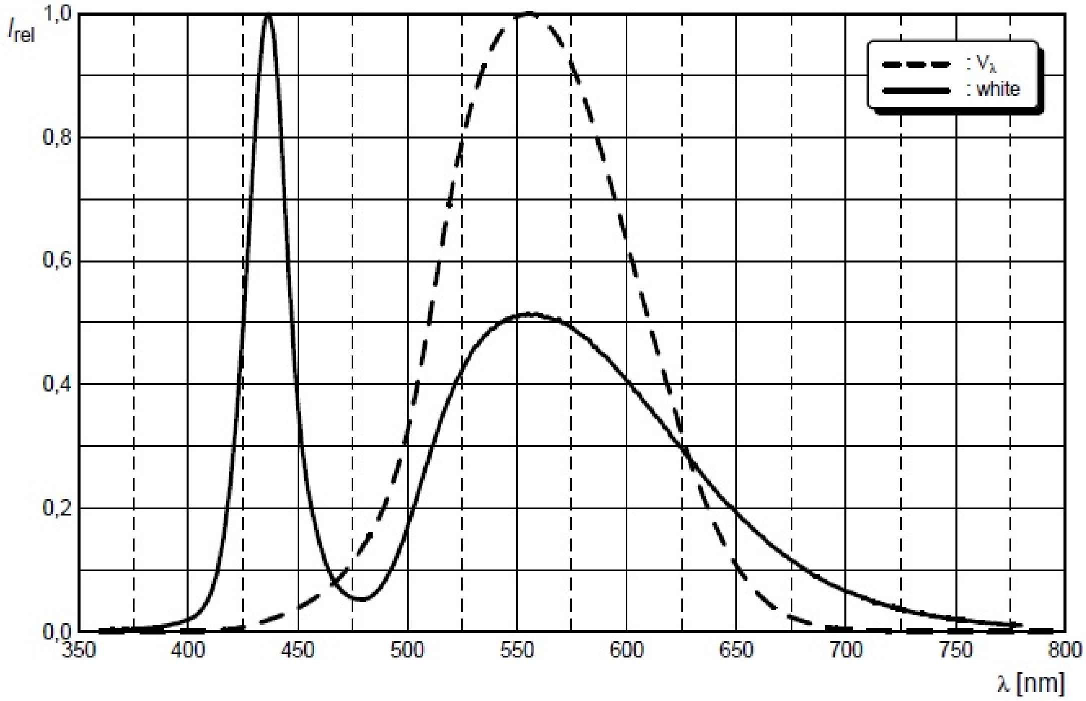

Figure 3.2 Spectral distribution for white LED.

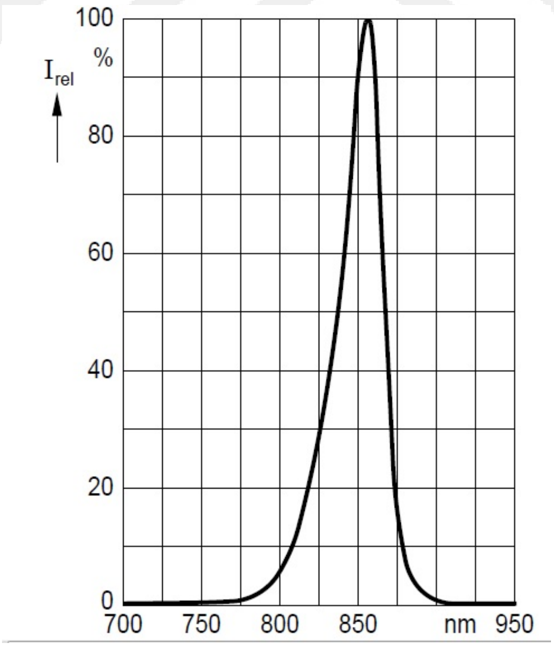

Figure 3.3 Spectral distribution for infrared LED.

3.3 Computer Aided Optical Design

3.3.1 Optical Path Length

The geometric path is the distance that the ray traces between any two points and the geometric path length between points A and B is calculated from:

$$GPL = \int_A^B ds = \int_A^B \sqrt{dx^2 + dy^2 + dz^2} \tag{3.2}$$

The optical path length is known as the product of the refractive index of the medium and the geometric path followed by the ray [28, 29]. Or mathematically, the optical path length is:

$$OPL = \int_A^B n(s)ds = c\int \frac{ds}{v} = c\int dt \tag{3.3}$$

This integral is calculated along the path of the rays which may change the medium on this path. This integral may take in any number of refraction and reflection. Path length is defined for virtual rays and this definition may be positive of negative which depends on the direction of the path.

Distance traveled by a light ray in optical medium, whose index of refraction is n, is $s = vt$ where v is the speed of the ray in the medium. Or time traveled by light in the same medium is

$$t = \frac{s}{v} = \frac{s}{c/n} = \frac{OPL}{c} \tag{3.4}$$

In optics, light travels a path by choosing shortest time needed to travel within possible different paths due to Fermat's principle. Fermats principle is related to optimum time. or it is equivalently related to optimum OPL since $t = OPL/c$. This principle can be written as *light travels in medium such that its total optical path length is optimum.*

Fermat's principle is used to derive law of refraction and law of reflection (Snell's law), paths of light in homogeneous and heterogeneous medium and finding geometric wavefronts [28].

In optical design one has to consider also the total internal reflection. It is a phenomenon that occurs when the light passes from a very dense medium to a less dense medium. When the light reaches a less dense medium, the rays normally goes away. For this reason, the output angle is greater than incident angle. This is called total internal reflection. The critical angle is $\theta_c = \arcsin \frac{n_2}{n_1}$.

3.3.2 Lens Design

OPL is one of the key objectives of optical designers. In this project, a free form lens having specific geometry is designed using OPL idea. The aim of the project is to manufacture a prototype lens for long range IR and visible illumination. First, the light source (LED) is assumed to be a point-like source for simplicity. Then, four surfaces are determined to form the lens; a parabola, a hyperbola, a circle and a plane, Figure 3.4. These are used to focus light rays from LED emitted at obtuse (wide) angle.

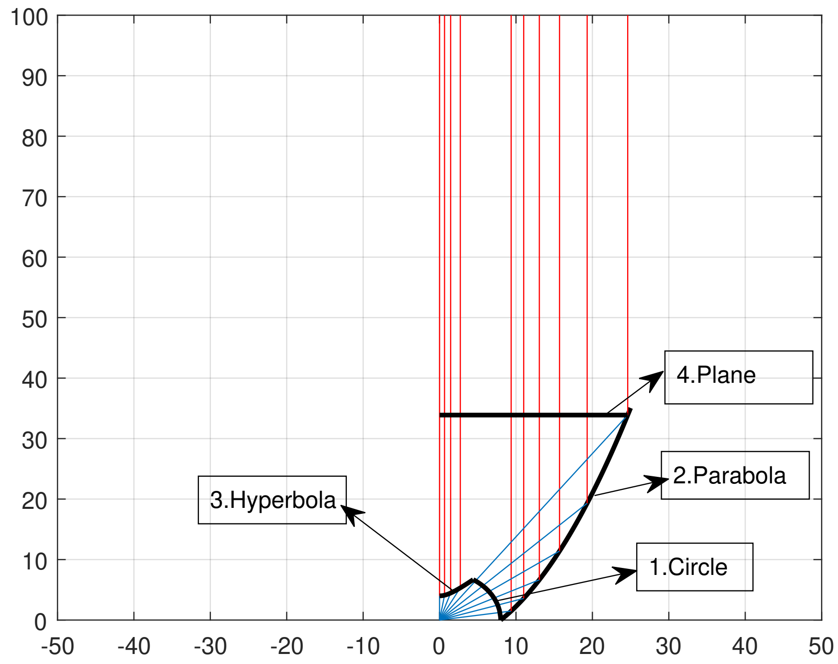

Figure 3.4 Four surfaces of the lens.

The description of the surfaces are as follows:

- The outer part of the lens is parabolic surface where LED is placed its focus. All the rays from LED hitting this parabolic surface will be reflected according to the total internal reflection idea.

- The surface closest to the LED is an hyperbola such that rays from the source will leave this surface parallel to y-axis.

- The circle is used to pass the rays from LED without refracting and to reach them to parabolic surface.

- The flat surface is used to exit all parallel rays from the lens.

LED is placed at the point (0, 0, 0). The radius of the circle is selected as R and it has the simple form:

$$x^2 + y^2 = R^2 \tag{3.5}$$

Then, using OPL, one can find the equation of parabola whose focus is at origin as:

$$y = \frac{x^2 - R^2}{2R} \tag{3.6}$$

and hyperbola whose one of the focus at origin as:

$$y = \frac{p(n-1)n + \sqrt{(p^2n^2(n-1)^2 - (n^2-1)(p^2(n-1)^2 - x^2))}}{n^2 - 1} \tag{3.7}$$

where n is the index and p is the shortest distance between LED and hyperbola.

These equations and point-like source are implemented in MATLAB, a highly computable and drawing program [31]. For two dimensional geometry, MATLAB m-file, whose output is shown in Figure 3.4, can be found in Appendix E.

The SolidWorks program is used to do 3D solid modeling of the lens. This program is a powerful and user-friendly CAD program that allows you to easily model solid and allow you to assign materials to the designed product. At the same time this program allows you to do a lot of feature information and some tests on the designed product. Some of these tests are stress test, thermal test, etc. In the design, SolidWorks 2013 version has been used [32]. To start SolidWorks the command File ⇒ New ⇒ Part is invoked and the screen-shoot is given in Figure 3.5.

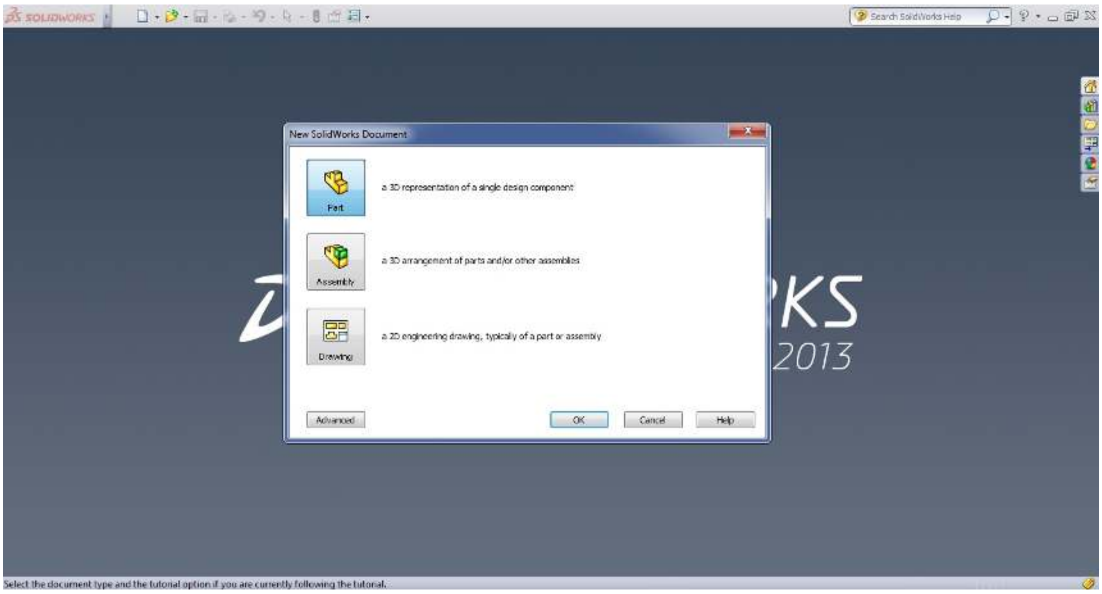

Figure 3.5 SolidWorks part selection.

Then, a plane is selected from the FeatureManager Desing Tree section. We select the front plane for drawing as shown in the Figure 3.6.

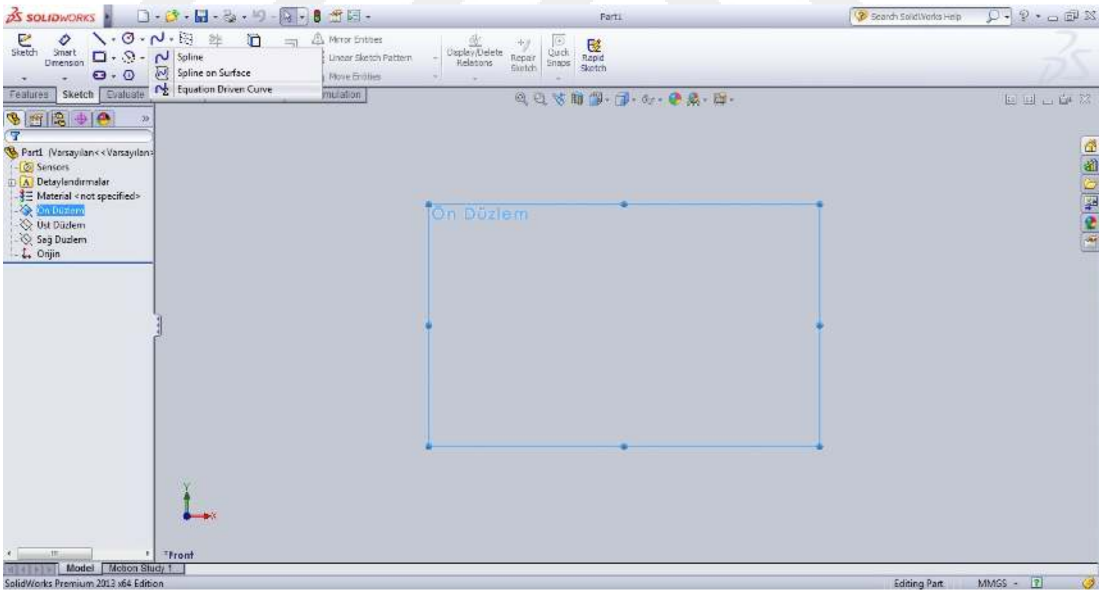

Figure 3.6 SolidWorks drawing surface selection.

The drawing process can now be started. The shape to draw is selected from Sketch Menu. We start with a parabola by entering the equation we obtained from MATLAB. Figures 3.6 and 3.7.

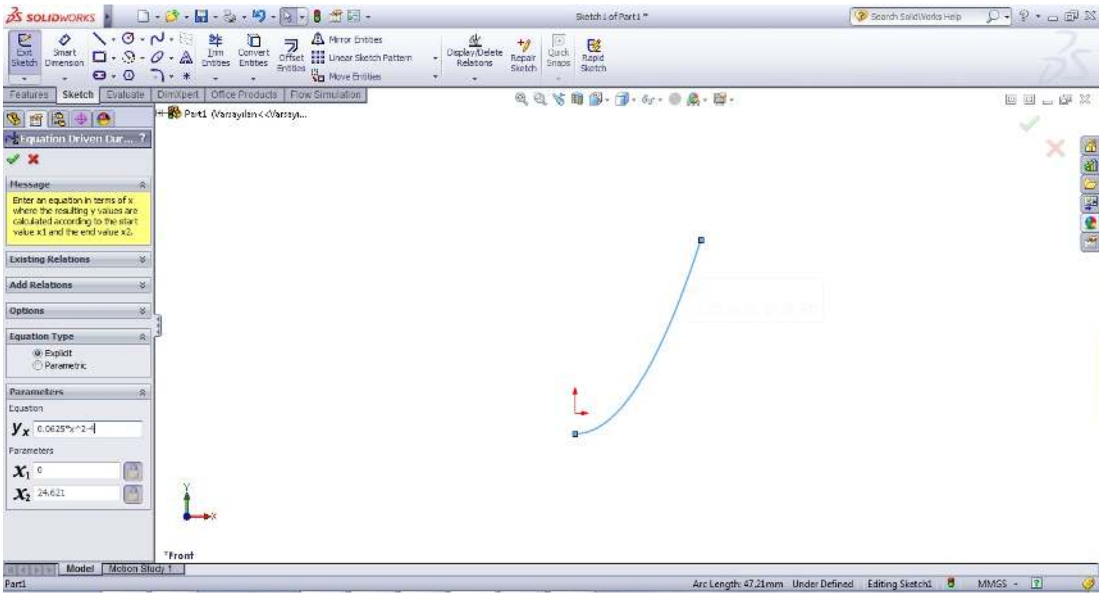

Figure 3.7 SolidWorks (quadratic) spline equation command.

Similarly the hyperbola and circle can be implemented as in Figure 3.8.

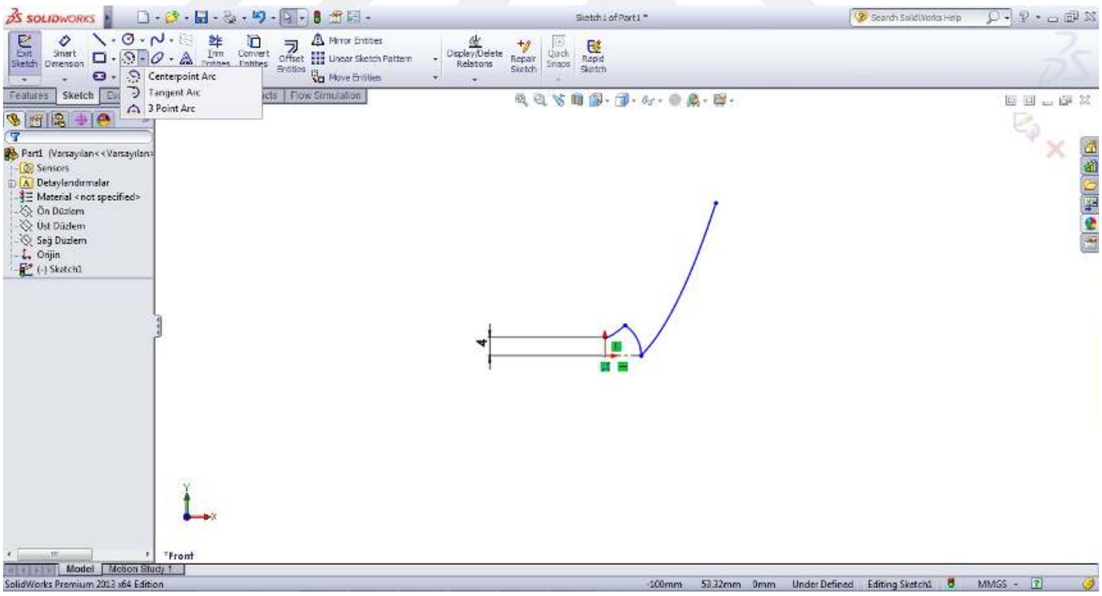

Figure 3.8 Lens components.

To make this drawing 3D, the open surfaces are joined with the line command. The 2D shape of the lens and the measurements are shown in Figure 3.9.

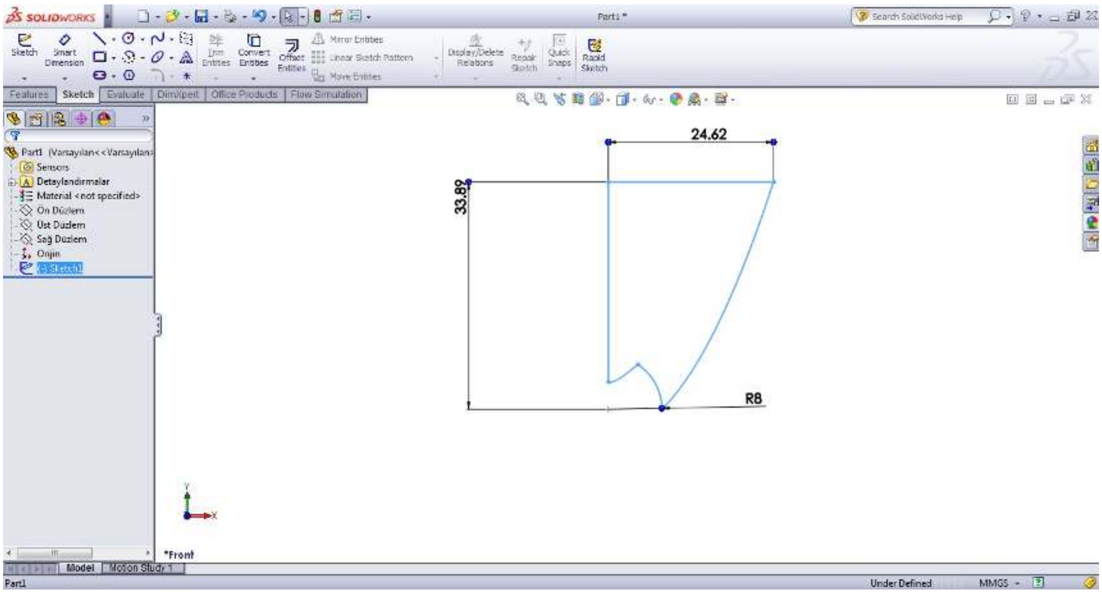

Figure 3.9 Final 2D lens. Measurement unit is millimeters.

The 2D drawing can be rendered in 3D using the command Features ⇒ Revolved Boss/Base. The final 3D shape of the lens is shown in Figure 3.10 and 3.11.

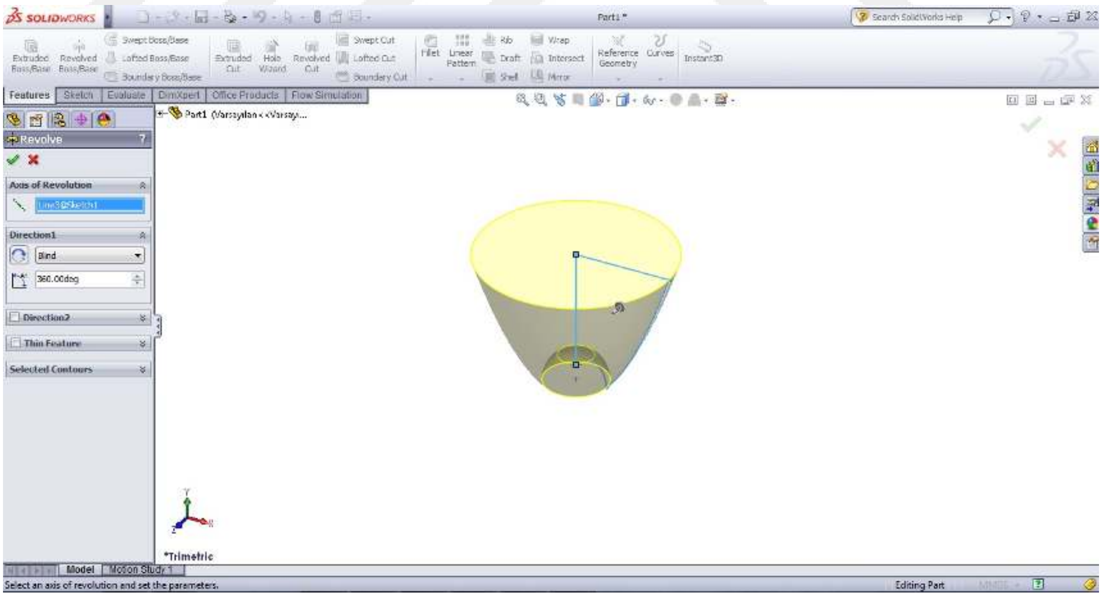

Figure 3.10 SolidWorks Revolved Boss/Base command

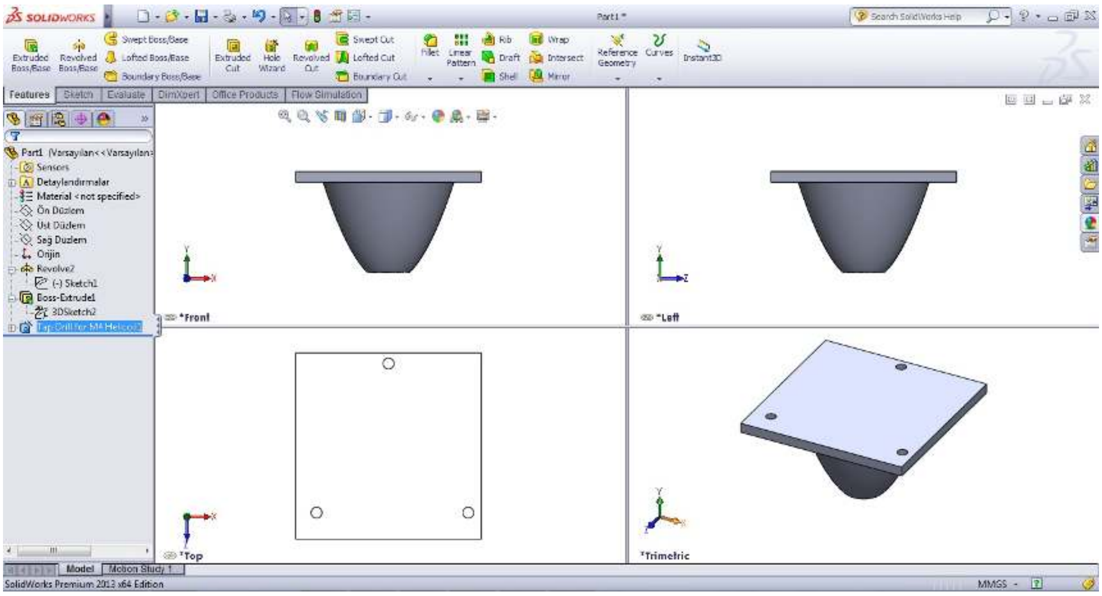

Figure 3.11 3D shape of the lens with an end-cap for mechanical installation of the lens.

Material assignment are invoked by using the command: FeatureManager Desing Tree ⇒ Material ⇒ Edit ⇒ Material ⇒ Plastic ⇒ PMMA commands to select material. An example result is shown in Figure 3.12.

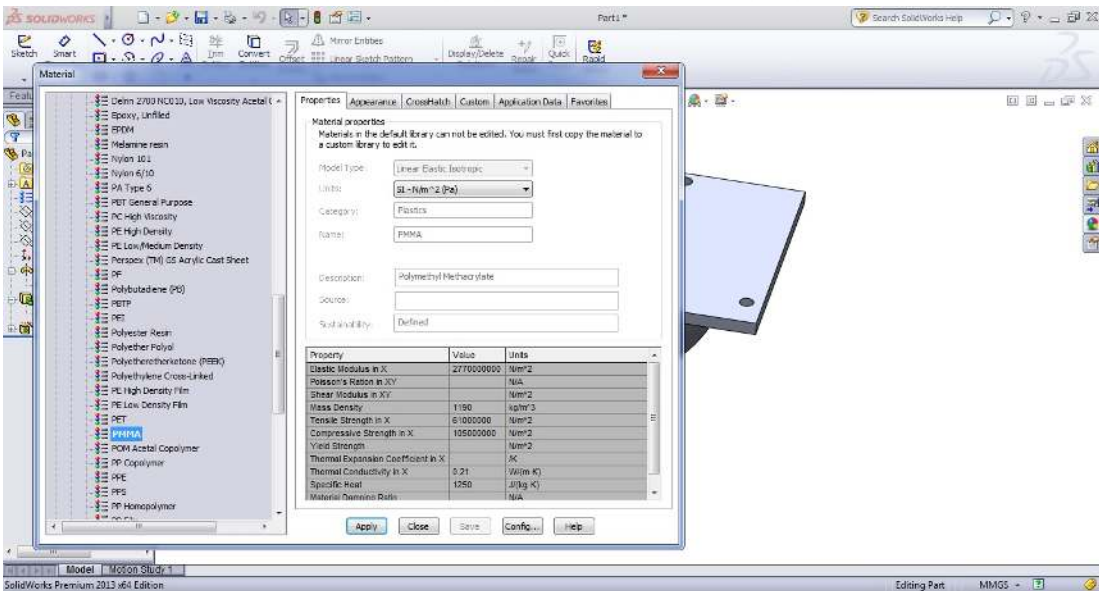

Figure 3.12 SolidWorks Material assignment.

To obtain the mass of the designed lens, Evaluate Mass properties command will be given as shown in Figure 3.13.

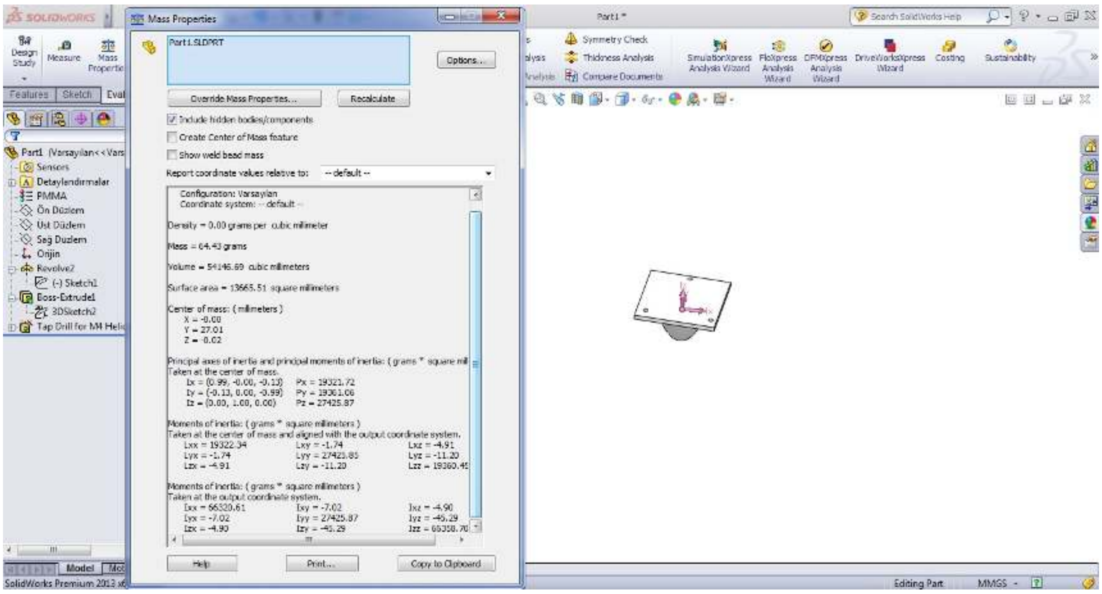

Figure 3.13 Mass properties of the lens.

3.4 ZEMAX

ZEMAX is widely used software in optics. This is an optical design program and analyze imaging system like camera lenses in addition illumination system. ZEMAX is the first optical design software written for Windows systems and written by Ken Moore in 1990. The name of the first version of program was Max and afterwards the name changed Zemax. This program works by ray tracing and modeling the propagation of rays via an optical system. It can model the effect of optical elements like simple lenses, aspheric lenses, mirrors and diffractive optical elements. It can produce standard analysis diagrams such as spot diagrams and ray-fan projects. This program also simulates coatings on optical surfaces. Zemax can carry out standard sequential ray tracing via optical elements, non-sequential ray tracing for analysis of stray light, and physical optics beam propagation. In addition, it has a tolerancing capability and thus makes it possible to analyze production and assembly faults. Optimization tools of Zemax can be used to maximize the performance and to minimize the deviations on developing the lens design by adjusting parameters [17, 33]. This program consist of two main modes; the sequential mode and the non-sequential mode. In this study, we have used the version ZEMAX June 9, 2009.

3.4.1 Sequential Mode

Ray tracing is a widely used technique for modeling the propagation of light through an optical system. Modeling of light propagation by means of ray tracing is called geometric optics. In sequential ray tracing, rays are viewed along a predefined surface sequence that moves from the object surface to the image surface. Rays will hit only ones per surface in the order of surface definitions. Imaging systems are well defined by sequential surfaces. Sequential ray tracing is computationally fast and very useful for designing, optimizing, and tolerancing imaging systems. Deviation calculations such as ray fan drawings, diffraction calculations, and wavefront aberration calculations can be done using sequential ray tracing [34]. Figure 3.14 shows an example screen shoot of ZEMAX for designing a beam expander containing four lenses.

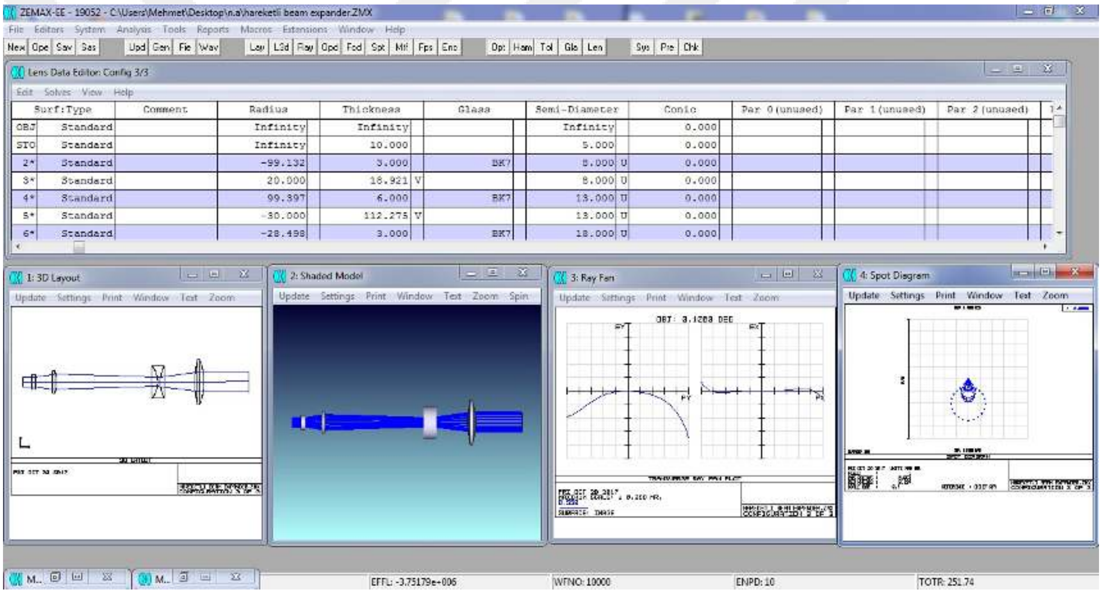

Figure 3.14 An example usage of Zemax sequential mode for a beam expander.

3.4.2 Non-Sequential Mode

Non-sequential ray tracing means that there is not a predefined set of surfaces that must strike the tracked rays. The objects hit by rays are determined solely by the physical locations of the objects, their properties, and the directions of the rays. Rays can strike non-sequential objects anywhere and can hit the same object multiple times or never hit. In non-sequential mode, optical components are modeled as real three-dimensional objects or as surfaces and solid objects. Each object is placed in an independent x, y, z coordinate with a defined orientation independently. Non-sequential mode is used to analyze deviated light, scatter and illumination in both imaging and non-imaging systems. There are many types of optical components that can not be modeled using sequential mode. Such objects must be modeled as real 3D components. Some examples of objects that use non-sequential mode include : light pipes, complex prisms, objects created in CAD programs and embedded volume objects [35]. Figure 3.15 shows an example screen shoot of ZEMAX for digital projector containing reflectors and lenses.

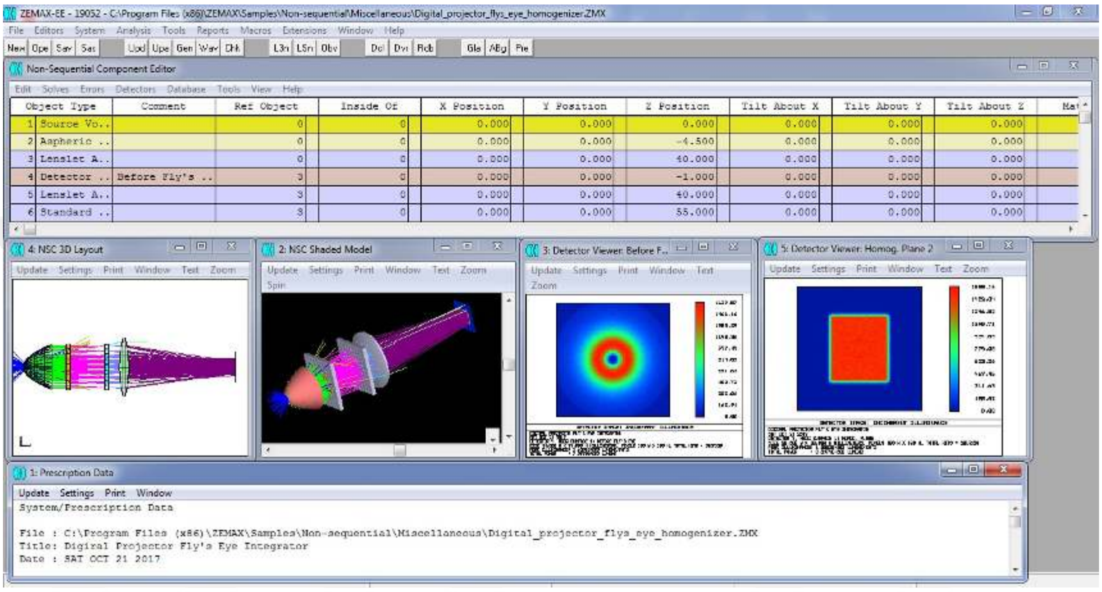

Figure 3.15 An example usage of ZEMAX non-sequential mode for a digital projector.

The optical simulations of the lens modeled in Solidworks has been made in the non-sequantial mode. In ZEMAX 2009, the extension of the lens file can be `.iges` or `.step`. This modified file extension is then inserted into the CAD files folder where ZEMAX has been installed, e.g:
`C:/Program Files (x86)/ZEMAX/Objects/CAD Files`.

In order to use LED as light source in optical design softwares, LED manufacturing companies presents to their users some file types containing the geometry of LED and rays originating from LED. These are known as eulumdat, source file, geometry, spectrum and thermal simulation files. The LED geometry file should be placed into the folder:
`C:/Program Files (x86)/ZEMAX/Objects/CAD Files`.
The eulumdat file having extention `.ldt` contains photometric data for a real lamp. Eulumdat allows us to use LED as a *point-like source* and mostly preferred

by designers. This file should be placed into the folder:
`C:/Program Files (x86)/ZEMAX/Objects/Sources/EULUMDAT`.

Two different detectors are used in the non-sequential in the optical simulation. They are the rectangular detector and the polar detector.

- **Detector Rectangle:** The rays from the light source strikes the surface of the detector and the energy data of the striking rays are recorded by the detector rectangle. The type of distribution of these stored data is determined by the selected data type parameter. The data type parameter is described in the detector parameters section. If you want this detector to have a reflective, transparent or absorbing surface, then the surface material is assigned using the material parameter. The material to be assigned may be MIRROR for reflective, ABSORB for absorbing or blank for transparent.

- **Detector Polar :** The rays from the light source strikes the surface of the detector and the power and visual light color data of the striking rays are recorded by the detector polar. The stored data distributions may be look at for incoherent light in the angular domains. If you want this detector to have a reflective, transparent or absorbing surface, then the surface material is assigned using the material parameter. The material to be assigned may be MIRROR for reflective, ABSORB for absorbing or blank for transparent. The size of the detector can be determined by the user.

To start non-sequential mode, user must invoke the command File ⇒ Non-Sequential Mode. This command start Non-Sequential Component Editor as shown in Figure 3.16 and 3.17.

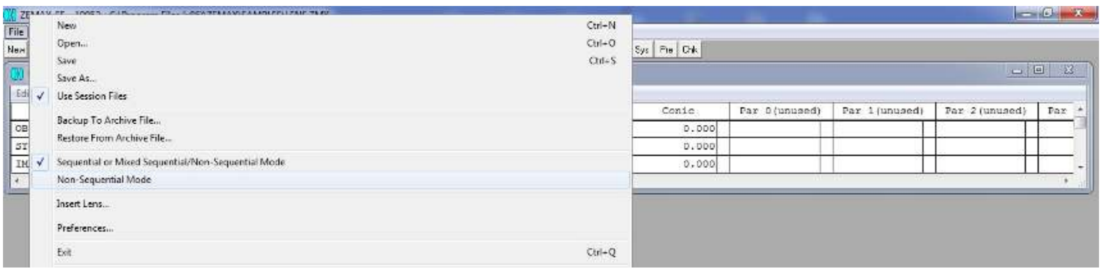

Figure 3.16 ZEMAX non-sequential mode (simulation)

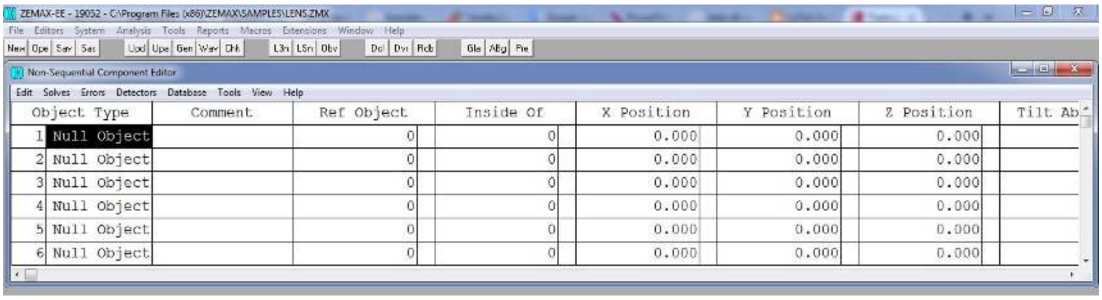

Figure 3.17 Non-Sequential Component Editor

Then, press insert key a few times to open newlines (or click Insert Object in Edit menu) to add the light source (LED), the lens, the detector and related objects. In this simulation, we use five objects which are shown in the below Figure 3.18 .

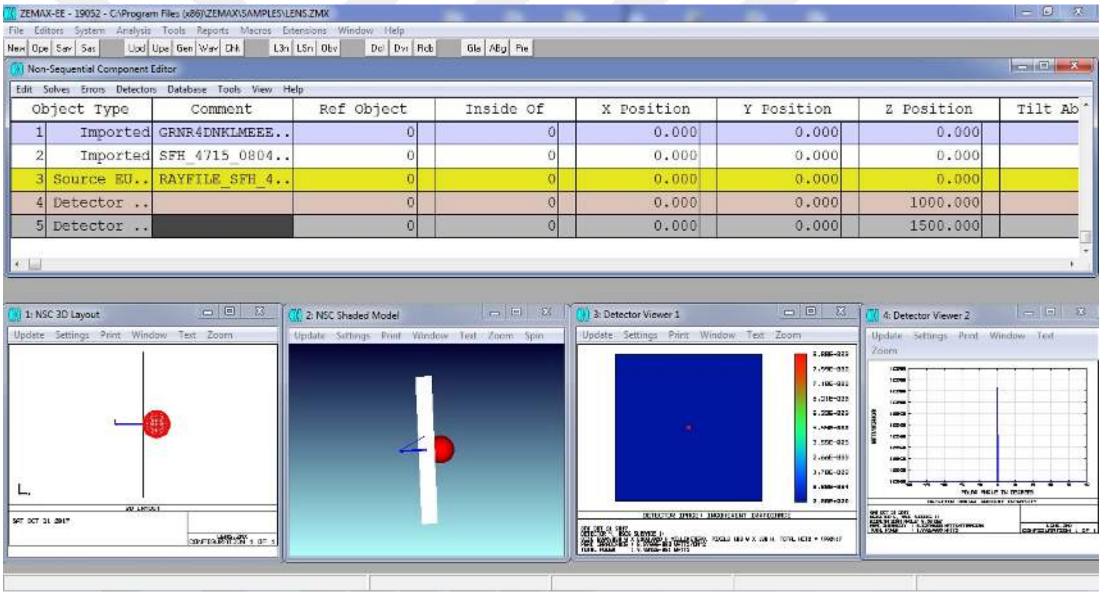

Figure 3.18 An example usage of Non-Sequential Component Editor for this study.

There are some parameters that the user should enter in the editor. Most of them are geometrical parameters such as x-position, y-position, tilt about z, etc. The rest of them are specific to the optical material assignment and the statistical analysis like layout rays, analysis rays and power of source, etc.

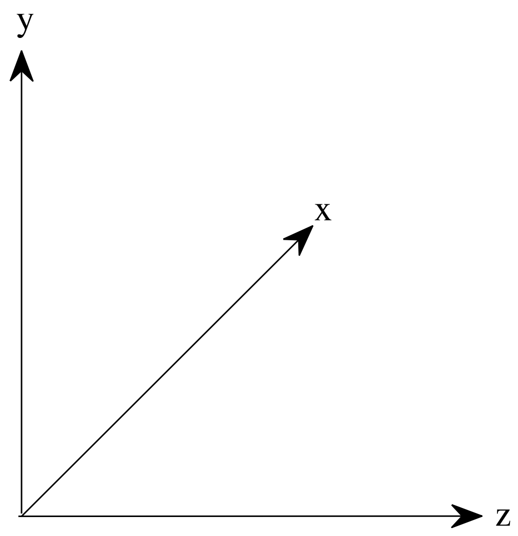

Figure 3.19 Coordinate system

- **x, y and z Position** are used to ensure that the inserted object is positioned and moved in the desired coordinate. The ZEMAX coordinate system is shown in Figure 3.19.
- **Tilt About x, y and z** are used to ensure that the inserted object is placed at the desired angle.
- **Material** parameter is used to specify the material from which the object is to be used. This parameter is used for objects such as lenses and mirrors.

When the light source is added to the system, one requires special parameters like layout rays, analysis rays and power besides the standard parameters.

- **Layout Rays** is the parameter that will allow you to enter the number of beams to be shown when simulating the program. The maximum value to be entered here is 20000 and the speed of the program which is the maximum value to be entered here is slowed down.
- **Analysis Rays** is the parameter that allows us to enter the number of rays to be analyzed. The value to enter here is limited by the file size that the manufacturer company will give us. The ray file that we used contains maximum 5 million rays.

- **Power** parameter is related with the optical power of LED and its electrical power.

In Non-Squential Component Editor, if you double-click an empty line (Null Object) you will see corresponding object properties. In the Type and Data File are selected. Similarly, the ray file and the spectrum file of the source are added to the system. Note that, the spectrum file contains the color model of the light source used. It contains information such as the wavelength of the light source and the weight of this wavelength. Spectrum file is in ASCII text format and extension `.SPC`. The spectrum file must be placed to the folder:
`C:/Program Files (x86)/ZEMAX/Objects/Sources/Spectrum Files`.
How to add LED source in ZEMAX are shown in Figure 3.20, 3.21 and 3.22.

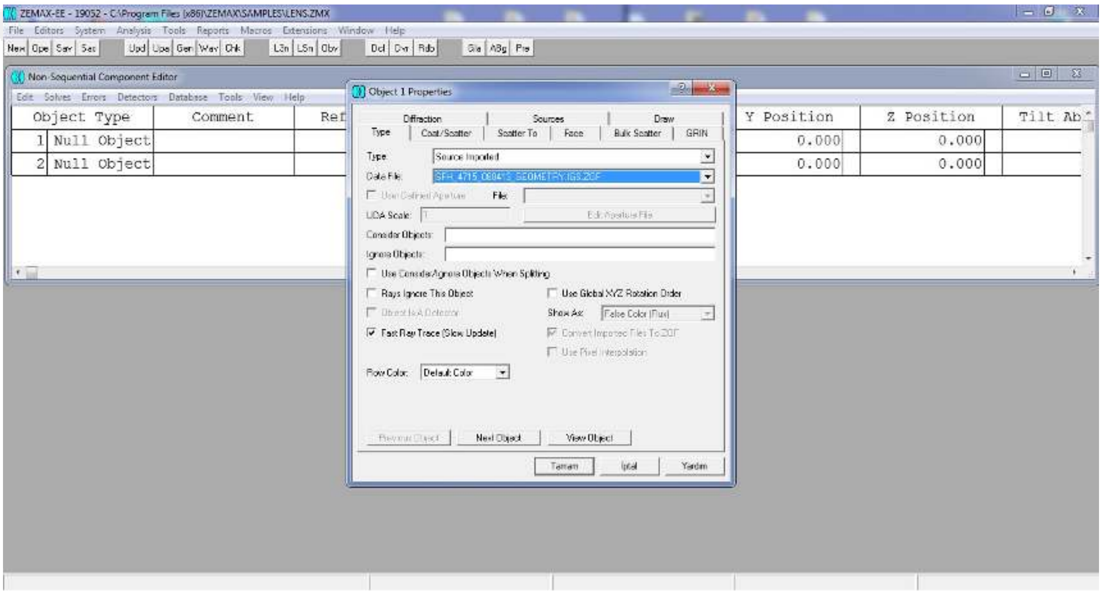

Figure 3.20 Importing the source file.

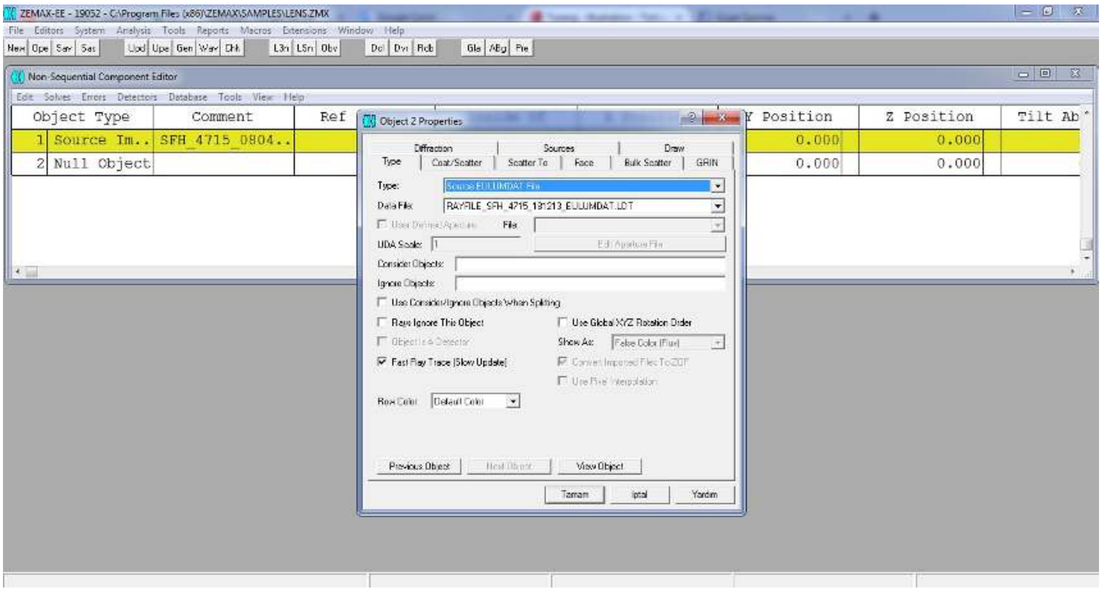

Figure 3.21 Importing the ray file.

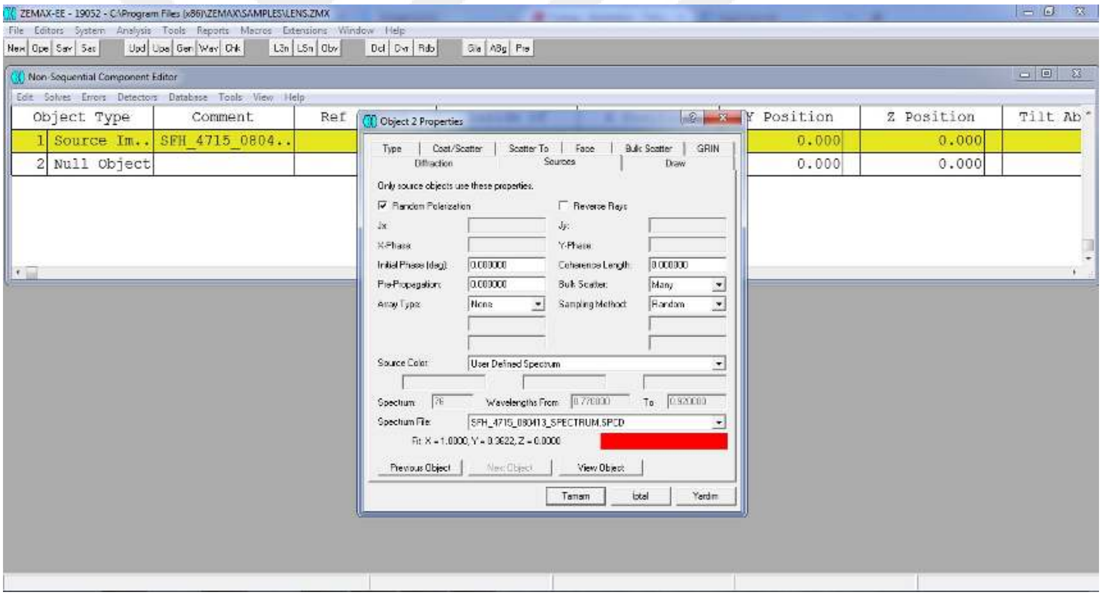

Figure 3.22 Importing the spectrum file.

After adding the light source, the designed lens will be added to the system as follows. There is no special parameter for the lens. Only the lens material (PMMA, PC [or polycarb in ZEMAX], PS [or polystyr in ZEMAX]) must be given. Figure 3.23 shows how to add the lens to the system.

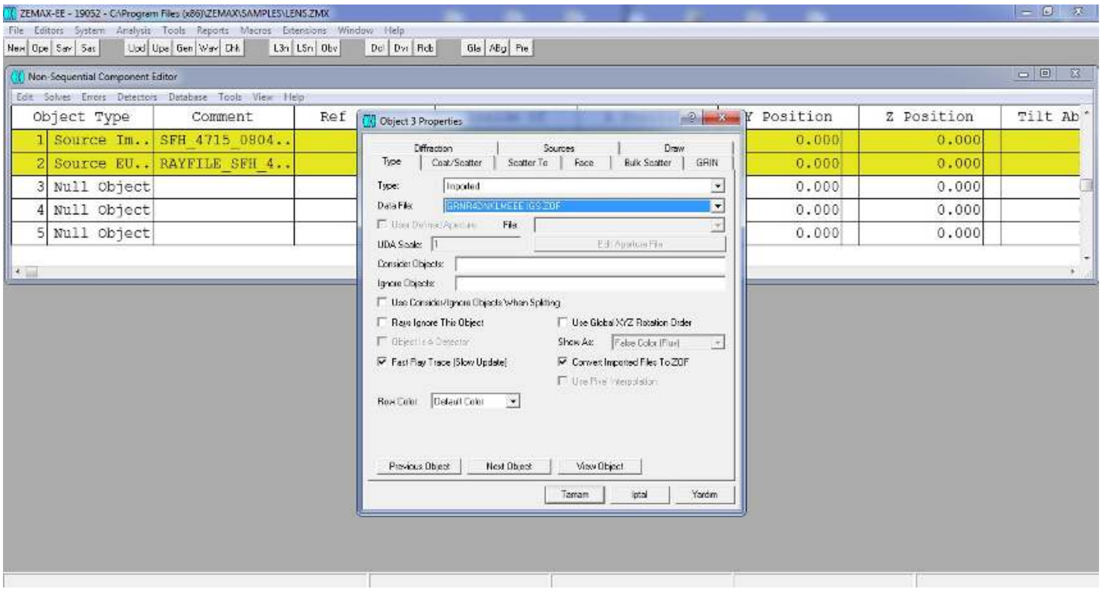

Figure 3.23 Lens imported

The last object that should be added to the system to simulate the detector which is basically counter of rays falling on it. Two detectors are added to the system; detector rectangle and detector polar. The parameters we will use in these detectors are X Half Width, Y Half Width, number of X Pixel, number of Y Pixel, Data Type, Color, Maximum Angle, Radial Size, number of P Pixel, number of A Pixel and Mirroring.
Detector Rectangle parameters:

- **X Half Width** is half of the desired width value in the x axis of the detector.
- **Y Half Width** is half of the desired height value in the y axis of the dedector.
- **Number of X Pixel** is the number of pixels to enter the x axis of the detector. The maximum number of pixel is 5000.
- **Number of Y Pixel** is the number of pixels to enter the y axis of the detector. The maximum number of pixel is 5000.
- **Data Type** defines the physical quantities of the analysis such as radiometric or photometric calculations.
- **Color** We may change the color output interface of the detector by this parameter. (0 for Grey Scale, 1 for Inverse Grey Scale, 2 for False Color, 3 for Inverse False Color).

Detector Polar parameters:

- **Maximum Angle** The polar angle unit is degrees, and the value to be entered must be between 1 and 180.
- **Radial Size** is the size of the radius of the detector in lens unit (such as mm).
- **Number of P Pixel** is the number of pixels in the polar angle direction. The value to be entered must be between 10 and 721.
- **Number of A Pixel:** is the number of pixels in the azimuth angle direction. The value to be entered must be between 12 and 720, and must be a multiple of 4.
- **Mirroring** allows the symmetry make use of the by using the detector of incident rays. All of the rays in the detector is divided into parts, and each portion of the detector beam into symmetrical mirror images are copied.

Inserting the detector to the system are shown in Figures 3.24, 3.25 and 3.26 respectively.

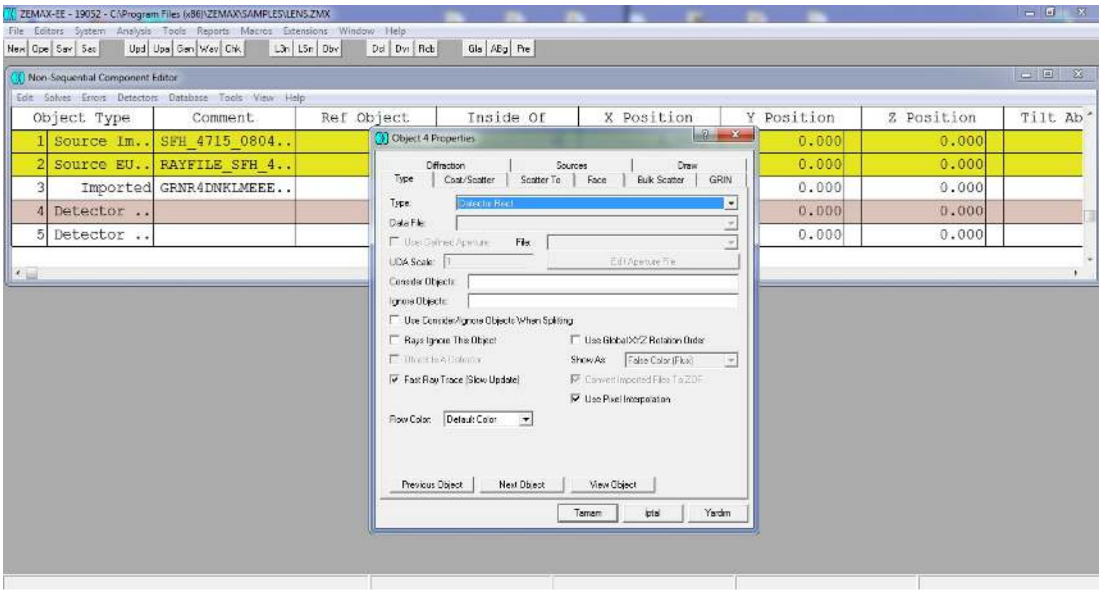

Figure 3.24 Adding Detector Rectangle.

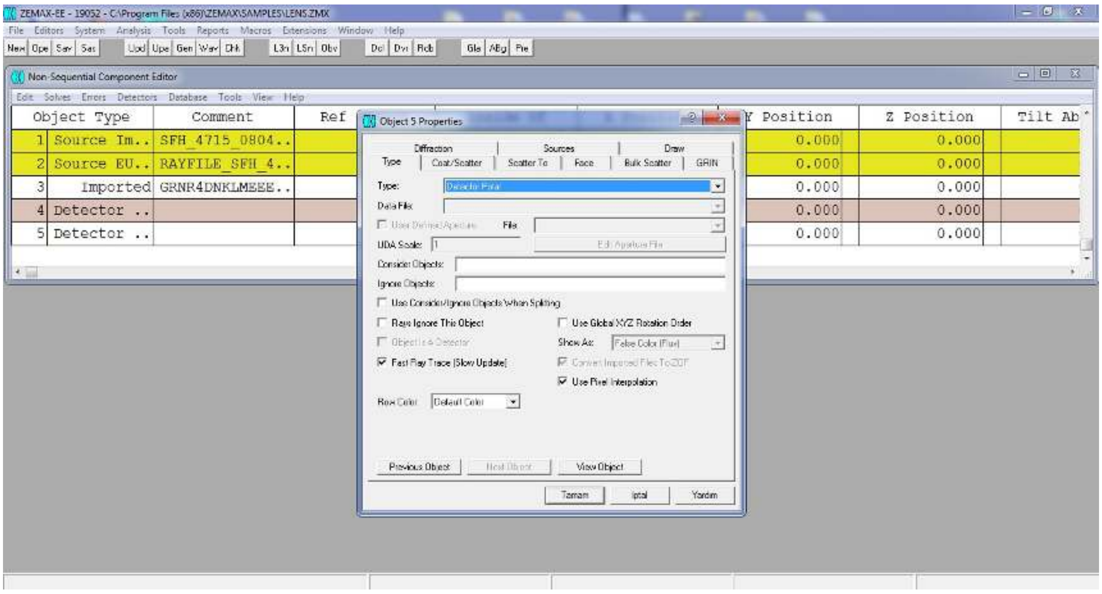

Figure 3.25 Adding Detector Polar.

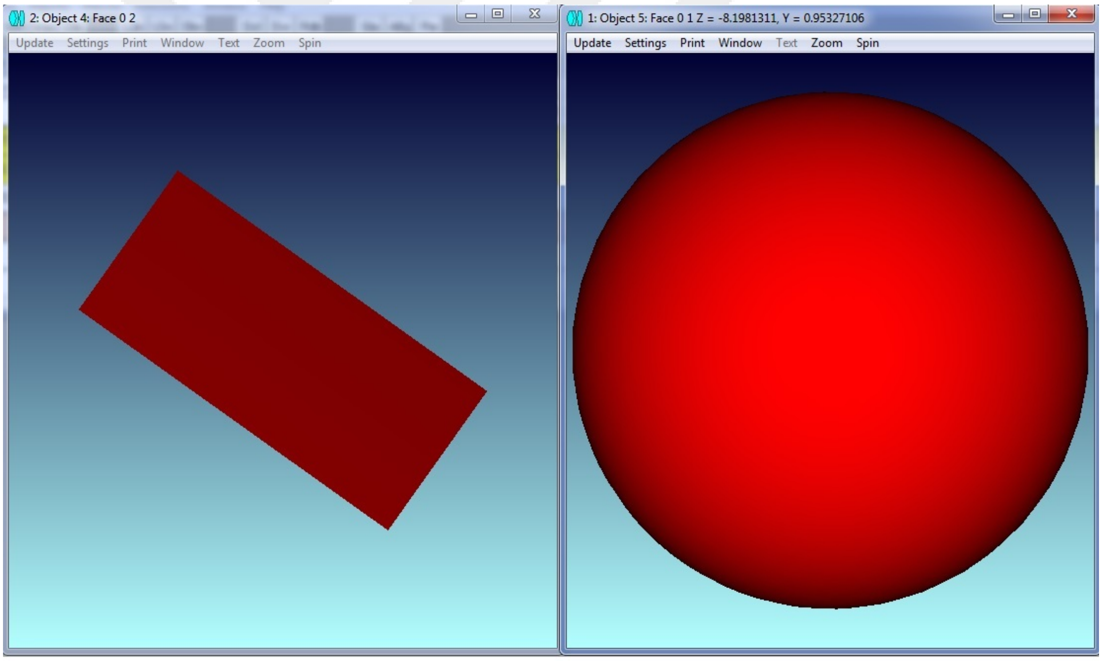

a **b**

Figure 3.26 a) Detector Rect b) Detector Polar

Simulation in ZEMAX

After completing the steps above, one can start the simulation. Simulations are based on the counting number photon hits and the calculation of equivalent optical power on the detector. Totally 5M rays are emitted from LED. The spot diagrams are obtained on the rectangular detector, whose size is 5.3 m × 5.3 m, for the positions 1 m, 10 m, 25 m, 50 m, 100 m, 250 m and 500 m.

To start the simulation, the Detector Control Surface command is invoked by pressing Dcl button. An example screen shoot is shown in Figure 3.27.

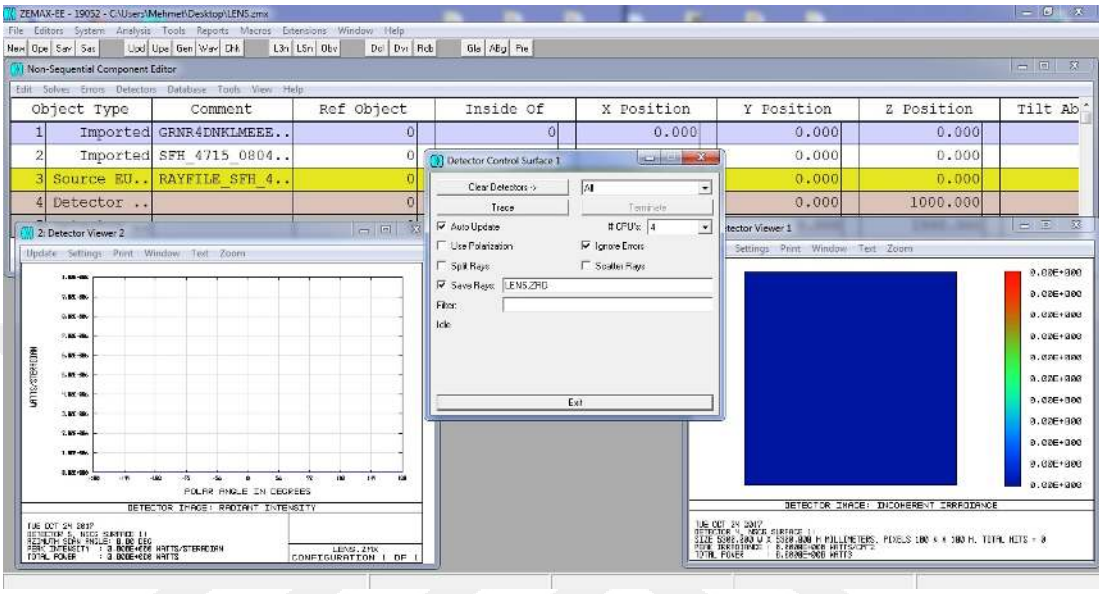

Figure 3.27 Detector Control Surface to start simulation.

The setting parameters are as follows.

- **Clear Detector** is used to clear up the results of previous simulation.
- **Trace/Terminate** is used to start/stop the simulation process.
- **Auto Update** command prints the simulation results to the screen at certain intervals while simulating.
- **Ignore Errors** is used to cancel simple faults at startup and ongoing simulation.
- **Split Rays** When a beam hits a surface, some of the energy it has is reflected, some are transmitted, and some are absorbed, depending on the surface properties. Ray split command calculates the path of the refracted and reflected beam and continues to record the path information of these rays. The save rays command must be selected to use this command.

- **Scatter Rays** keeps a record of the rays scattered by the surface feature and records this information. The save rays command must be selected to use this command.

- **Save Rays** command calculates the paths the beams use when simulating, and saves the information in .ZRD (ZEMAX Ray Database) format, such as whether the beams reach the target. If this information is to be checked later, it is displayed in non-sequential mode in text file format with .RDB (Ray Database Viewer) command. Sample file shown in Figure 3.28.

- **Filter** is used to filter data when saving simulation data. If left alone, all rays used in the simulation will be saved in the .ZRD file.

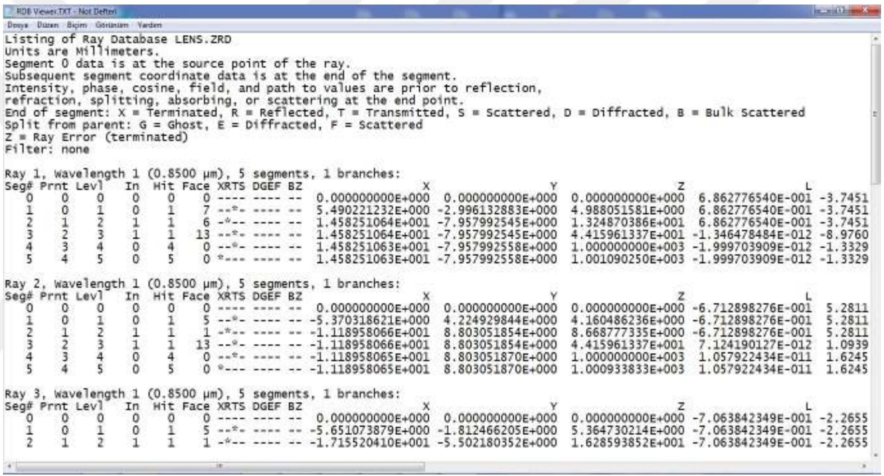

```
Listing of Ray Database LENS.ZRD
Units are Millimeters.
Segment 0 data is at the source point of the ray.
Subsequent segment coordinate data is at the end of the segment.
Intensity, phase, cosine, field, and path to values are prior to reflection,
refraction, splitting, absorbing, or scattering at the end point.
End of segment: X = Terminated, R = Reflected, T = Transmitted, S = Scattered, D = Diffracted, B = Bulk Scattered
Split from parent: G = Ghost, E = Diffracted, F = Scattered
Z = Ray Error (terminated)
Filter: none

Ray 1, Wavelength 1 (0.8500 µm), 5 segments, 1 branches:
Seg# Prnt Levl   In  Hit Face XRTS DGEF BZ                X                 Y                 Z                 L
   0    0    0    0    0    0 ---- ---- --  0.000000000E+000  0.000000000E+000  0.000000000E+000  6.862776540E-001 -3.7451
   1    0    1    0    1    7 --*- ---- --  5.490221232E+000 -2.996132883E+000  4.988051581E+000  6.862776540E-001 -3.7451
   2    1    2    1    1    6 -*-- ---- --  1.458251064E+001 -7.957992545E+000  1.324870386E+001  6.862776540E-001 -3.7451
   3    2    3    1    1   13 --*- ---- --  1.458251064E+001 -7.957992545E+000  4.415961337E+001 -1.346478484E-012 -8.9760
   4    3    4    0    4    0 --*- ---- --  1.458251063E+001 -7.957992558E+000  1.000000000E+003 -1.999703909E-012 -1.3329
   5    4    5    0    5    0 *--- ---- --  1.458251063E+001 -7.957992558E+000  1.001090250E+003 -1.999703909E-012 -1.3329

Ray 2, Wavelength 1 (0.8500 µm), 5 segments, 1 branches:
Seg# Prnt Levl   In  Hit Face XRTS DGEF BZ                X                 Y                 Z                 L
   0    0    0    0    0    0 ---- ---- --  0.000000000E+000  0.000000000E+000  0.000000000E+000 -6.712898276E-001  5.2811
   1    0    1    0    1    5 --*- ---- -- -5.370318621E+000  4.224929844E+000  4.160486236E+000 -6.712898276E-001  5.2811
   2    1    2    1    1    1 -*-- ---- -- -1.118958066E+001  8.803051854E+000  8.668777335E+000 -6.712898276E-001  5.2811
   3    2    3    1    1   13 --*- ---- -- -1.118958066E+001  8.803051854E+000  4.415961337E+001  7.124190127E-012  1.0939
   4    3    4    0    4    0 --*- ---- -- -1.118958065E+001  8.803051870E+000  1.000000000E+003  1.057922434E-011  1.6245
   5    4    5    0    5    0 *--- ---- -- -1.118958065E+001  8.803051870E+000  1.000933833E+003  1.057922434E-011  1.6245

Ray 3, Wavelength 1 (0.8500 µm), 5 segments, 1 branches:
Seg# Prnt Levl   In  Hit Face XRTS DGEF BZ                X                 Y                 Z                 L
   0    0    0    0    0    0 ---- ---- --  0.000000000E+000  0.000000000E+000  0.000000000E+000 -7.063842349E-001 -2.2655
   1    0    1    0    1    5 --*- ---- -- -5.651073879E+000 -1.812466205E+000  5.364730214E+000 -7.063842349E-001 -2.2655
   2    1    2    1    1    1 -*-- ---- -- -1.715520410E+001 -5.502180352E+000  1.628593852E+001 -7.063842349E-001 -2.2655
```

Figure 3.28 An example of ZEMAX RDB (Ray DataBase) file.

The simulation results using Eulumdat files are shown in Figures 3.29, 3.30, 3.31 and 3.32, and Tables 3.6 and 3.7, and in Appendix A and B.

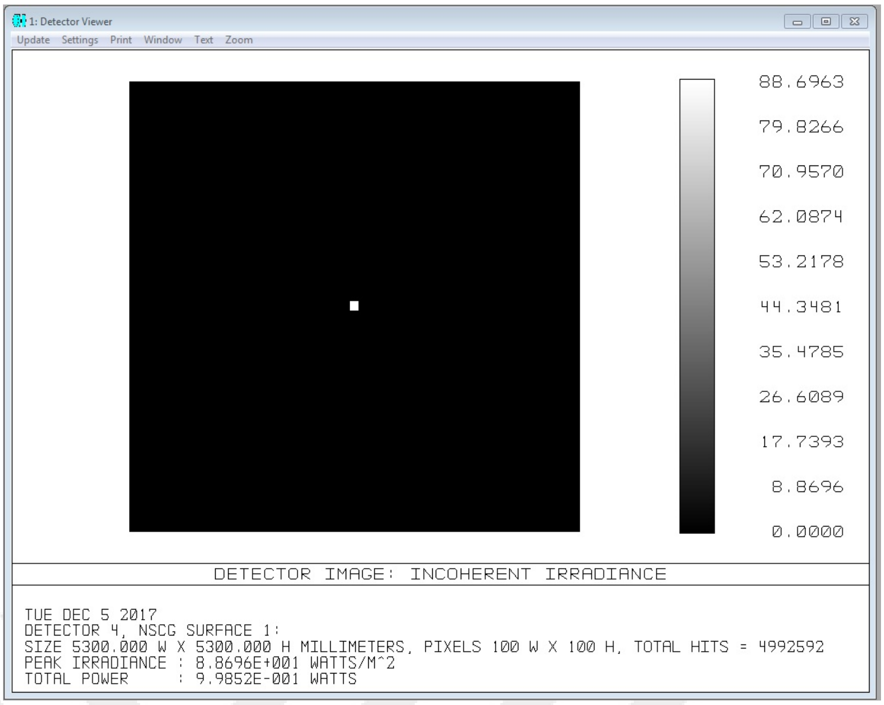

Figure 3.29 Spot diagram obtained for the detector position at 1 m using OSRAM SFH4715.

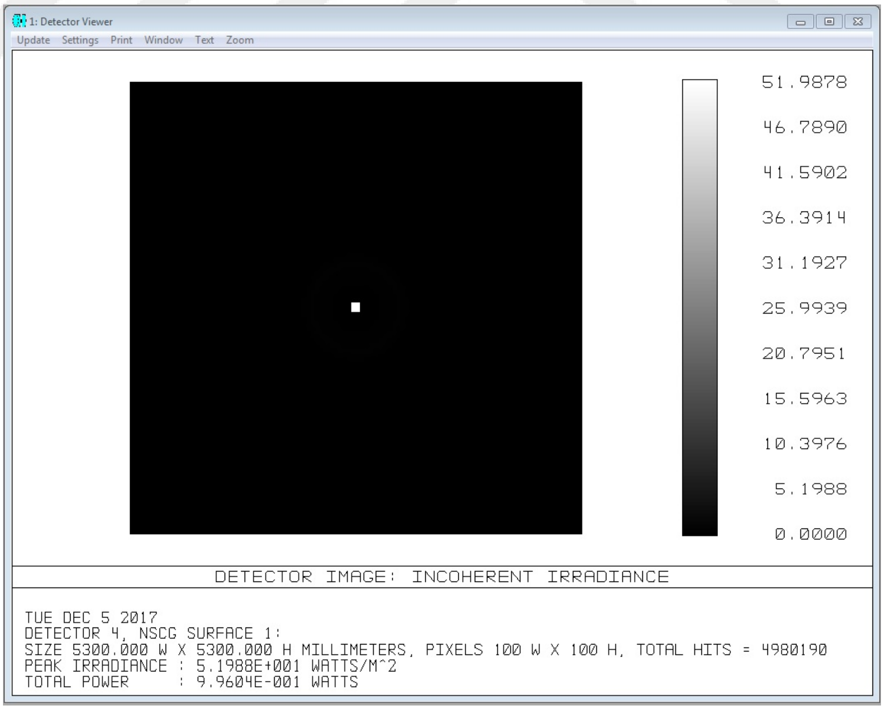

Figure 3.30 Spot diagram obtained for the detector position at 100 m using OSRAM SFH4715.

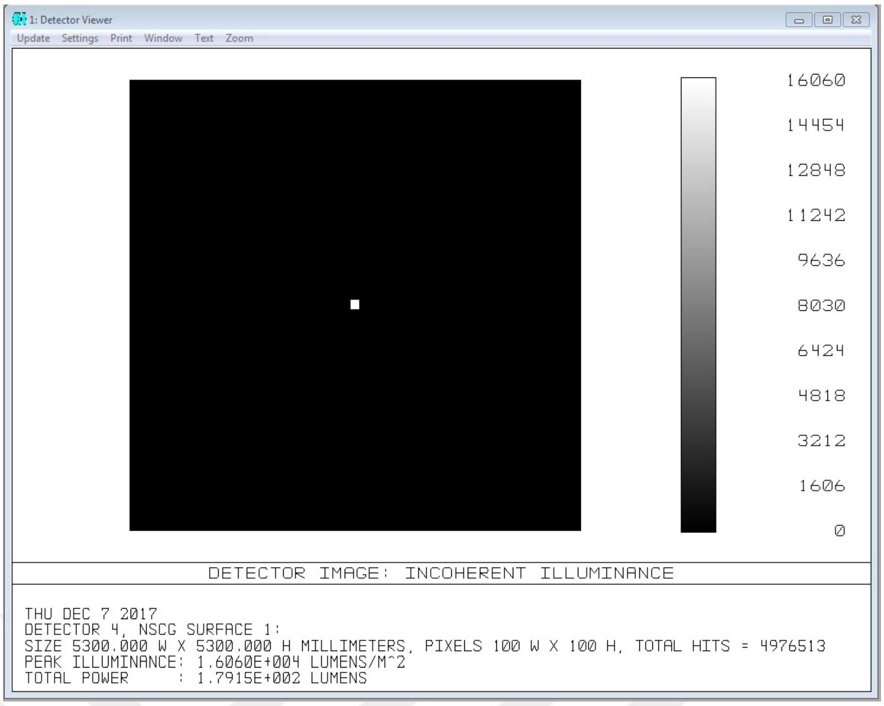

Figure 3.31 Spot diagram obtained for the detector position at 1 m using OSRAM LUW CVBP.

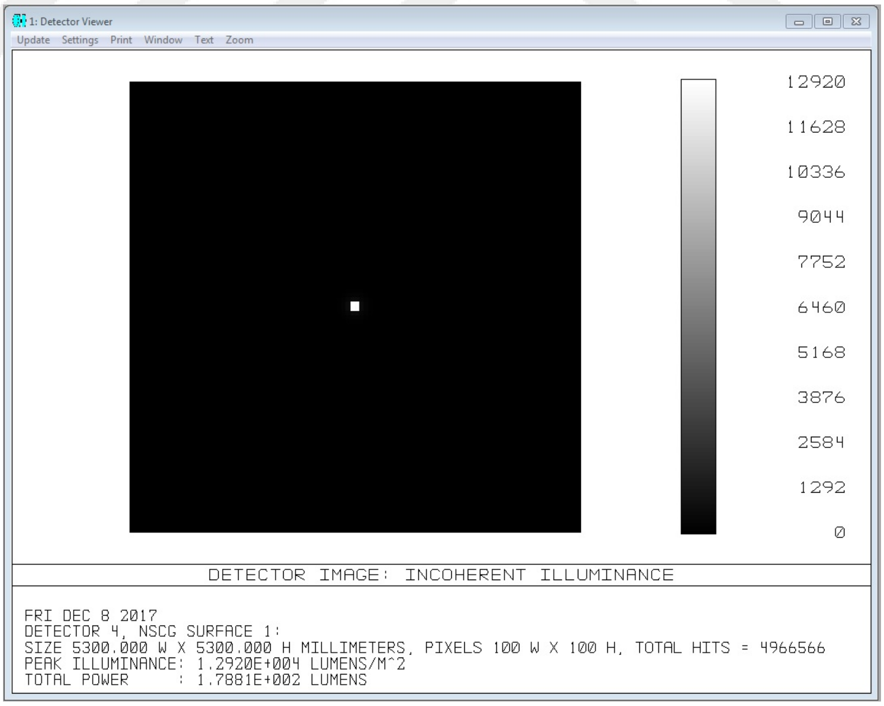

Figure 3.32 Spot diagram obtained for the detector position at 100 m using OSRAM LUW CVBP.

Table 3.6 Simulation results for PMMA at some distances using eulumdat file for OSRAM SFH4715.

Distance(meter)	Total Hits	Total Power (mW)	mW/m^2
1	4992592	998.52	88696
10	4980329	996.07	75312
25	4980296	996.06	54431
50	4980199	996.04	52358
100	4980190	996.04	51988
250	4980214	996.04	51798
500	4571067	914.21	51662

Table 3.7 Simulation results for PMMA at some distances using eulumdat file for OSRAM LUW CVBP.

Distance(meter)	Total Hits	Total Power (lm)	lux
1	4976513	179.15	16060
10	4966738	178.87	16064
25	4967221	178.84	15649
50	4966991	178.80	14319
100	4966566	178.81	12290
250	4966867	178.75	11867
500	4966974	178.77	11499

Results show that the optical power loss is very low when using eulumdat files for both visible and IR LED sources. That is to say the optical performance of the designed lens is perfect if one uses the LED's eulumdat file representing point-like source in the simulation.

However, one can use the source (or ray) file of LED to model light source realistically. That a source file represents actual light distribution instead of point-like source. Source files includes coordinate, angles and intensity data of the rays. The extension of this file is `.DAT` and are placed in the folder: `C:/Program Files (x86)/ZEMAX/Objects/Sources/Source Files`. The source file of LED to be used can be obtained from the LED manufacturer web page. The comparison of emitted rays by using eulumdat and source files for IR LED used in the study are shown in Figure 3.33a and 3.33b respectively.

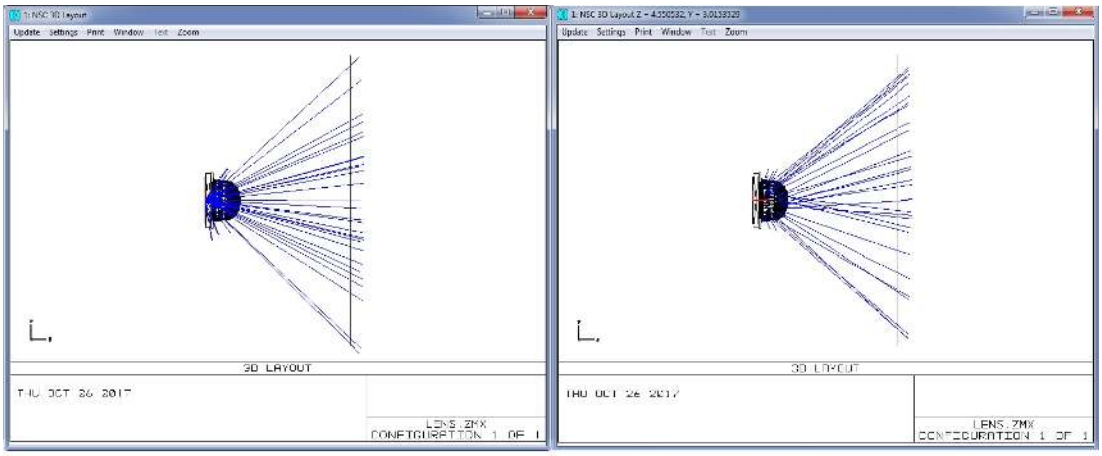

a b

Figure 3.33 Light ray distribution for OSRAM SFH4715 using (a) eulumdat file and (b) source file.

The results of the first simulation with the source files are shown in Figures 3.34 and 3.35 where detector position is 10 away from the source. For both cases the LED position is selected as (0,0,0). In Figure 3.34 lens position is (0,0,0) while in Figure 3.35 the lens position is (0,0,0.36 mm).

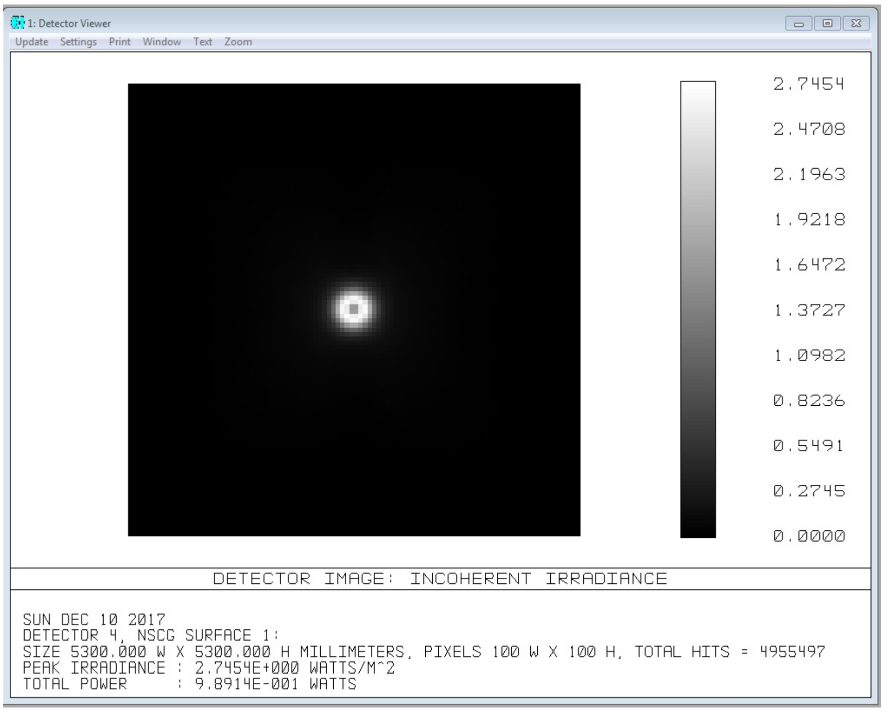

Figure 3.34 The lens is located at points (0,0,0) in the coordinate system.

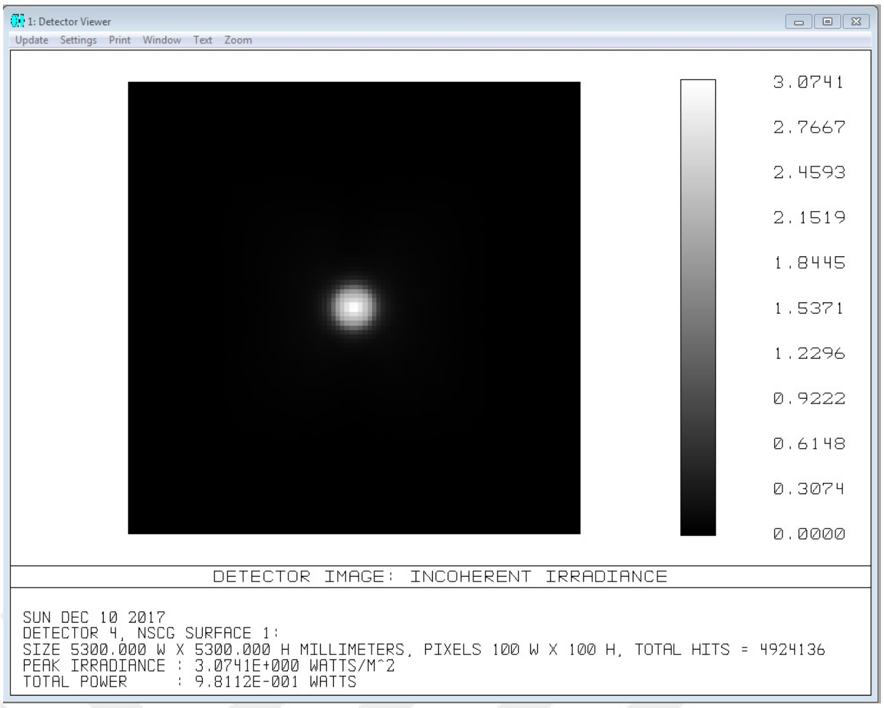

Figure 3.35 The lens is located at points (0,0,0.36) in the coordinate system

It is clear that the total number of hits depend on the lens and LED positions. Therefore, the distance between the lens and the LED can optimized such that the maximum number of hits are obtained. The graph for total number of hits vs lens position of IR and visible LED are shown in Figures 3.36 and 3.37 respectively for three optical materials. It is obvious that PMMA exhibits a better performance in terms of number of photons on the detector same detector position.

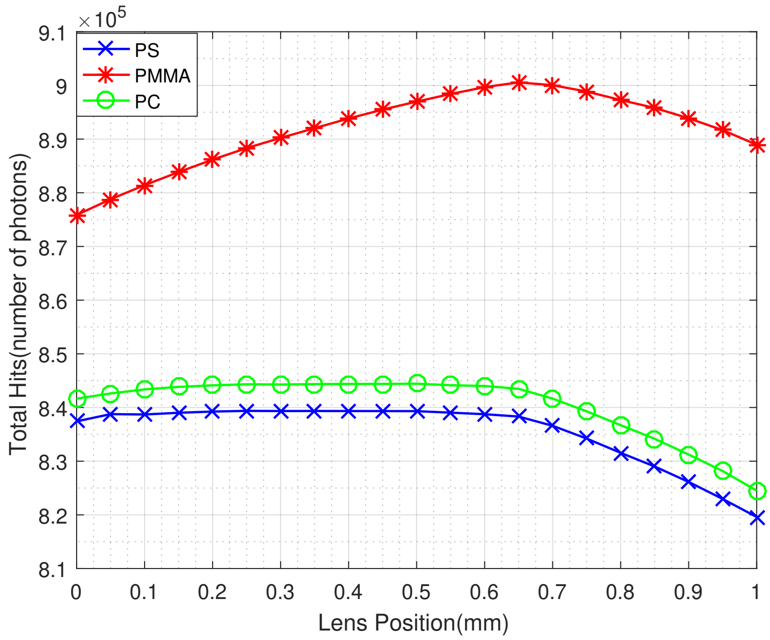

Figure 3.36 Total number of hits as a function of distance between for IR LED (OSRAM SFH4715) and lens for three different materials.

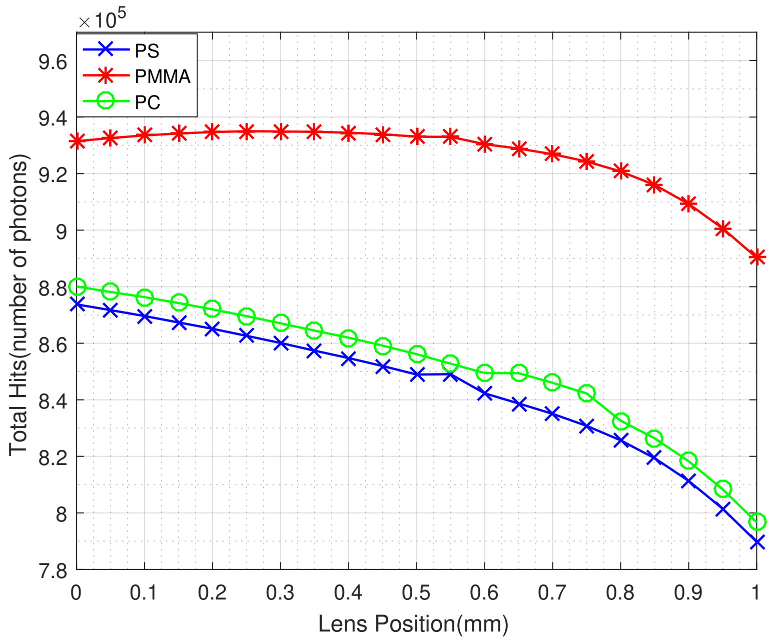

Figure 3.37 Total number of hits as a function of distance between for visible LED (OSRAM LUW CVBP) and lens for three different materials.

After setting the Z position, the lens was simulated with infrared LED for different materials. The spot diagrams on the detector (1 m and and 100

m) for three materials and IR LED are shown in Figures 3.38, 3.39 and 3.40, respectively. Simulation results for the other lengths are shown in Appendix C and D. In addition, the relative intensity vs detector distance plot is shown in Figure 3.41 and in Table 3.8.

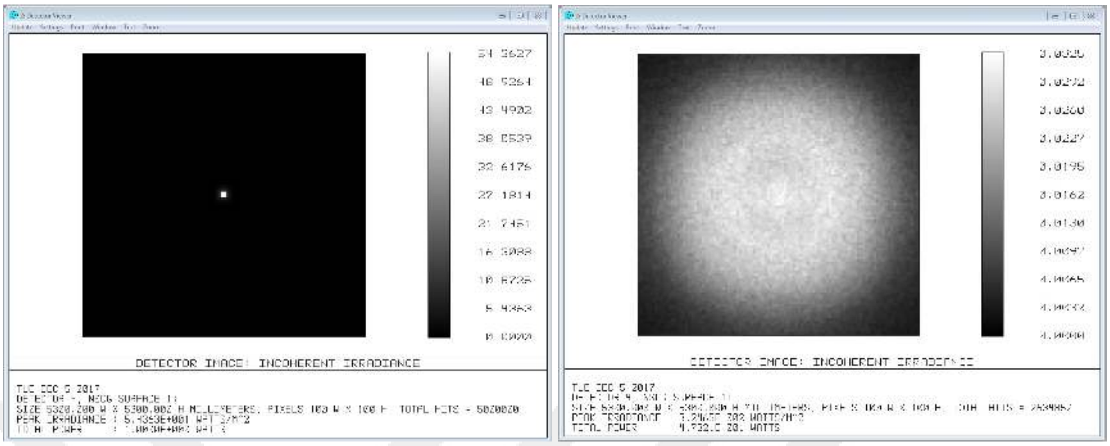

(a) **(b)**

Figure 3.38 (a) Spot diagram at 1 m for PMMA lens. (b) Spot diagram at 100 m for PMMA lens.

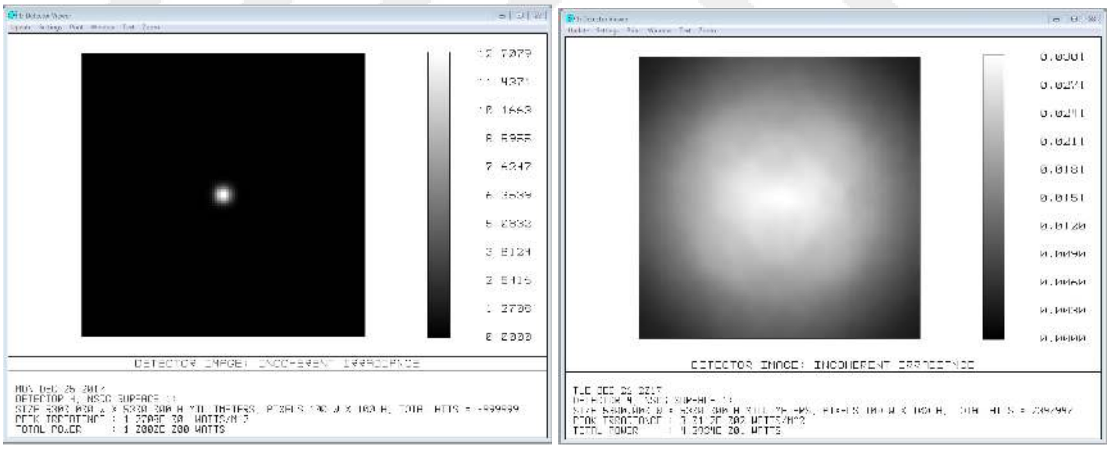

(a) **(b)**

Figure 3.39 (a) Spot diagram at 1 m for PC lens. (b) Spot diagram at 100 m for PC lens.

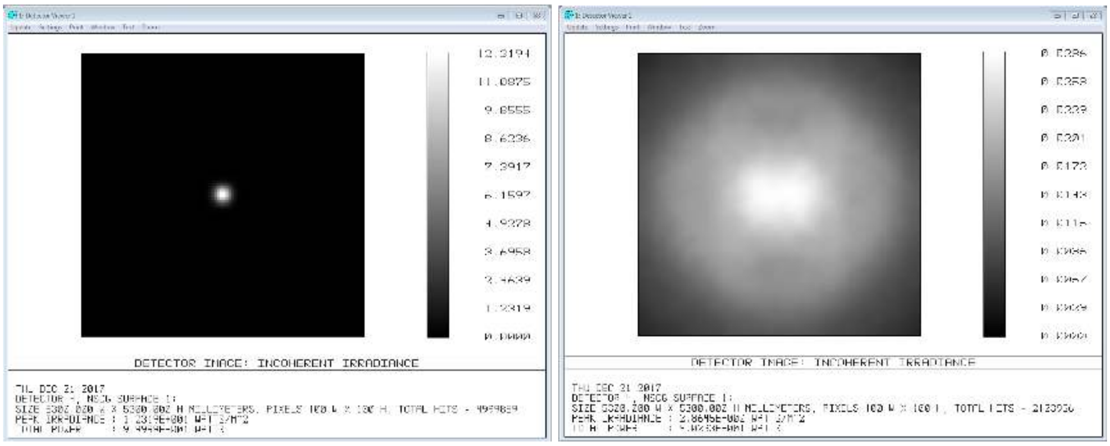

(a) **(b)**

Figure 3.40 (a) Spot diagram at 1 m for PS lens. (b) Spot diagram at 100 m for PS lens.

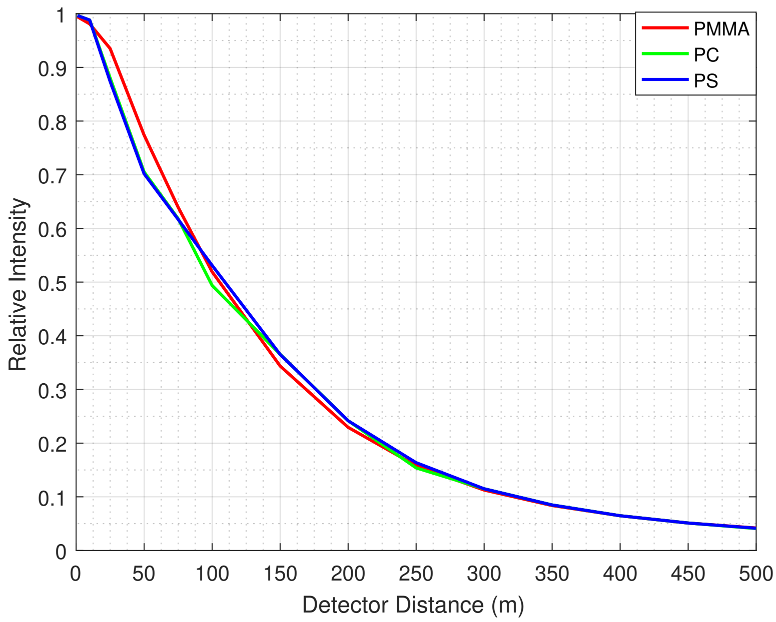

Figure 3.41 Relative intensity vs LED and detector distance for IR LED. It is clear that the inverse-square-law holds.

Table 3.8 Simulation results for IR LED.

	PMMA				PC				PS			
Distance (m)	Total Hits	Total Power (mW)	Peak Irradiance (mW/m^2)	Efficiency (%)	Total Hits	Total Power (mW)	Peak Irradiance (mW/m^2)	Efficiency (%)	Total Hits	Total Power (mW)	Peak Irradiance (mW/m^2)	Efficiency (%)
1	5000000	1000	54300.0	100.00	4999999	1000	12708	100.00	4999859	999.9	12319	100.00
10	4924141	981.1	3074.2	98.48	4915063	978.6	2168	98.30	4906491	976.3	1886.6	98.13
25	4461535	845.3	507.0	89.23	4223006	768.0	450.5	84.46	4119762	735.2	735.2	82.40
50	3735061	650.1	127.0	74.70	3549433	607.9	118.1	70.99	3491500	596.7	596.7	69.83
100	2634852	473.2	32.5	52.70	2397947	439.3	30.1	47.96	2123956	402.3	402.3	42.48
250	708477	125.1	6.5	14.17	575478	116.2	5.0	11.51	469758	103.3	4.8	9.40
500	188240	31.4	3.5	3.76	147782	31.6	1.4	2.96	127540	30.2	1.3	2.55

* Efficiency is ratio of detector hits to total number of rays.

Same study is repeated for the visible LED (OSRAM LUW CVBP). Results are shown in Figure 3.42, 3.43, 3.44, , 3.45 respectively and in Table 3.9.

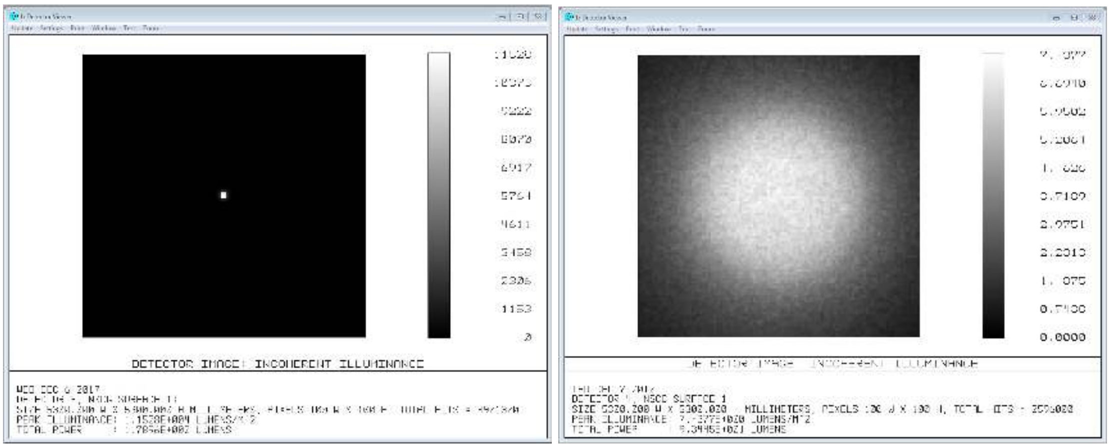

(a) **(b)**

Figure 3.42 (a) Spot diagram at 1 m for PMMA lens. (b) Spot diagram at 100 m for PMMA lens.

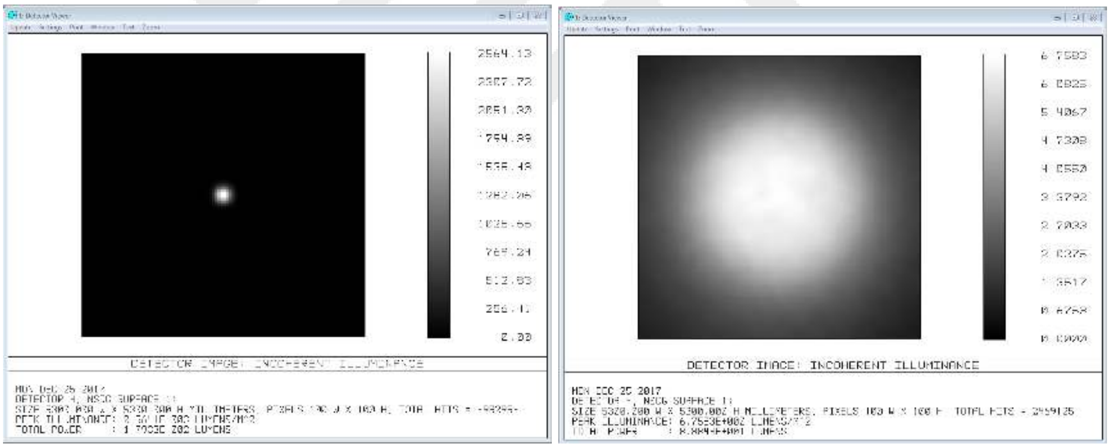

(a) **(b)**

Figure 3.43 (a) Spot diagram at 1 m for PC lens. (b) Spot diagram at 100 m for PC lens.

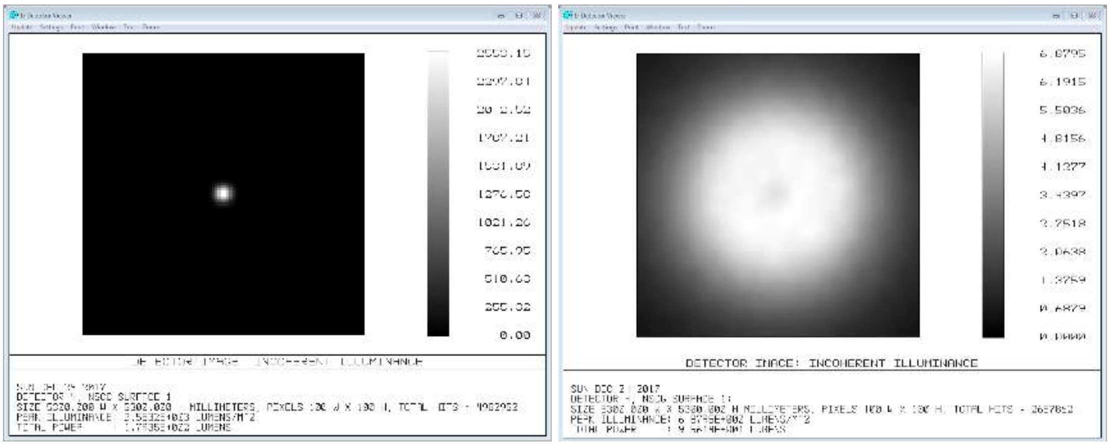

(a) (b)

Figure 3.44 (a) Spot diagram at 1 m for PS lens. (b) Spot diagram at 100 m for PS lens.

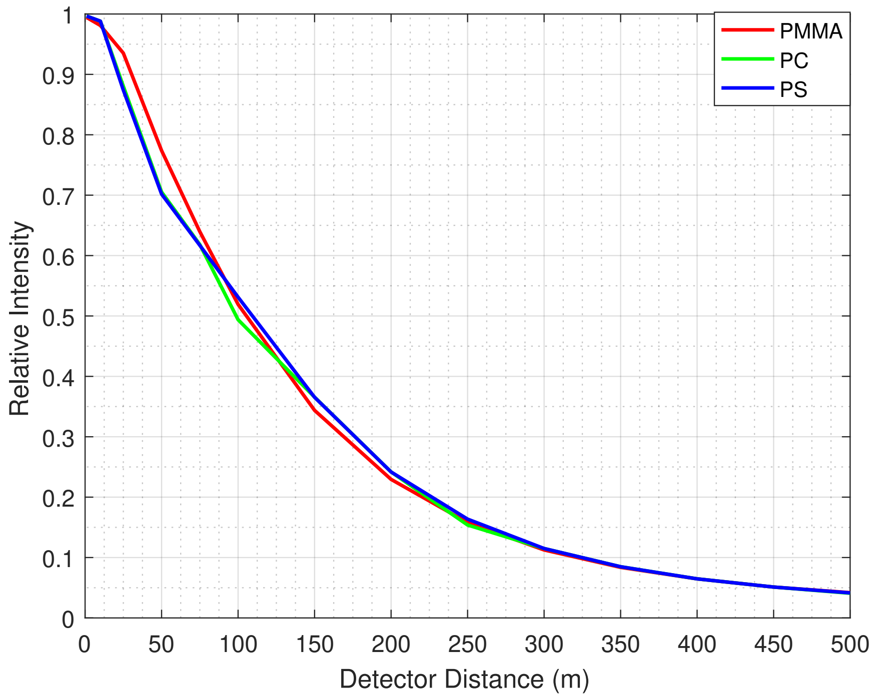

Figure 3.45 Relative intensity vs LED and detector distance for visible LED. It is clear that the inverse-square-law holds.

Table 3.9 Simulation results for visible LED.

	PMMA				PC				PS			
Distance (m)	Total Hits	Total Power (lm)	Peak Illuminance (lux)	Efficiency (%)	Total Hits	Total Power (lm)	Peak Illuminance (lux)	Efficiency (%	Total Hits	Total Power (lm)	Peak Illuminance (lux)	Efficiency (%
1	4971370	178.96	11528	99.43	4982954	179.38	2564.1	99.66	4982952	179.35	2553.2	99.66
10	4904966	176.58	669.81	98.10	4940747	177.81	565.37	98.81	4940789	177.87	565.20	98.82
25	4676005	168.23	110.22	93.52	4401602	158.10	106.20	88.03	4369832	156.90	106.31	87.40
50	3869220	139.16	28.09	77.38	3526219	126.70	27.11	70.52	3508973	126.11	27.07	70.18
100	2596000	93.45	7.44	51.92	2469125	88.84	6.76	49.38	2657862	95.6	6.87	53.16
250	789107	28.39	1.42	15.78	769355	27.70	1.14	15.39	818099	29.46	1.14	16.36
500	209454	7.53	0.49	4.19	204408	7.37	0.31	4.09	207343	7.45	0.32	4.15

Finally, all the spot radii of the illumination on the detector are calculated. In this study spot radius is defined as the full width of the central pattern on the detector at half maximum, FWHM. The simulation results are shown in Table 3.10 3.11 respectively.

Table 3.10 Infrared LED Spot Radius vs distance of the detector.

	FWHM (m)		
Distance(m)	PMMA	PC	PS
1	0.0663	0.0663	0.0663
10	0.1457	0.1192	0.1192
25	0.2783	0.2783	0.2783
50	0.5433	0.5167	0.5167
100	1.0865	1.0335	1.0335

Table 3.11 Visible LED Spot Radius vs distance of the detector.

	FWHM (m)		
Distance(m)	PMMA	PC	PS
1	0.0663	0.0663	0.0663
10	0.1457	0.1192	0.1192
25	0.2650	0.2385	0.2517
50	0.5035	0.4902	0.4902
100	0.9938	0.9143	0.9672

CHAPTER 4

PRODUCTION OF THE LENS AND OPTICAL MEASUREMENTS

4.1 Introduction

This chapter describes the production and optical measurements of the lens whose simulation is given in the Chapter 3. A plastic injection method is used for the manufacturing of the lens. Optical analysis based on light intensity measurements are preformed within 50 meters. It is found that the measurement results are around half of simulation results.

4.2 Production

4.2.1 Injection Molding Machine

It is a machine used for the production of plastic products by injection molding method. This machine has two different versions as horizontal orientation injection molding and vertical orientation injection molding. In general, horizontal orientation injection molding devices are used. However, vertically oriented injection devices are used in applications that will benefit from gravity. Injection molding machines consist of two main mechanisms. These are the compression mechanism and the injection mechanism. The drawing of an injection molding machine is shown in Figure 4.1.

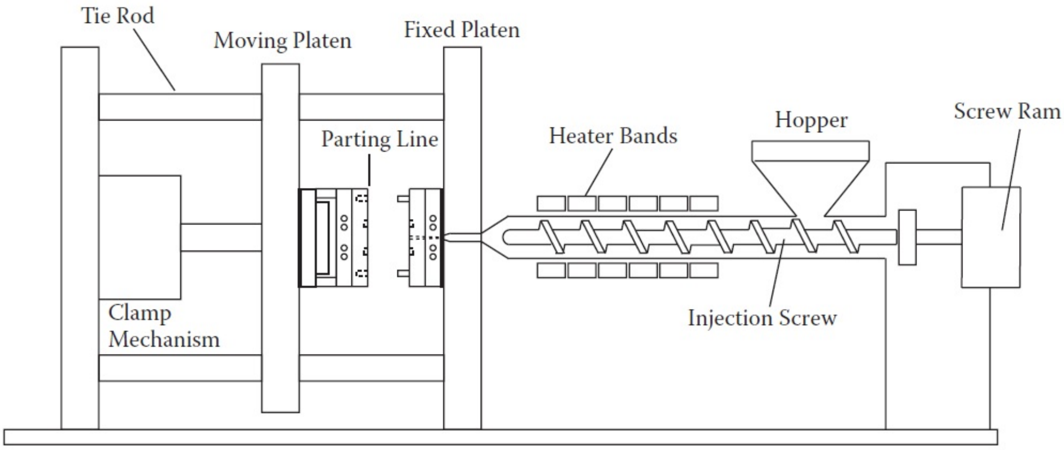

Figure 4.1 The injection molding machine, [37].

The clamping mechanism is used to close, open and hold the mold. The injection mechanism is used to inject the plastic into the mold. Due to the compression mechanism, these devices are also called injection presses. Except for injection points, these machines do not directly press the material inside the mold. The compression mechanism applies a high pressure on the mold. During the injection of plastic, thousands of tons of pressure per square centimeter can be produced. Therefore the pressure to be applied by the compression mechanism must be higher. For this reason, the compression forces of these devices are unit content to tone. Compression pressures of injection machines are between 5 and 2500 tons. The pressures of the machines to be used for optical dies are between 10 and 50 tons. The compression mechanism moves to open and close the mold, except to keep the mold closed during injection. It is also used during the separation of the produced product from the mold [36].

The compression mechanism consists of two large metal plates. These are a means of providing the clamping force and a hinge used to apply this force. It is called metal plated platen. One of these plates is fixed to the injection machine and this piece is called a fixed platen. The other platen is attached to the clamping cylinder and allows the die to move back and forth. This piece is also called a moving platen. In old devices, hydraulic systems were used to provide compressive strength. Nowadays, electric servo mechanism is used to provide compression force to many machines. The reason for preferring these machines is that superior control and repeatability capabilities are better than hydraulic devices.

A hopper to hold the plastic material injection molding machine of the mechanism, injection screw and barrel consists of. The barrel has a heating mechanism like bands of the heater. The purpose of these tapes is to melt the material and bring the material to the desired temperature for injection. Screw sizes for plastic optical molding are about 1 meter, which is suitable for machine and die sizes. The amount of material that this screw can inject in one shot is called the shot size. Injection screws are usually made from cast iron used in molds. This is why it can interact with the material to be molded or with the weak fill of the mold. When the mold material is injected, the injection mechanism seals the mold by injection. This keeps the pressure on the injected material [37].

4.2.2 Injection Molding

The most important part used in the production of high-quality plastic optical parts is mold. Structures that consist of a series of plates containing various parts are called molds. The molds consist of two halves, one of which is attached to the stationary fixed while the other is attached to the moving plate. This plate is called a fixed and moving halves or cavity and core. Each mold halves has a thermal insulator plate. These plates are also used to connect halves to the mold [38]. An example mold is shown in Figure 4.2. The parts of the mold are as follows:

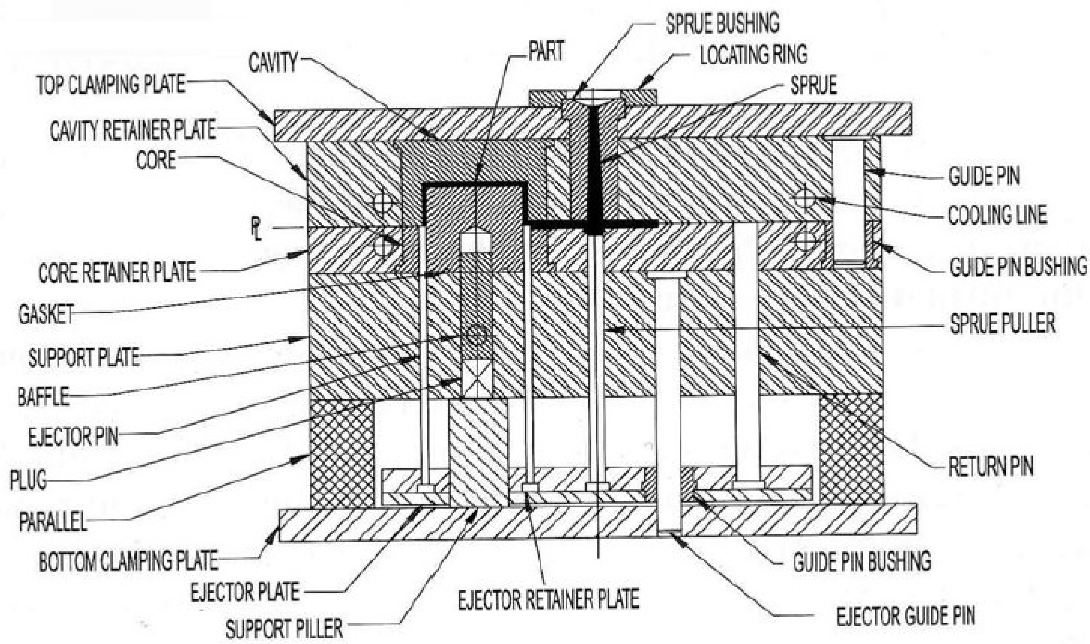

Figure 4.2 An example steel mold for plastic injection machine by courtesy of [39].

- **Core Insert :** It's the male part of the mold. This part forms the inner surface of the part to be produced.
- **Cavity Insert :** It is the female part of the mold and there is a gap in this part. This gap forms the outer part of the product.
- **Core Plate :** It's the part of the male part of the mold. The part entering the circuit in the opening and closing movement of the mold is called the core plate.
- **Cavity Plate :** It is the part that holds the female part of the mold. This plate has a sprue bush that provides molten plastic access.
- **Back Plate :** These plates are placed underneath the core plate and above the gap plate. These plates do not allow the core and gap insert to come out of the plates.
- **Parallel Block :** It provides sufficient clearance for movement of the ejector plate and can be found from the simple equation:
  Parallel Block Height = Thickness of Injection Group + Rest Button Head Thickness + Required Movement
- **Ejector Plate :** This plate is placed in the base of the ejector retainer and clamped. This does not allow the ejector pins and return pins to exit from the ejector retainer. This plate has the ability to hold the ejector rod. At the same time, this plate transmits the spraying force through the ejector rod.
- **Ejector Retainer :** This part holds the ejector pins and return pins.
- **Ejector Pins :** The ejector pins are fixed to the core plate from the ejector retainer. These pins are used to remove the product from the core plate.
- **Return Pins :** When the mold is closed, return the ejector plate.
- **Rest Button :** The rest buttons are used to reduce the effective seating area of the ejector plate.
- **Ejector Rod :** It facilitates the operation of the ejection system.
- **Sprue Bush :** The mold brings the material to the separation line.
- **Sprue Puller :** When the mold is opened, it draws the sprue together.
- **Register Ring :** The register ring aligns to the center of the machine.

- **Guide Pillers :** It is fixed to the cavity part of the mold.Guide pillers is used to center the movable and stationary halves of the mold.
- **Guide Bushes :** It is fixed to the core part of the mold.Guide bushes is used to center the movable and stationary halves of the mold.

The cavity, core and exact shape of the lens mold designed for this study are shown in Figures 4.3, 4.4 and 4.5, respectively.

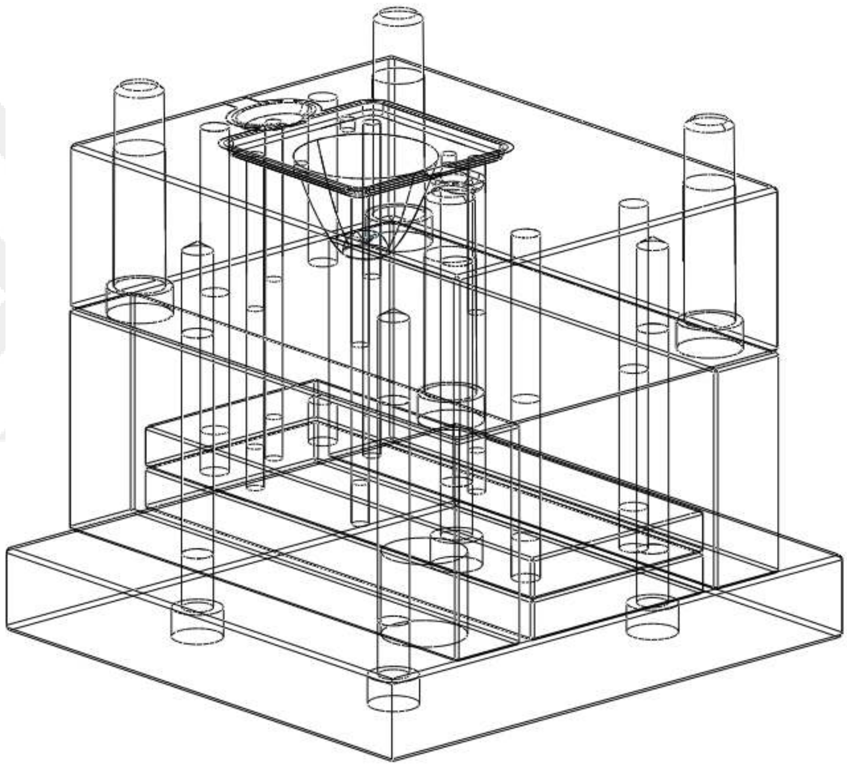

Figure 4.3 The cavity parts of lens mold.

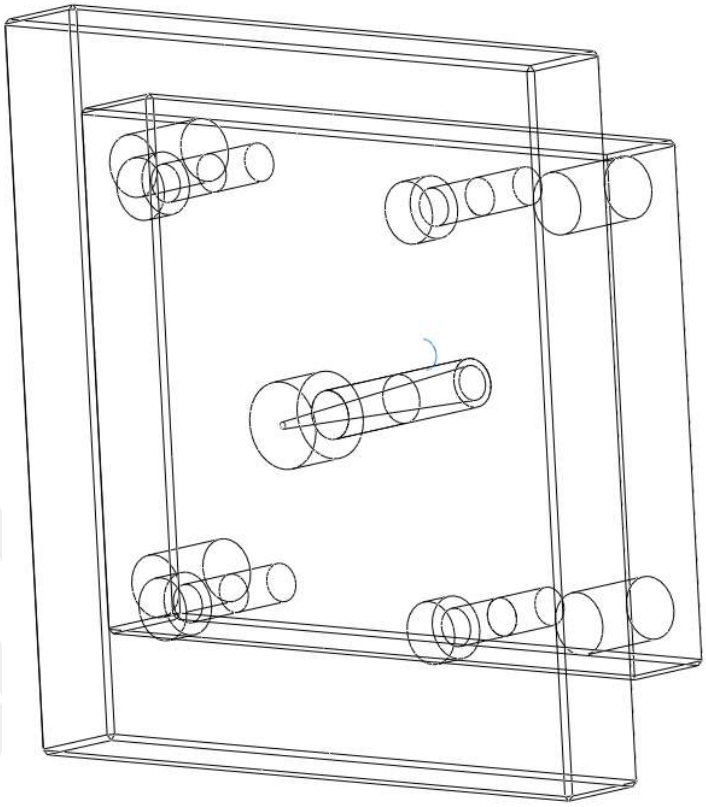

Figure 4.4 The core parts of lens mold.

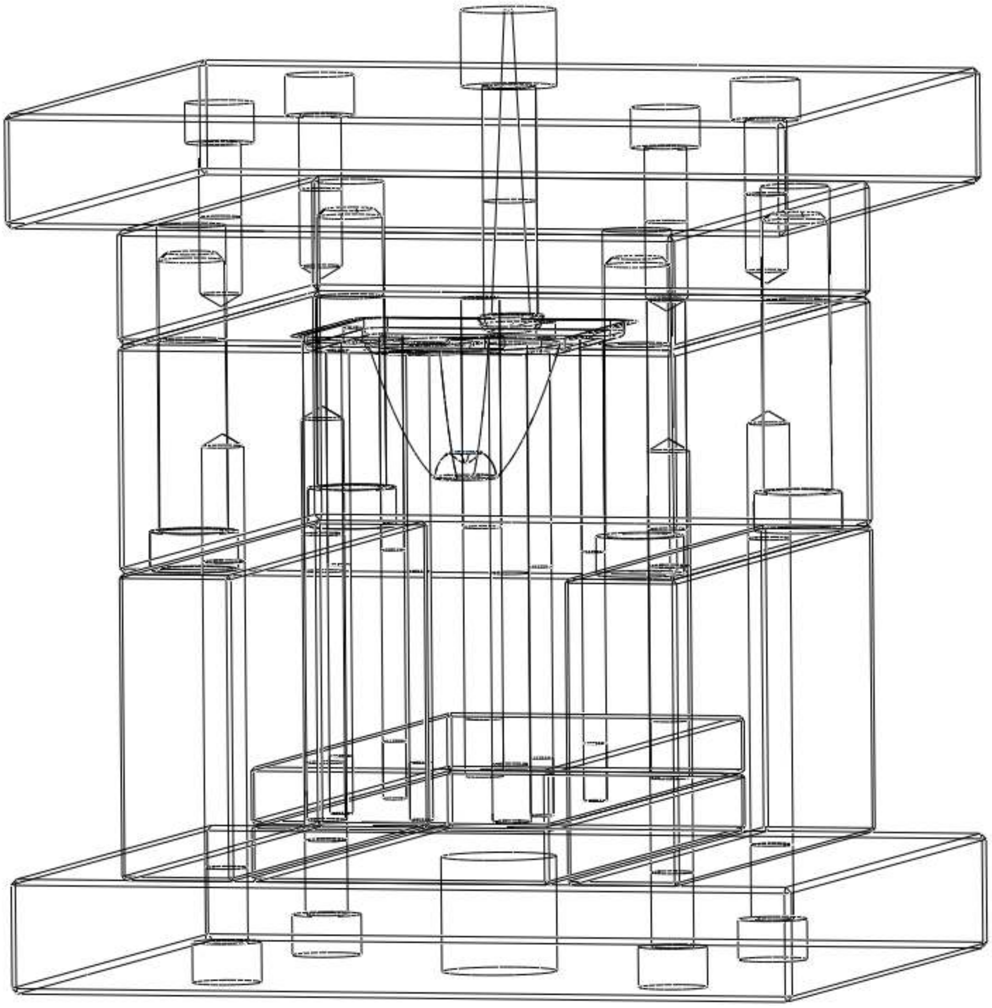

Figure 4.5 The full lens mold used in the production in this study.

Production is started by connecting the manufactured mold to the injection device. The first lens produced is shown in Figure 4.6 is imperfect. The reason is that the temperature setting of the plastic injection device and the amount of material are not adjusted correctly.

Figure 4.6 First produced lens having a lot of troubles.

In later experiments, the machine settings have been changed properly and the production steps continued. The results of updates in the production are shown in Figure 4.7, from the worst product, Figure 4.7a, to the best product, which is used in the single lens optical measurements, Figure 4.7d.

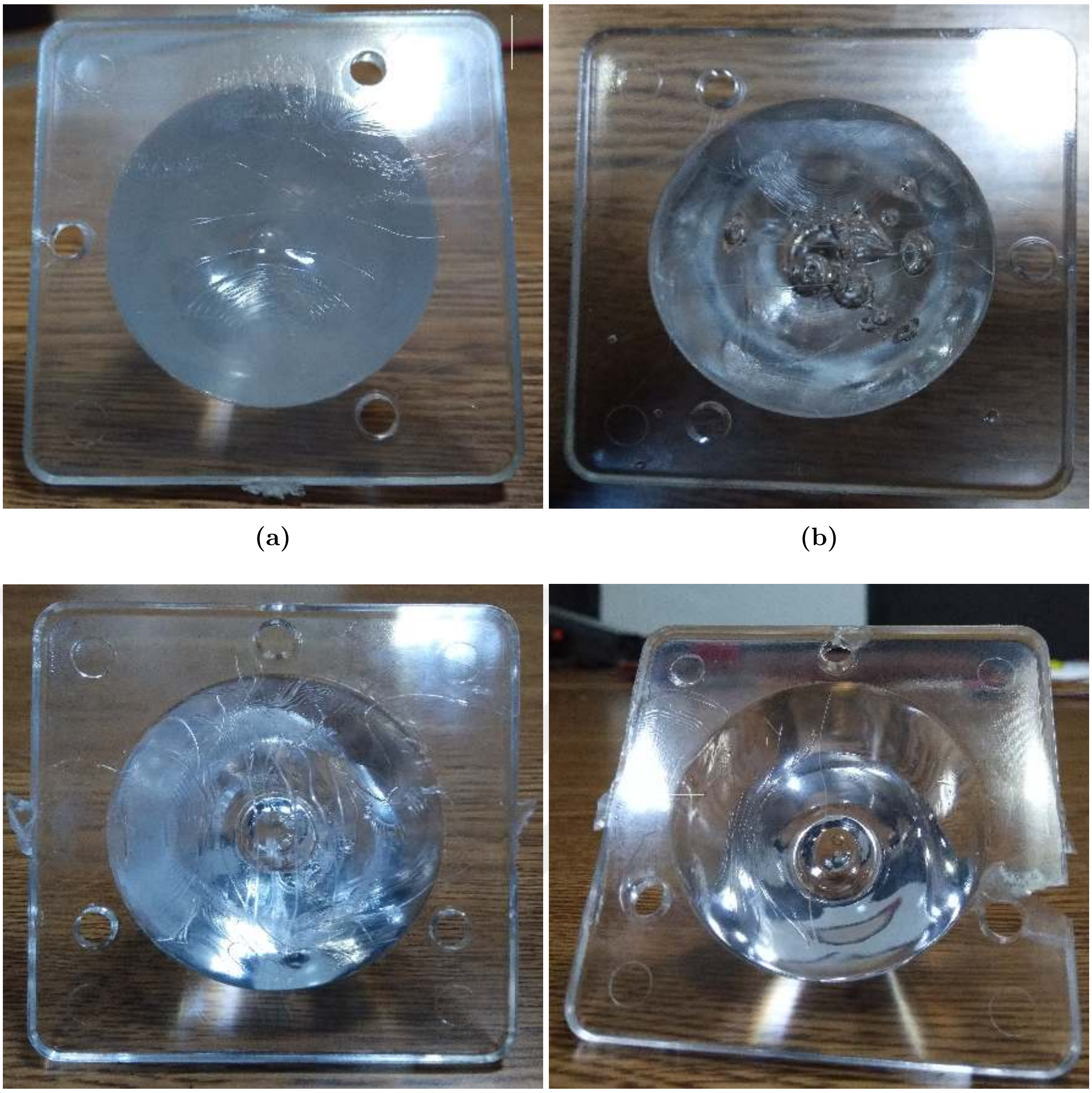

(a) (b) (c) (d)

Figure 4.7 The lens photos taken from the production steps. (a) The lens is not transparent since the material is not melted at the proper temperature. (b) There are same air bubbles inside the lens since the material contains moisture which is not fully dried. (c) There are scratches on the lens. This is due to the fact that the plastic injection machine is not ironed properly. (d) This lens which is our best has fewer manufacturing defects than the other lenses and used in the optical measurements.

4.3 Optical Measurements

In order to test the optical performance the system consisting of single LED (OSRAM SFH4715 or OSRAM LUW CVBP) and single lens, two measurements are taken into account for IR and visible regions.

In the IR region at around 850 nm, optical powers are measured by using Newport Powermeter 843-R [40] whose active area is about 1 cm^2. Measurements are made at various distances. The results and comparison with simulations are shown in Table 4.1 Figure 4.10 for short distances (where the effect of lens are very clear) and 4.11 for long distances. The values for the perfect geometry in the simulation are around three times better than measurements. This may be due to misalignment of LED and lens. To model misalignment of LED-lens system, the tilt angle of the lens about Y-axis is changed for 1, 2 and 3 degrees. It is clear that the real data measurements and predictions from the simulations are in good agreement for the tilt angle of 3 degrees. This is a strong indication that the LED and lens alignment are very significant.

Figure 4.8 shows the photo of the corridor before (a) and after (b) IR illumination using single LED and lens. The setup of optical devices are shown in Figure 4.9 as well.

(a) (b)

Figure 4.8 (a) No infrared illumination in a 50-meter-long corridor. (b) Same corridor after IR illumination using a single lens.

(a) (b)

Figure 4.9 (a) LED + Lens system and powermeter before measuring the IR intensities. (b) Mustafa KILIN the Research Assistant is adjusting the powermeter.

Table 4.1 Optical measurement results as a function of detector distance for IR LED. The detector diameter of the powermeter is 10.3 mm.

Distance (m)	Power(mW) in simulation	Power (mW) in measurement
1	2.1866	1.4450
5	1.1291	0.0692
10	0.2798	0.0178
15	0.1166	0.0082
20	0.0591	0.0051
25	0.0408	0.0036
30	0.0277	0.0027
35	0.0248	0.0020
40	0.0201	0.0016
45	0.0153	0.0014

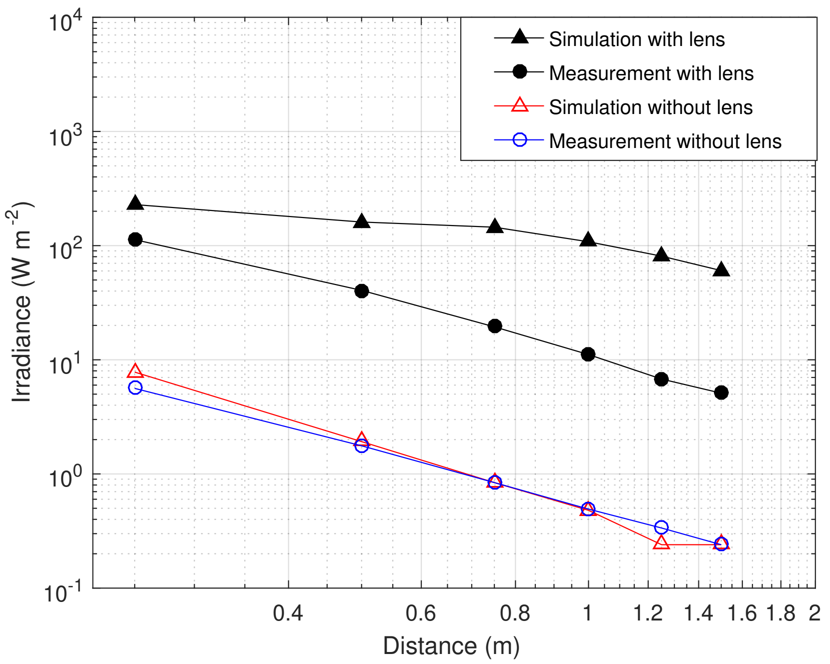

Figure 4.10 Optical measurements at short ranges for the IR LED-lens system with and without lens.

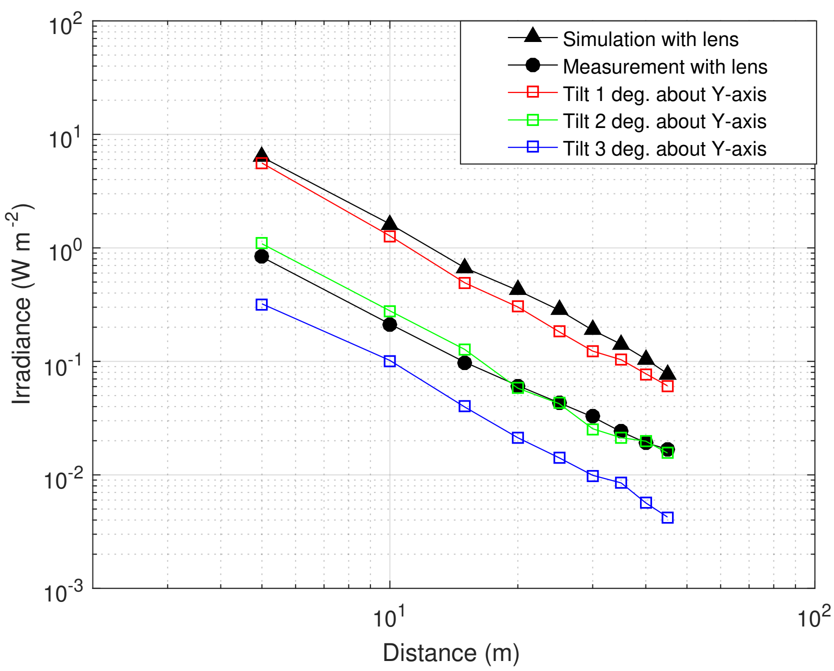

Figure 4.11 Optical measurements at long ranges for the IR LED-lens system. The misalignment of the system is modeled by changing the tilt angle of the lens about Y-axis at 1, 2 and 3 degrees.

The same study is repeated for the visible range by replacing IR LED with white one at 4500 K. Illuminations at various distances are measured by using Testo 435 Luxmeter [41] whose diameter is 30 mm. Results are shown in Figure 4.12, 4.13 and 4.14, and in Table 4.2. Again, these are due to the misalignment of LED-lens system and the production defects in the lens (scratches, bubbles, etc.).

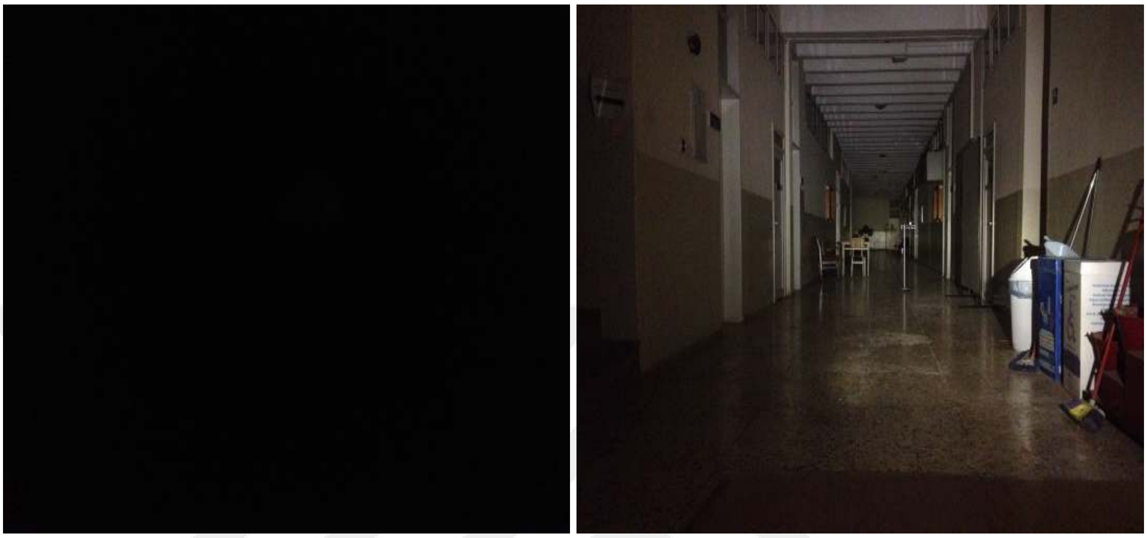

(a) (b)

Figure 4.12 (a) No illumination in a 50-meter-long corridor. (b) Same corridor after illumination using a single lens.

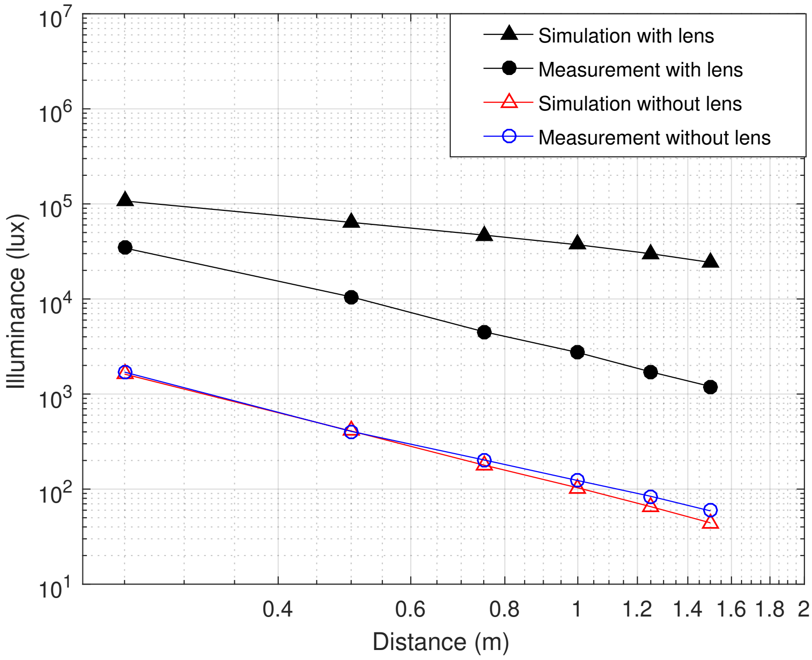

Figure 4.13 Optical measurements at short ranges for the Visible LED-lens system with and without lens.

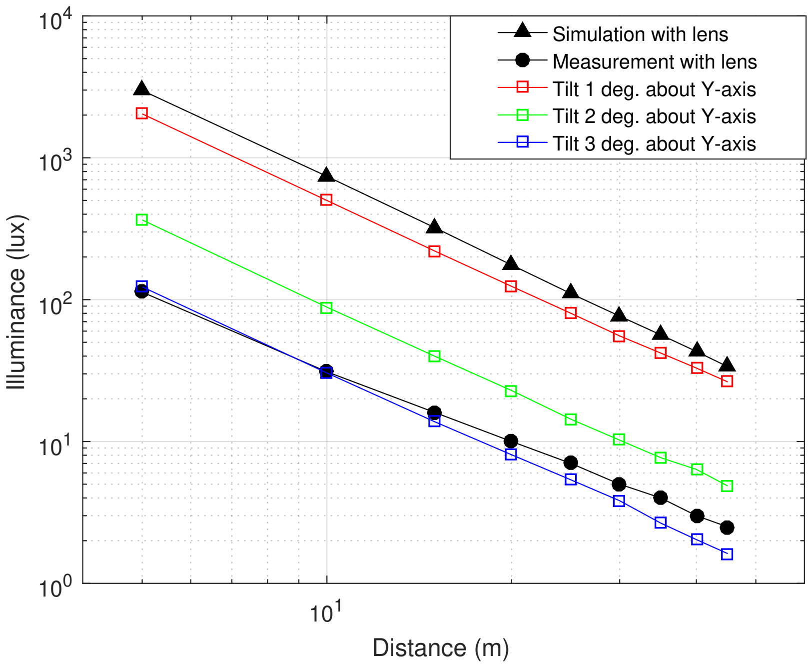

Figure 4.14 Optical measurements at long ranges for the Visible LED-lens system. The misalignment of the system is modeled by changing the tilt angle of the lens about Y-axis at 1, 2 and 3 degrees.

Table 4.2 Optical measurement results in lux as a function of detector distance for Visible LED.

Distance (m)	Illuminance (lux) in simulation	Illuminance (lux) in measurement
1	37184	2728
5	2981	113
10	739	31
15	321	16
20	175	10
25	110	7
30	77	5
35	57	4
40	43	3
45	34	2

CHAPTER 5

SUMMARY AND CONCLUSION

In this master thesis, a prototype of a free form lens which can be used for long range illumination is designed and manufactured. Various optical polymers (PMMA, PC and PS) are concerned as lens material. IR and visible LEDs are selected as light source since their light efficiency are very high. Optical performance of the LED and lens system is tested on a detector placed at short and long ranges.

The design of the lens is started by considering light rays emitting from point-like source to all directions. One needs a special lens to parallel all these rays for the long range illumination. So a free form geometry depending on the index of the refraction and LED-lens configuration is determined by using Fermat's principle in 2D. Then, a 3D bulk of the lens is obtained in SolidWorks program. LED and 3D lens are imported in ZEMAX 2009 in order to obtain the optical performance in the computer.

In the production of the lens PMMA is selected since it exhibits the best performance in terms of optical transmittance and optical power on the detector using simulation results performed using ZEMAX. The production is fulfilled by well known technique called the molding and plastic injection method in Gaziantep Industry. An example projector for commercial purpose containing four lenses are shown in Figure 5.1. We face with some production errors due to the large bulk of the lens such as intrinsic bubbles, scratches, collapsing of the polymer. Even though these defects and LED-lens miss alignments in the mounting, the optical measurements are in good agreement with the simulation.

Author suggests that such a lens and LED system can be used in the wireless optical communication, in illumination of football stadiums and car parks, and in military purpose for the security of border.

Figure 5.1 Final IR projector for commercial purpose.

REFERENCES

[1] Zhou, P., et al. (2004). Fly Eye lens array used in LCD projection display with high light efficiency. *Acta Polonica Sinica*. **24**, 587-591.

[2] Shen, M., et al. (2006). Method of reflective fly eye lens design for LED illuminating system. *Acta Polonica Sinica*.**35**, 93-95.

[3] Moisev, A.M., et al. (2008). Design of high efficient freeform lens for illumination of elongated rectangular region. *Optical Society of America*.**19**,17.

[4] Jiang, J., To, S., Lee, W.B., Cheung, B. (2010). Optical design of a freeform TIR lens for LED streetlight. *Urban&Fischer*.**121**, 1761-1765.

[5] Bortz, J., Shatz,N., Pitou, D. (2000). Optimal design of nonimaging projection lens for use with a LED source and a rectangular target. *SPIE*.**4092**, 130-138.

[6] Jacobson, B.A., Gengelbach, R.D. (2002).Lens for uniform LED illumination: an example of automated optimization using Monte Carlo ray tracing of an LED source. *SPIE*.**4446**, 130-138.

[7] Ding, Y. et al. (2008). Freeform LED lens for uniform illumination. *Optical society of America*. **16**, 17-30.

[8] Ramirez-Iniguez, R., Idrus, SM & Sun, Z. (2008). Optical Wireless Communications: IR for Wireless Connectivity.Auerbach Publications.

[9] Özyeğin Üniversitesi, OKATEM, `http://okatem.ozyegin.edu.tr`, 05.08.2017.

[10] Slaiman, I.,Hamid, N.H.B., Boon, T.T. (2014).Optical Wireless Communications Through Visible Light Leds: An Overview.*IJERT*.**3**, 1152-6.

[11] Wolfe, William L.1998. Introduction to Radiometry.TT29. SPIE.

[12] ILT. International Light Technologies.Light Measurement Handbook.1997.Available at : `https://www.intl-lighttech.com/form/ilt-light-measurement-handbook`, 12.10.2017.

[13] William Ross McCluney.1994.Introduction to Radiometry and Photometry.0-89006-678-7.Artech House.

[14] ZUMTOBEL.The Lighting Handbook.2004.Available at : `http://www.zumtobel.com/PDB/teaser/EN/lichthandbuch.pdf`, 12.10.2017.

[15] MATLAB Release. 2016a. The MathWorks. Inc. Natick, Massachusetts, United States.

[16] SolidWorks. Dassault Systmes SolidWorks Corporation. Wyman Street Waltham, United States.

[17] ZEMAX LLC. Kirkland, Washington, United States. https://www.zemax.com/opticstudio, 09.01.2017.

[18] Sultanova, N, et al, (2009) Dispersion Properties of Optical Polymers, ACTA PHYSICA POLONICA A, 116-4, Pages 585-587.

[19] Marvin J. Weber. 2003. Handbook of Optical Materials. CRC.

[20] Evonik Industries - Specialty Chemicals.PMMA 8N PLEXIGLASS Datasheet.
http://www.plexiglas.net/product/plexiglas/en/products/technical-data/pages/default.aspx, 12.09.2017.

[21] Properties of Polycarbonate
http://www.usglobalimages.stratasys.com/Main/Files/MaterialPropertyStudies/MMS_FDM_PCPropertiesReport.pdf?v=635784503840324549, 12.09.2017.

[22] Properties of Polycarbonate and Datasheet
www.kolumanplastik.com/pdf/pc-1150r-(easy-mold-release).pdf, 12.09.2017.

[23] Demir, M., Parlak, O., (2013). Anomalous transmittance of polystyrene-ceria nanocomposites at high particle loadingst. *J. Mater. Chem. C.***1**, 290.

[24] Properties of Polystyrene and Datasheet, web.rtcompany.com/info/data/permastat/PermaStat400.htm, 12.09.2017.

[25] Kasap S., Capper P. 2007. Springer Handbook of Electronic and Photonic Materials. Springer.

[26] OSRAM. SFH4715 Infrared Led Datasheet. http://www.osram-os.com/Graphics/XPic7/00204173_0.pdf, 12.01.2017.

[27] OSRAM. SFH4715 Infrared Led Datasheet. http://www.osram-os.com/Graphics/XPic7/00204173_0.pdf, 12.01.2017.

[28] Pedrotti F.L., Pedrotti L.M., Pedrotti L.S. 2006. Introduction to Optics. Pearson.

[29] Fischer, Robert E., Tadic-Galeb, Biljana, Yoder, Paul R. (2008). Optical System Design (2nd ed.). New York: McGraw-Hill.

[30] Smith, Warren J. (2007). Modern Optical Engineering (4th ed.). McGraw-Hill.

[31] MathWorks, User's Guide(R2016a). https://www.mathworks.com/help/pdf_doc/matlab/index.html, 20.03.2017.

[32] SolidWorks, User's Guide(2013). http://help.solidworks.com/2013/english/solidworks/install_guide/HID_STATE_MANUAL_DOWNLOAD.htm, 12.04.2017.

[33] Geary, Joseph M. (2002). Introduction to Lens Design: With Practical Zemax Examples. Willmann-Bell.

[34] ZEMAX Sequantial Mode http://customers.zemax.com/os/resources/learn/knowledgebase/exploring-sequential-mode-in-zemax, 20.02.2017.

[35] ZEMAX Non-Sequantial Mode http://customers.zemax.com/os/resources/learn/knowledgebase/exploring-non-sequential-mode-in-zemax, 20.02.2017.

[36] Herbert Rees. (2001). Understanding Injection Mold Design. Hanser.

[37] Michael Schaub, Jim Schwiegerling, Eric C. Fest, et al. (2011). Molded Optics Design and Manufacture. CRC Press.

[38] PRO/ENGINEER Mold Design Reference Guide. CADD CENTRE.

[39] Plastic Injection Molding and Injection System https://www.tasarimdanimalata.com/plastik-enjeksiyon-kalipciligi/plastik-enjeksiyon-kalplar-enjeksiyon-sistemi-2-638/ 10.01.2018

[40] Newport,v843-R Economical Handheld Laser Power Meter Datasheet. Newport Corporation, Irvine, California, United States. https://www.newport.com/p/843-R, 01.01.2018.

[41] Testo 435-4 - Multi-function Instrument for VAC & IAQ and Lux probe, for measuring light intensity. Testo Ltd, Alton, Hampshire, United Kingdom. http://www.testolimited.com/testo-435-4-multi-function-instrument-for-vac-iaq, 01.01.2018.

APPENDIX A

SIMULATION RESULTS USING EULUMDAT FILES FOR VISIBLE LED

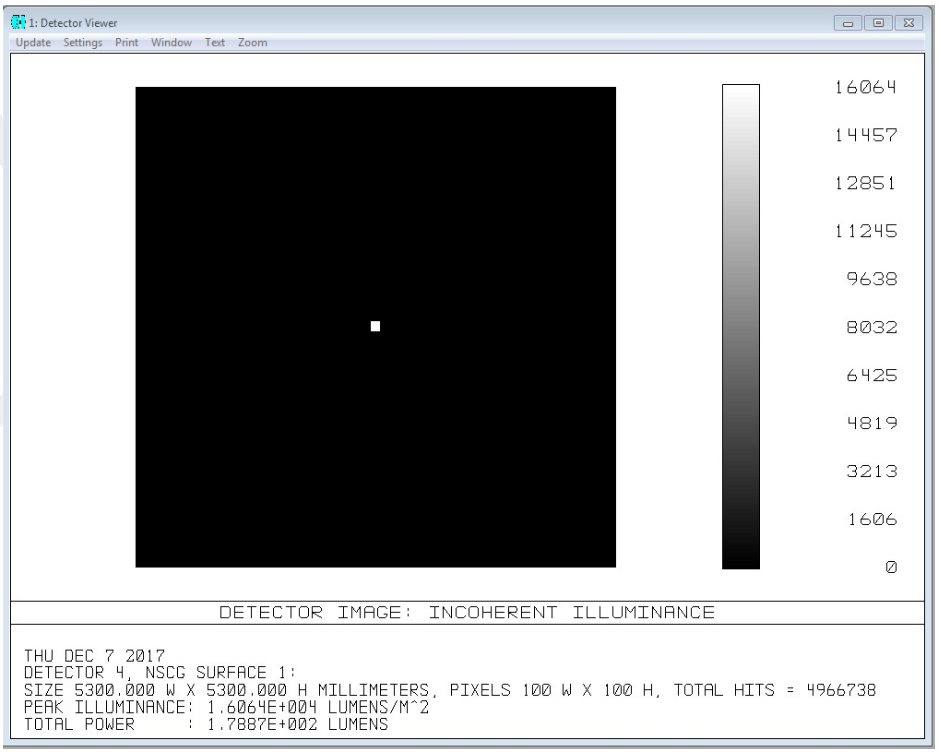

Figure A.1 Spot Diagram at 10 meter for OSRAM LUW CVBP LED and Lens.

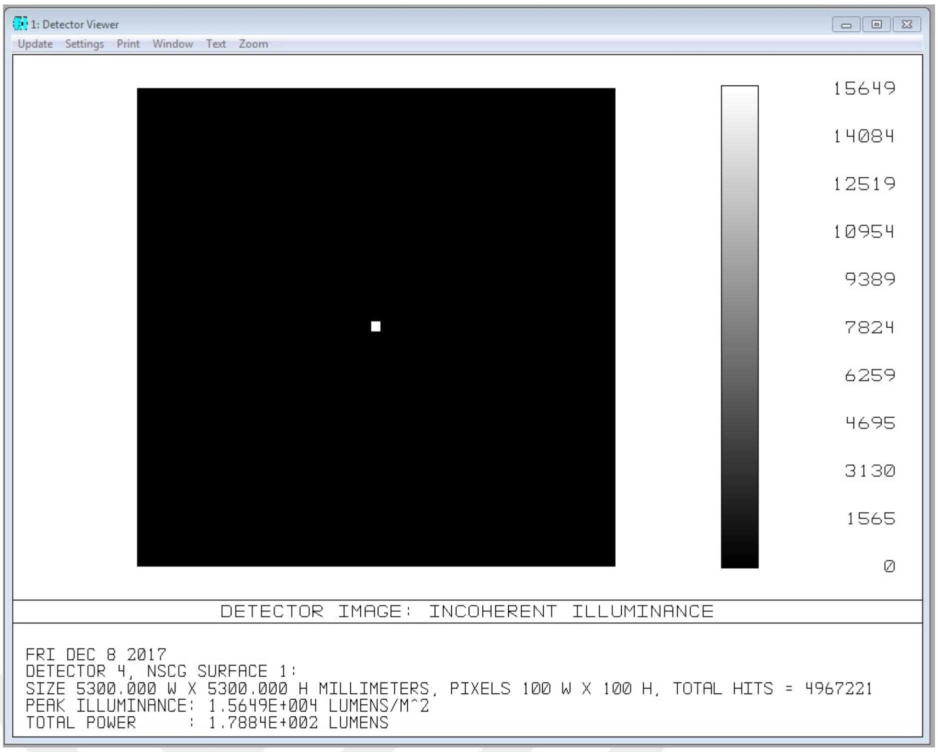

Figure A.2 Spot Diagram at 25 meter for OSRAM LUW CVBP LED and Lens.

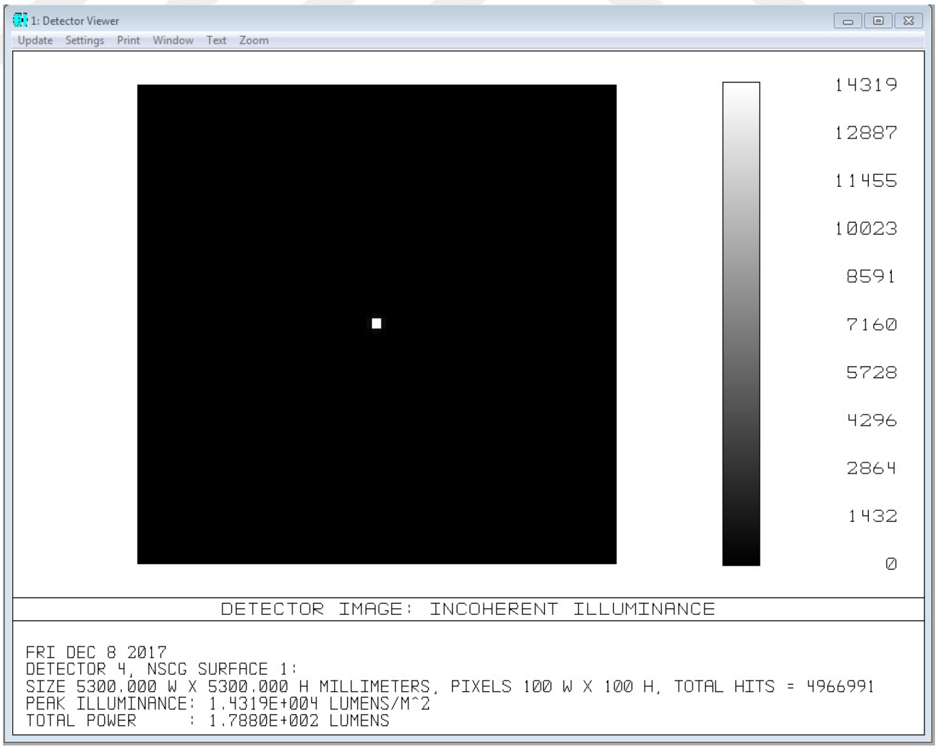

Figure A.3 Spot Diagram at 50 meter for OSRAM LUW CVBP LED and Lens.

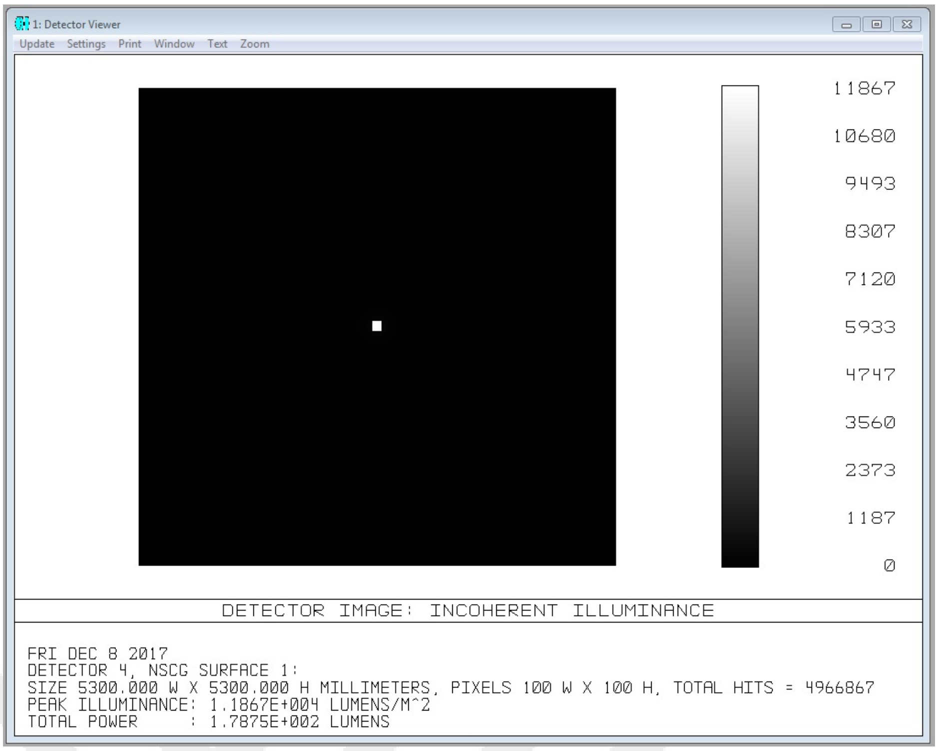

Figure A.4 Spot Diagram at 250 meter for OSRAM LUW CVBP LED and Lens.

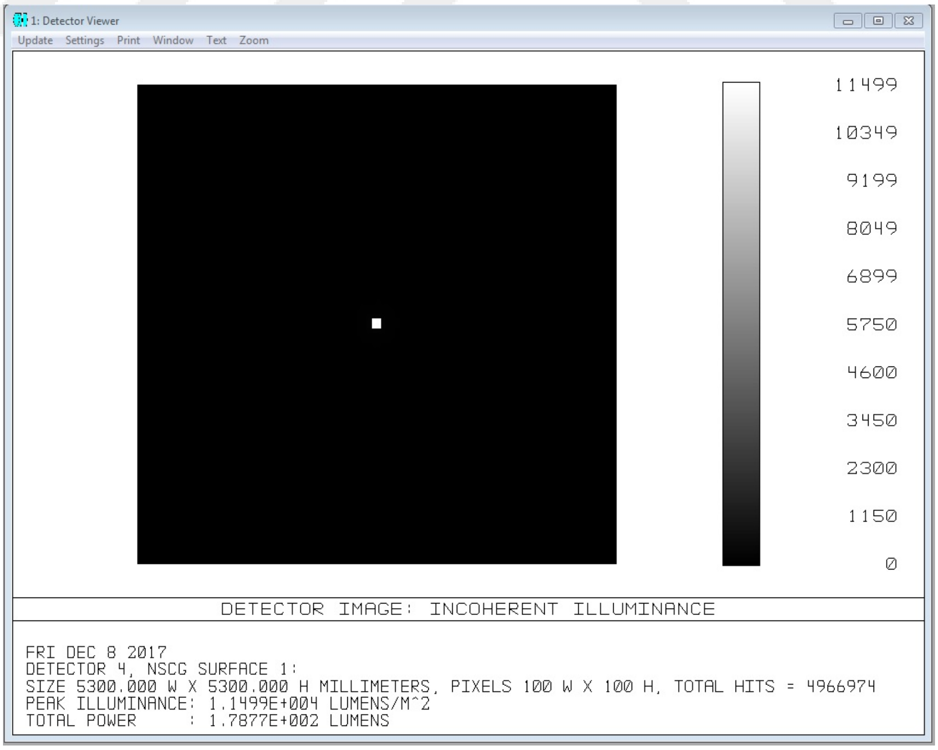

Figure A.5 Spot Diagram at 500 meter for OSRAM LUW CVBP LED and Lens.

APPENDIX B

SIMULATION RESULTS USING EULUMDAT FILES FOR IR LED

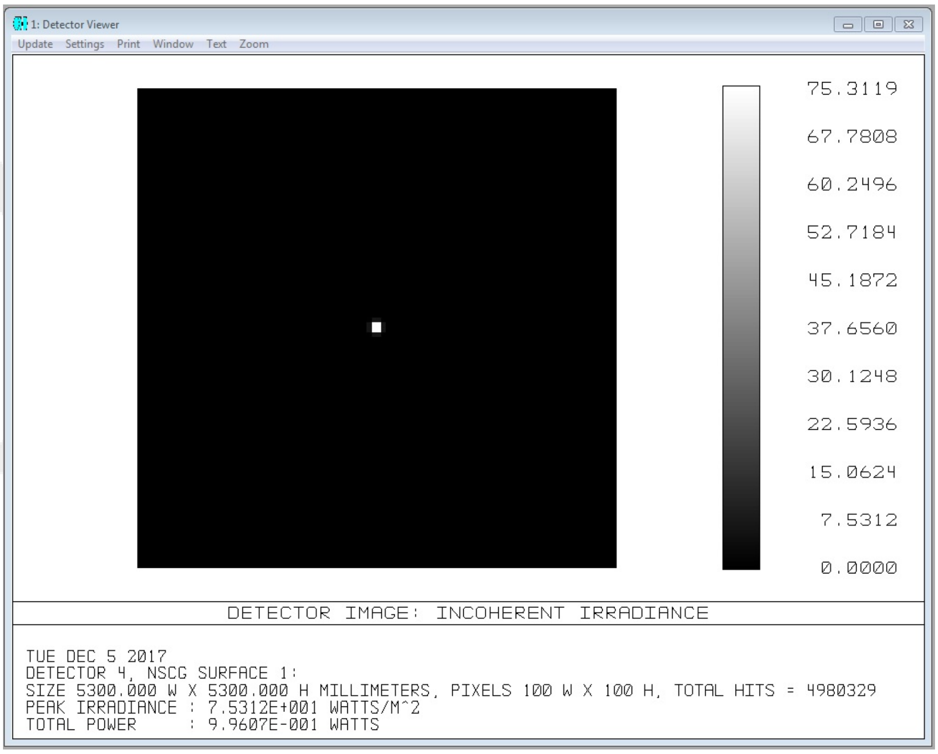

Figure B.1 Spot Diagram at 10 meter for OSRAM SFH4715 LED and Lens.

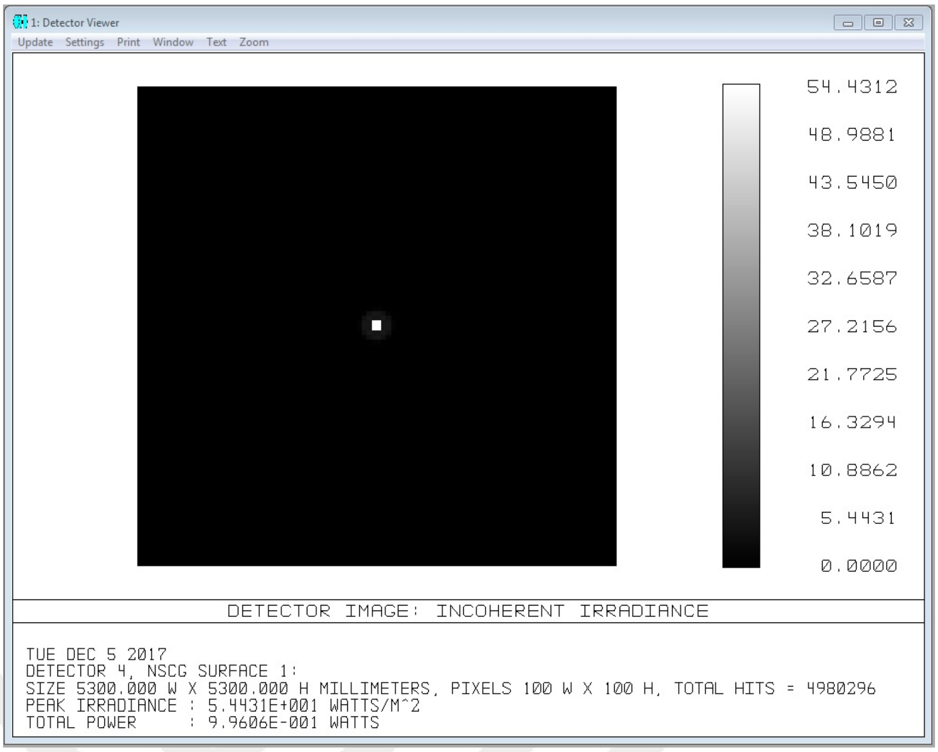

Figure B.2 Spot Diagram at 25 meter for OSRAM SFH4715 LED and Lens.

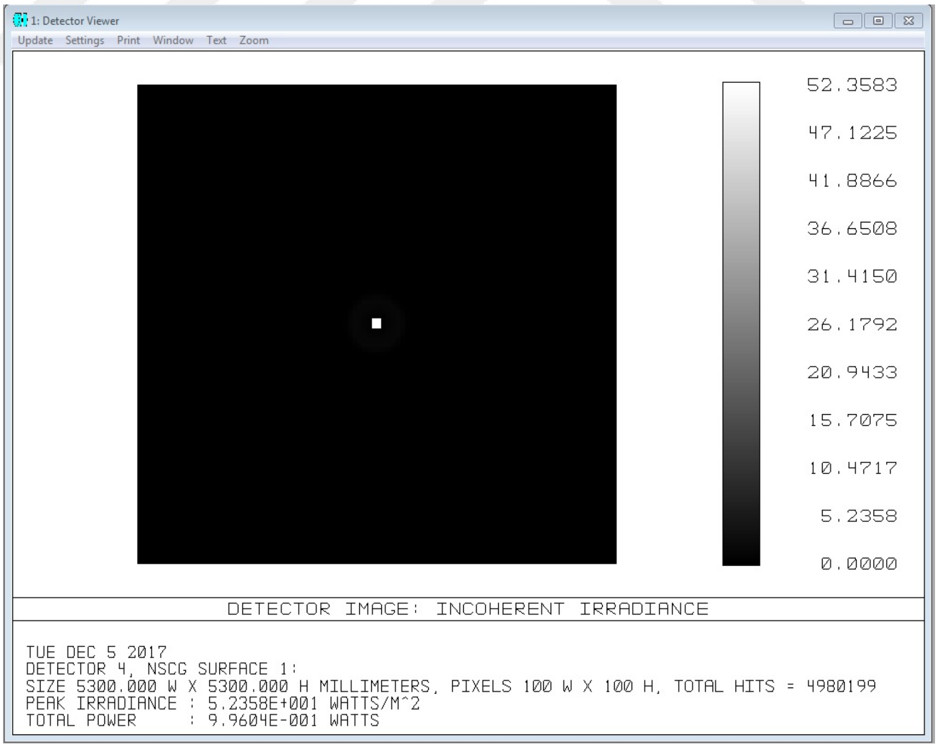

Figure B.3 Spot Diagram at 50 meter for OSRAM SFH4715 LED and Lens.

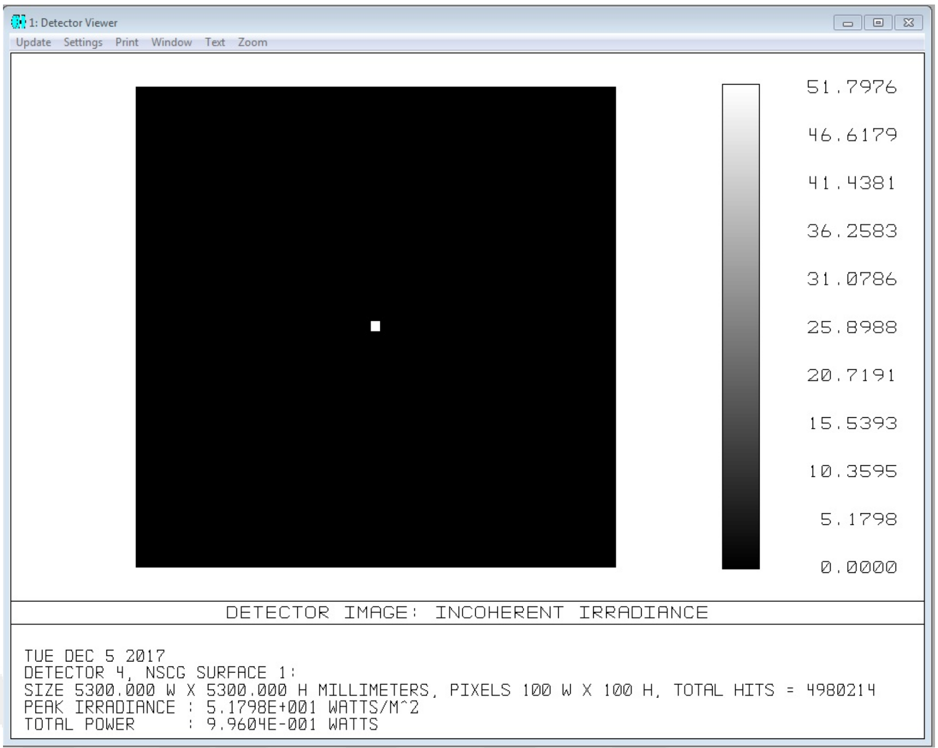

Figure B.4 Spot Diagram at 250 meter for OSRAM SFH4715 LED and Lens.

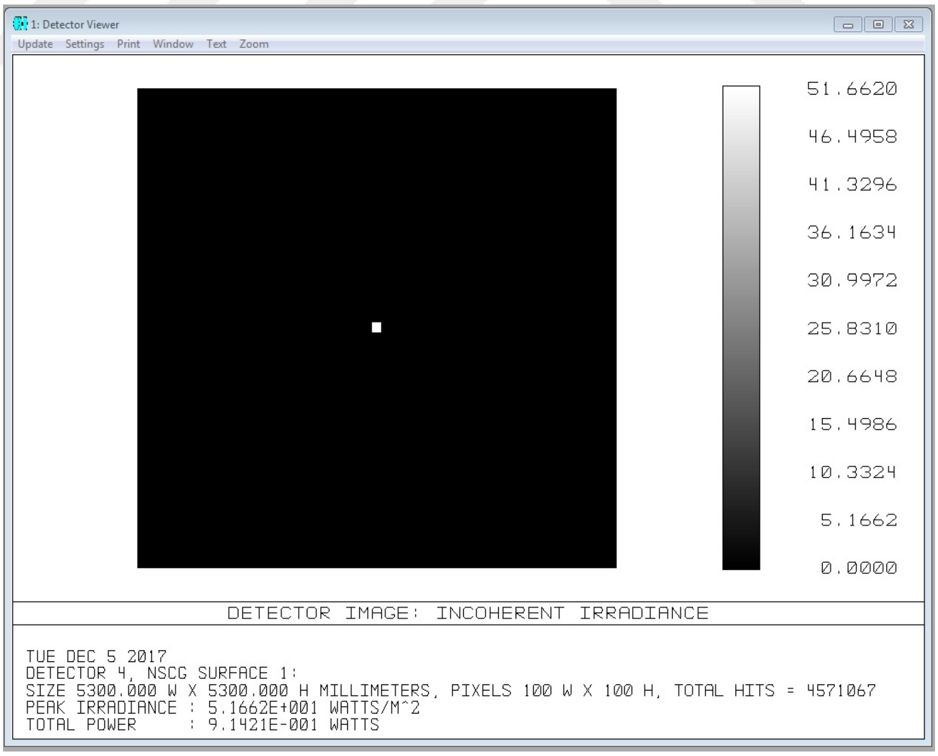

Figure B.5 Spot Diagram at 25 meter for OSRAM SFH4715 LED and Lens.

APPENDIX C

SIMULATION RESULTS FOR DIFFERENT MATERIALS USING VISIBLE LED

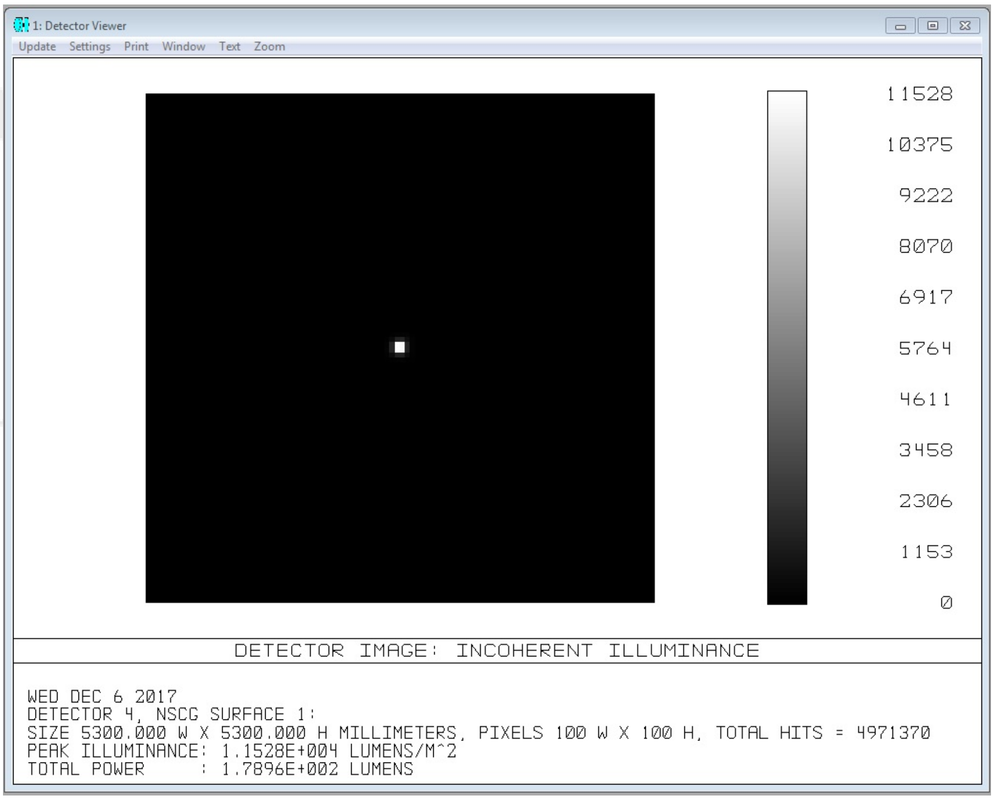

Figure C.1 Simulation result at 1 meter for PMMA lens.

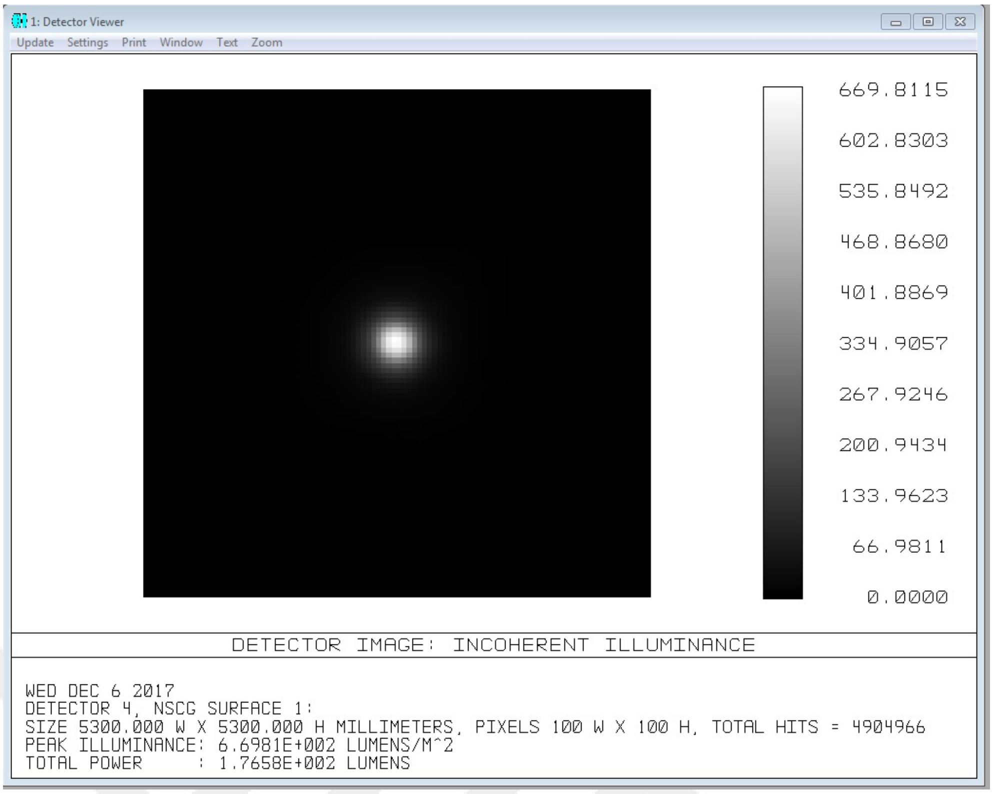

Figure C.2 Simulation result at 10 meter for PMMA lens.

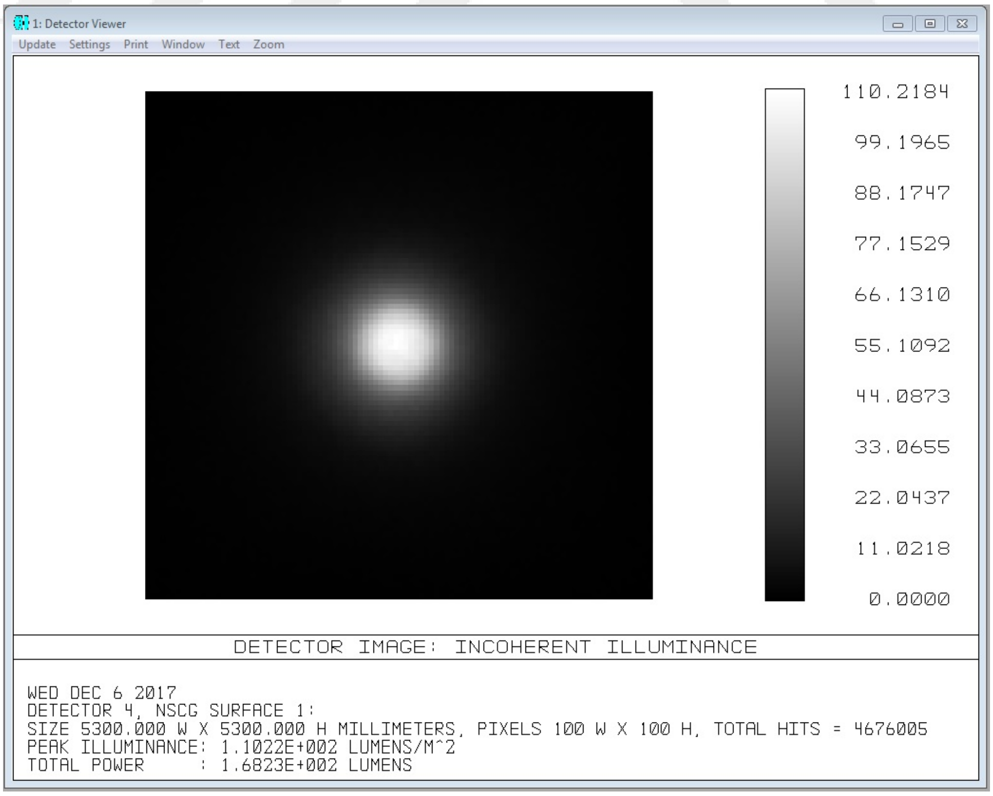

Figure C.3 Simulation result at 25 meter for PMMA lens.

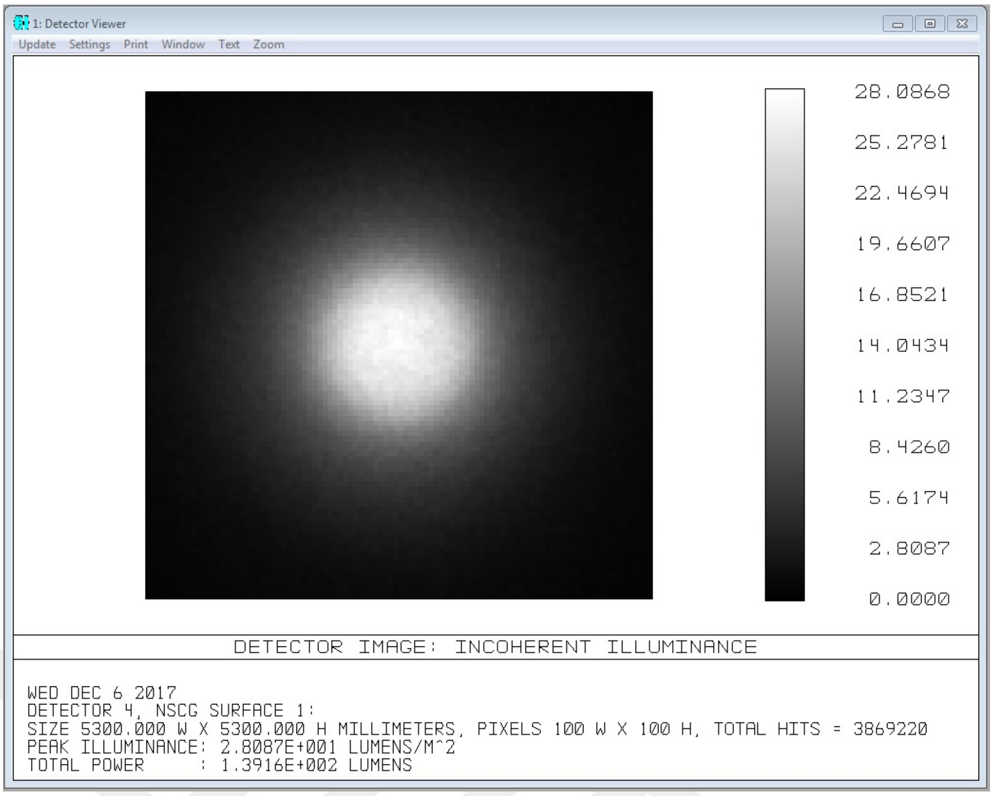

Figure C.4 Simulation result at 50 meter for PMMA lens.

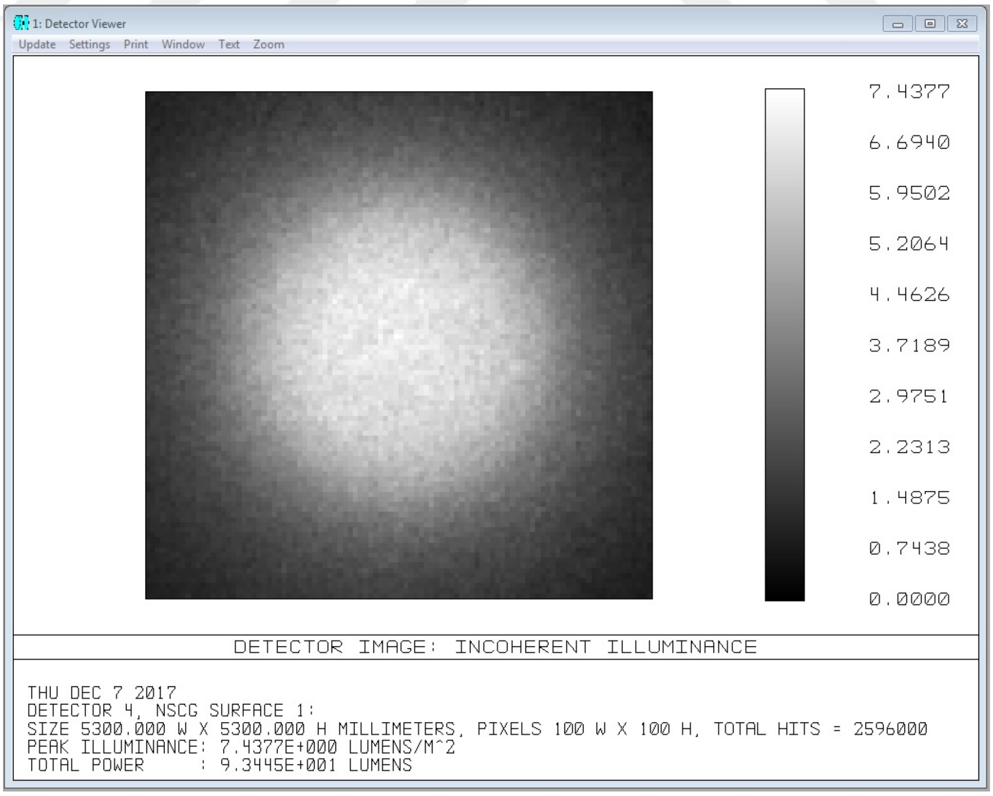

Figure C.5 Simulation result at 100 meter for PMMA lens.

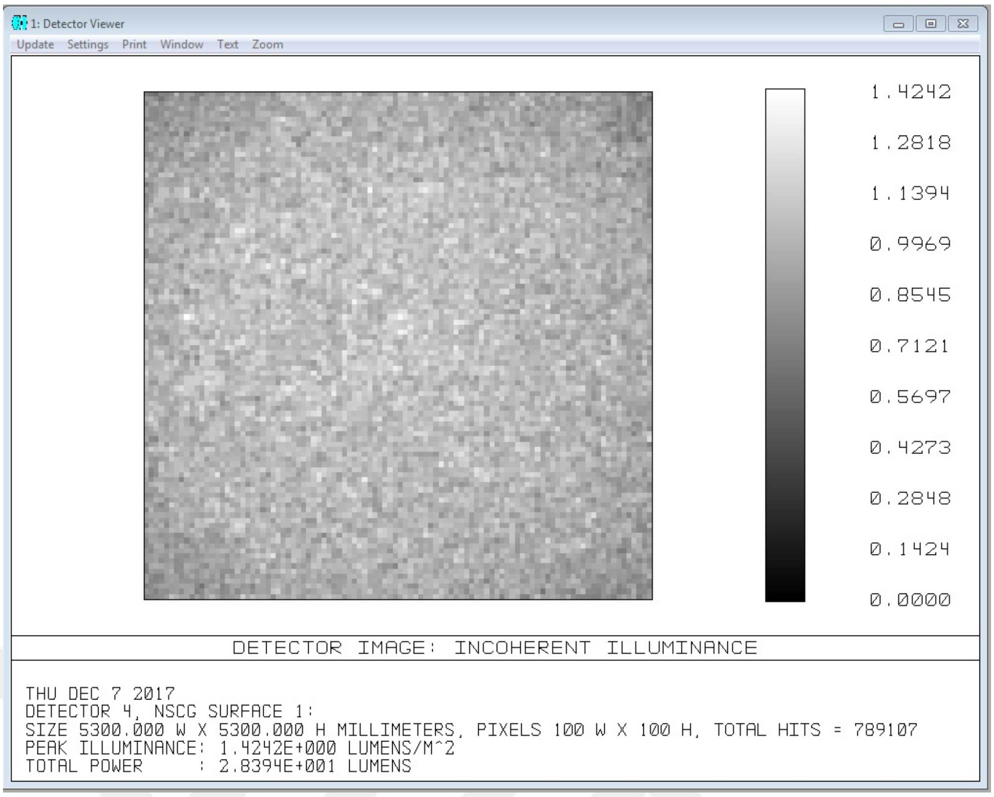

Figure C.6 Simulation result at 250 meter for PMMA lens.

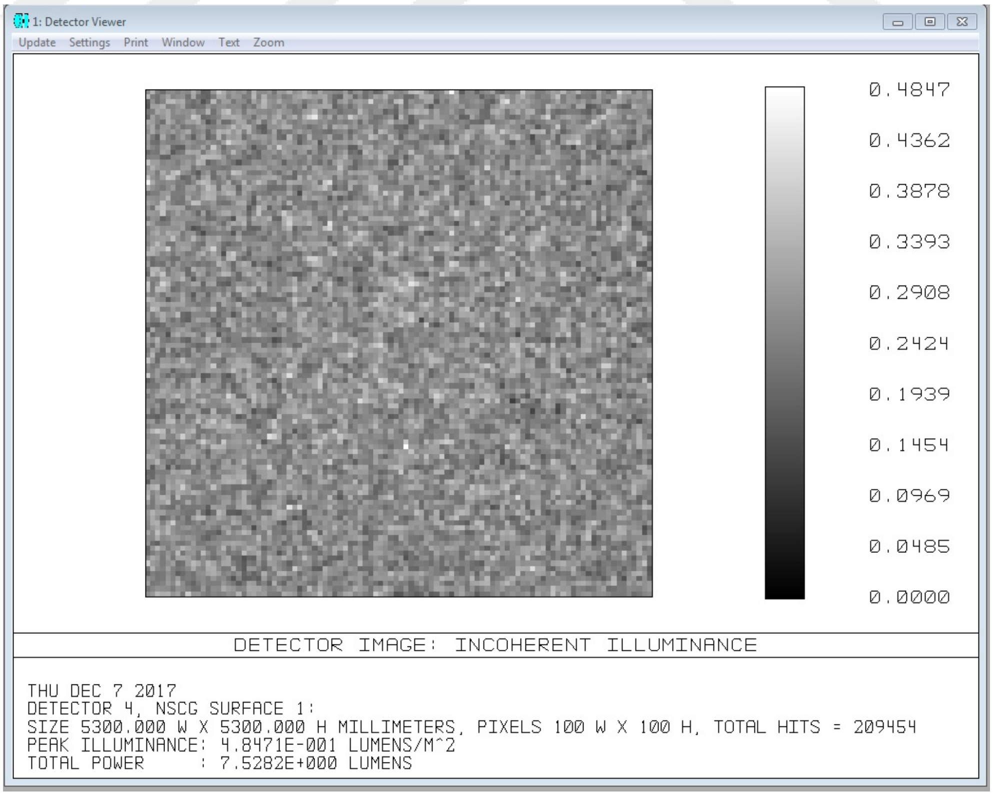

Figure C.7 Simulation result at 500 meter for PMMA lens.

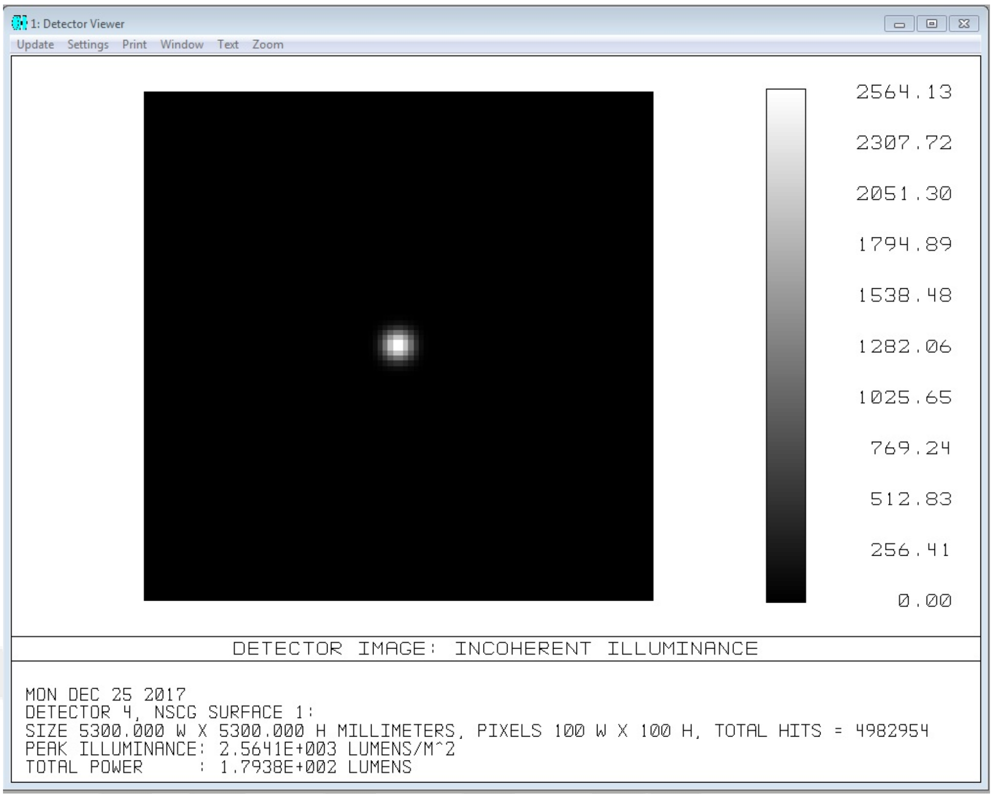

Figure C.8 Simulation result at 1 meter for PC lens.

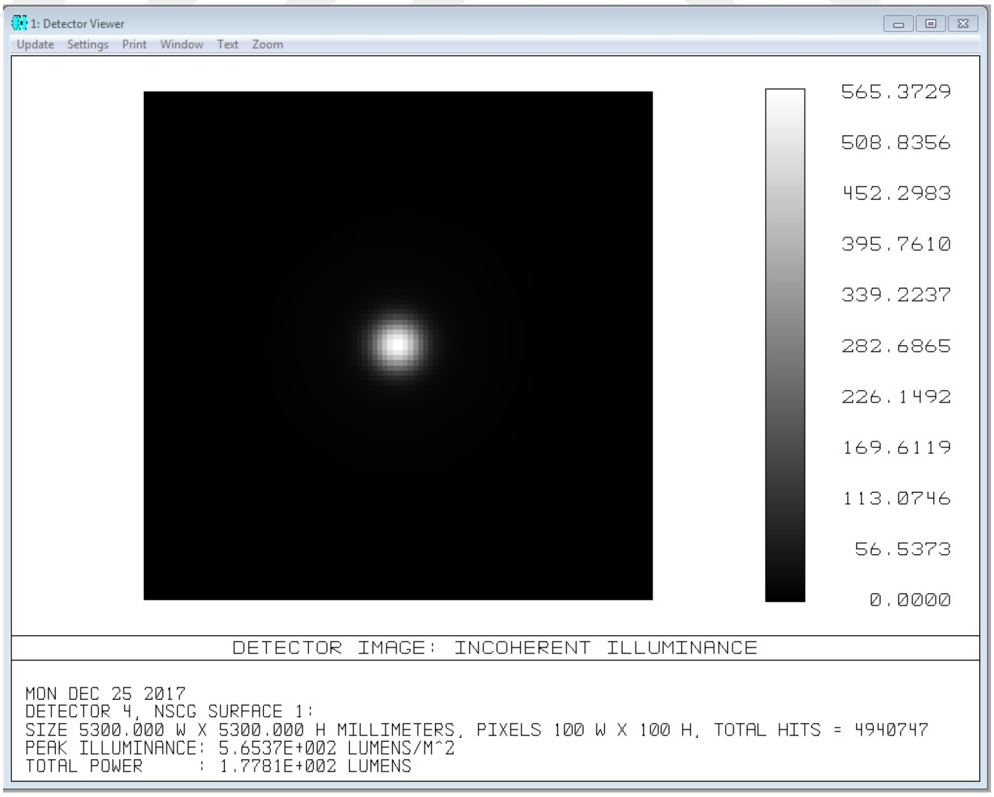

Figure C.9 Simulation result at 10 meter for PC lens.

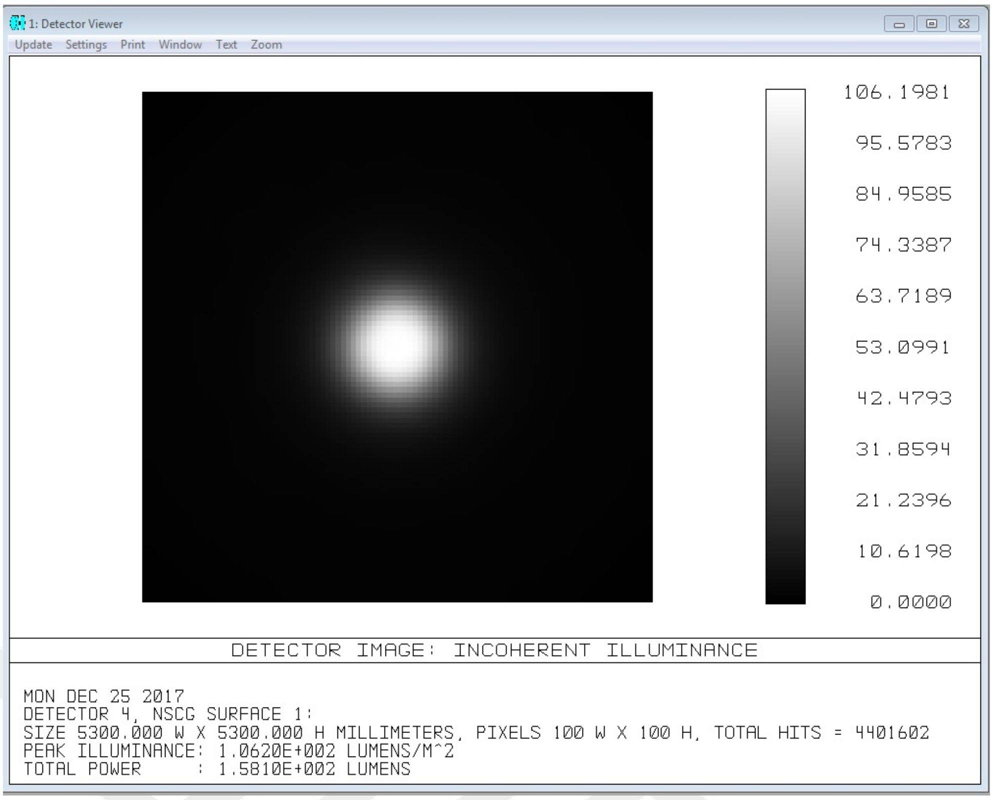

Figure C.10 Simulation result at 25 meter for PC lens.

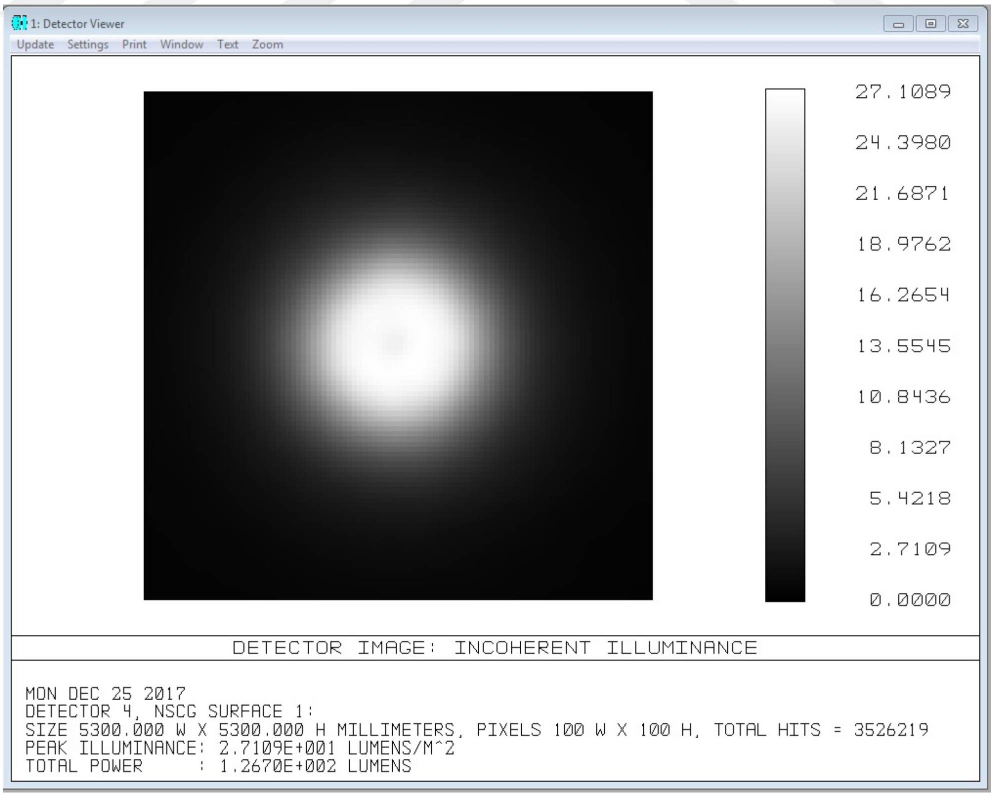

Figure C.11 Simulation result at 50 meter for PC lens.

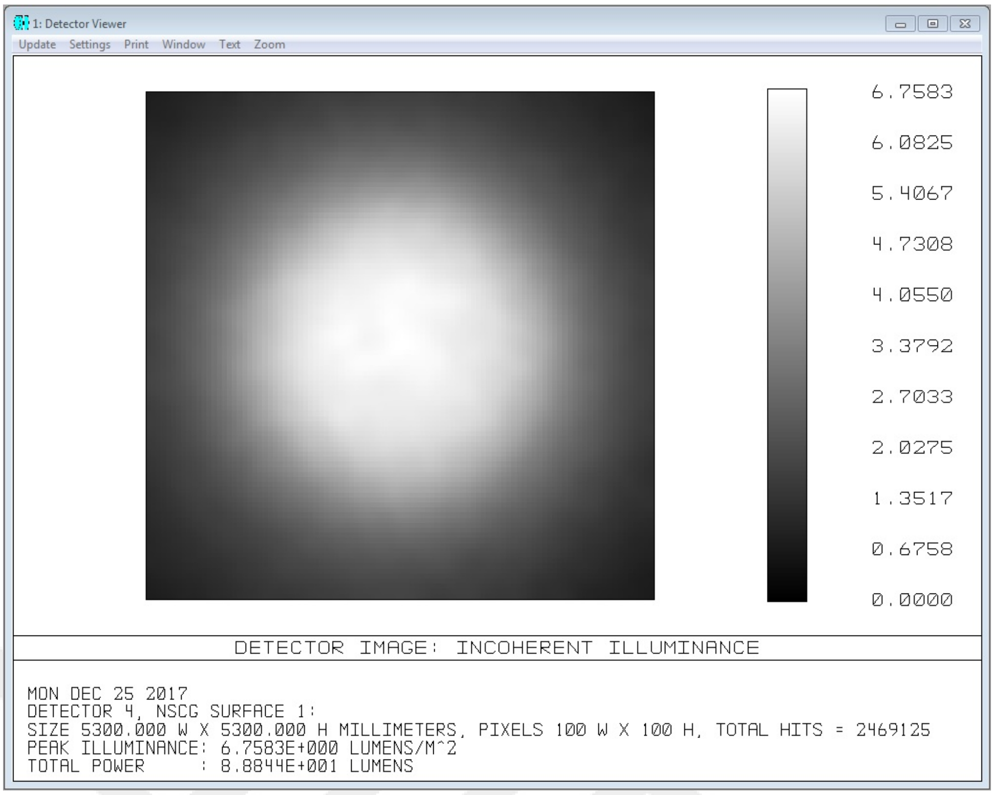

Figure C.12 Simulation result at 100 meter for PC lens.

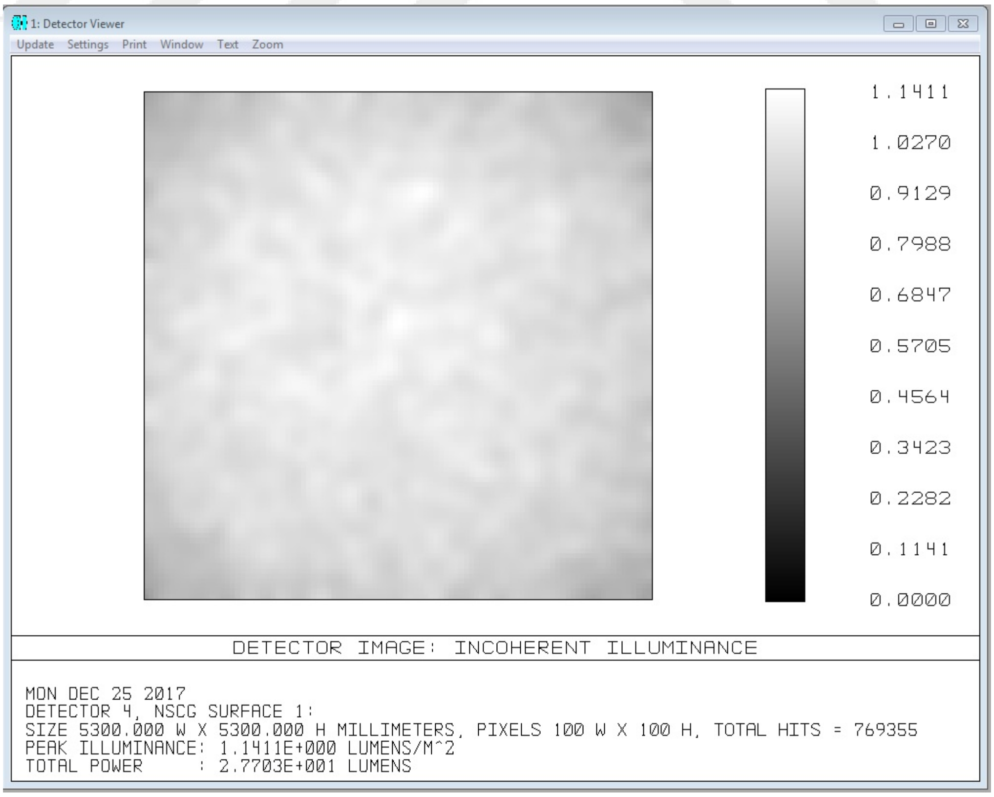

Figure C.13 Simulation result at 250 meter for PC lens.

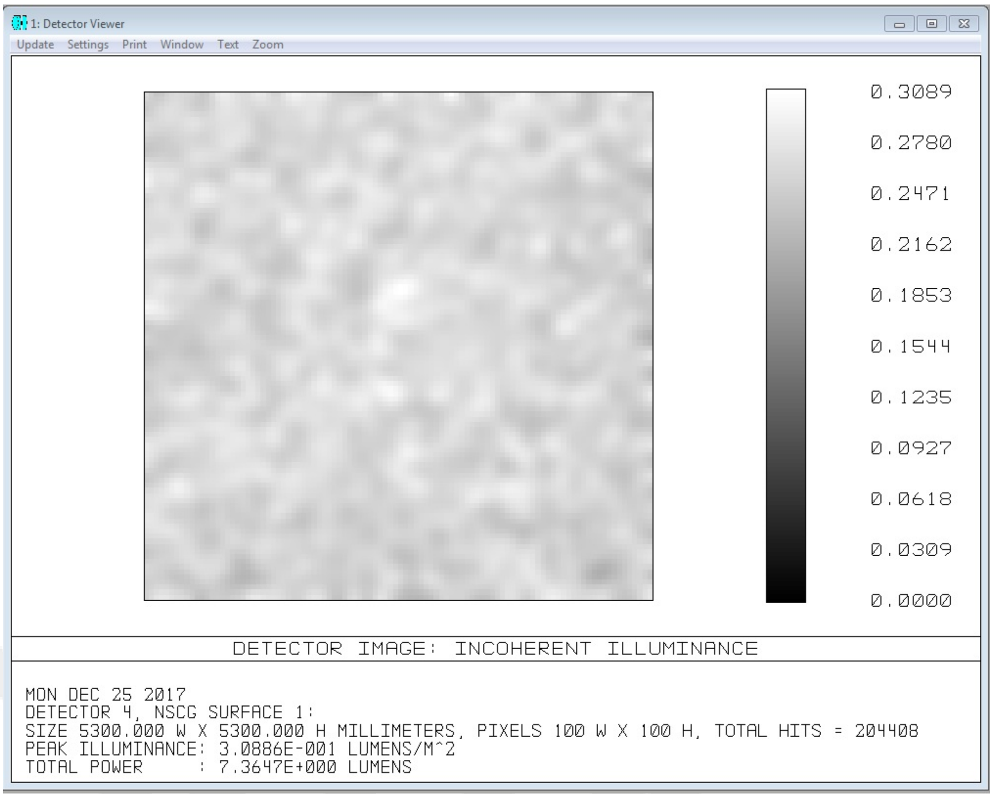

Figure C.14 Simulation result at 500 meter for PC lens.

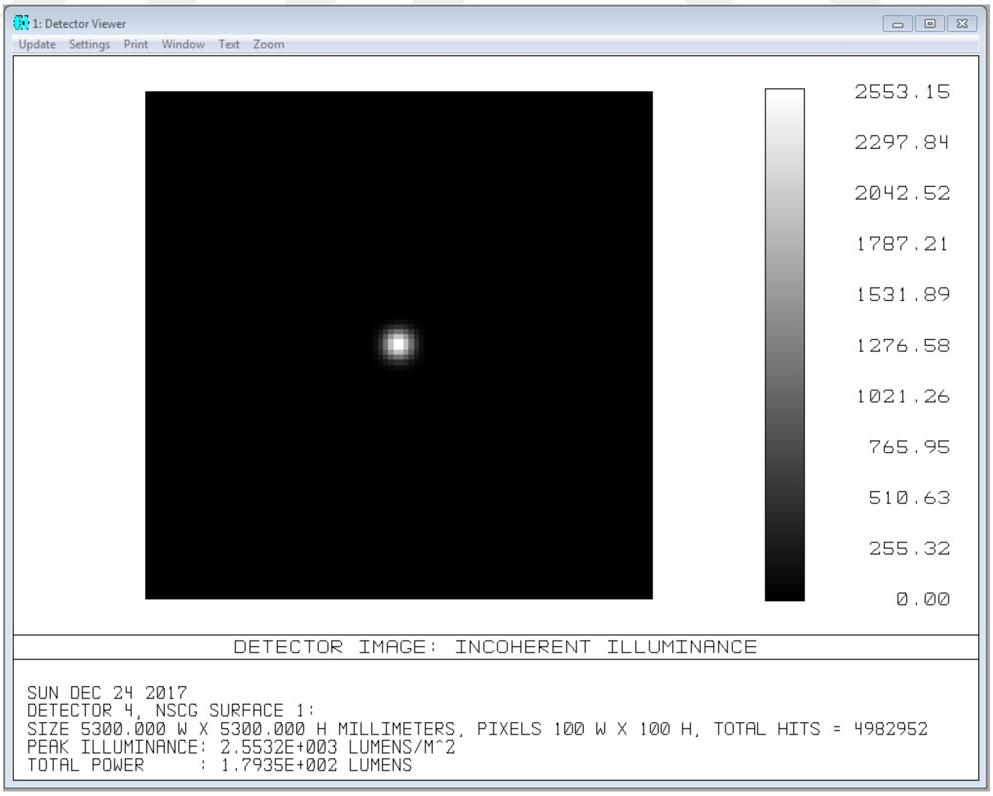

Figure C.15 Simulation result at 1 meter for PS lens.

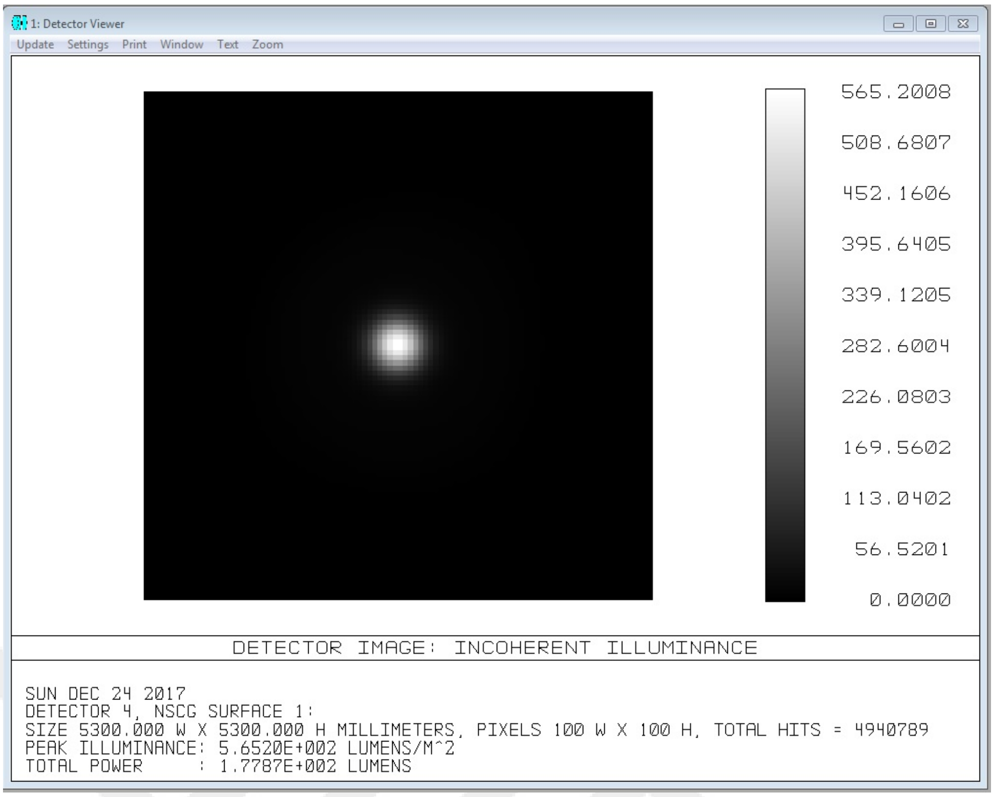

Figure C.16 Simulation result at 10 meter for PS lens.

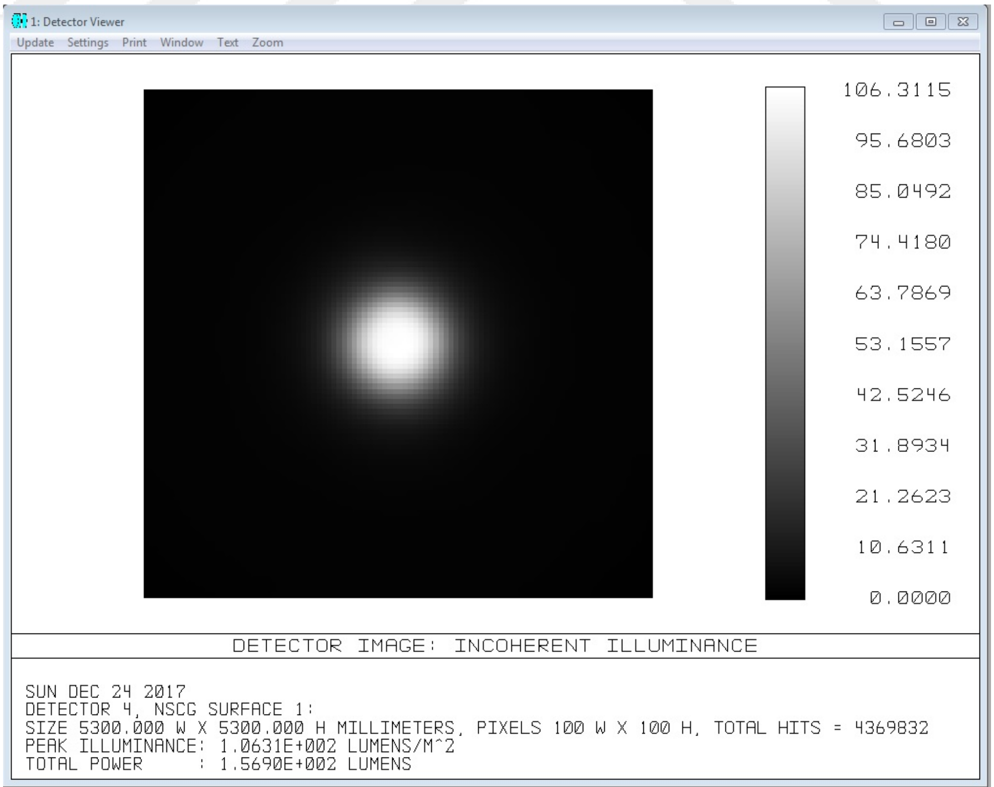

Figure C.17 Simulation result at 25 meter for PS lens.

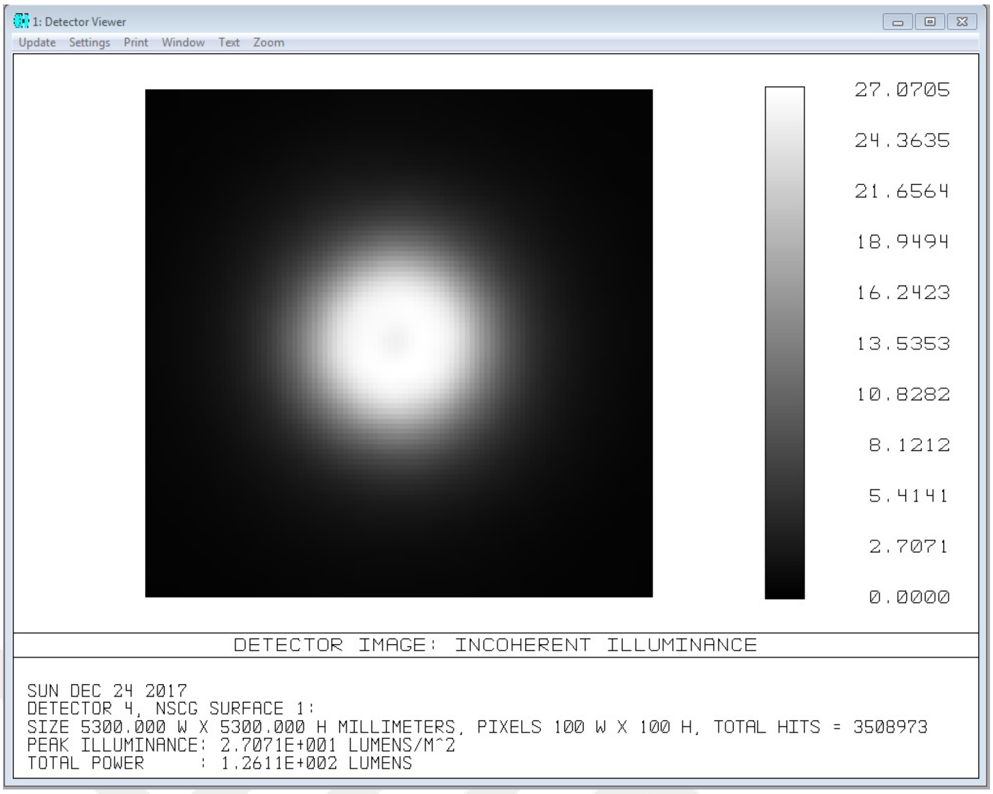

Figure C.18 Simulation result at 50 meter for PS lens.

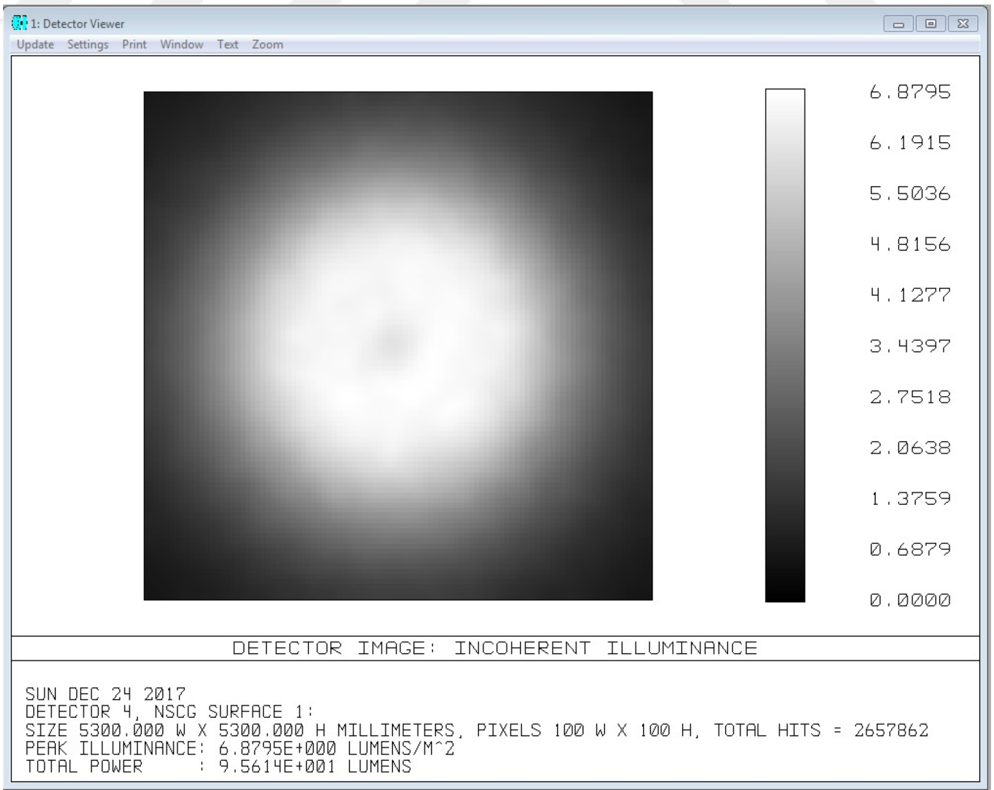

Figure C.19 Simulation result at 100 meter for PS lens.

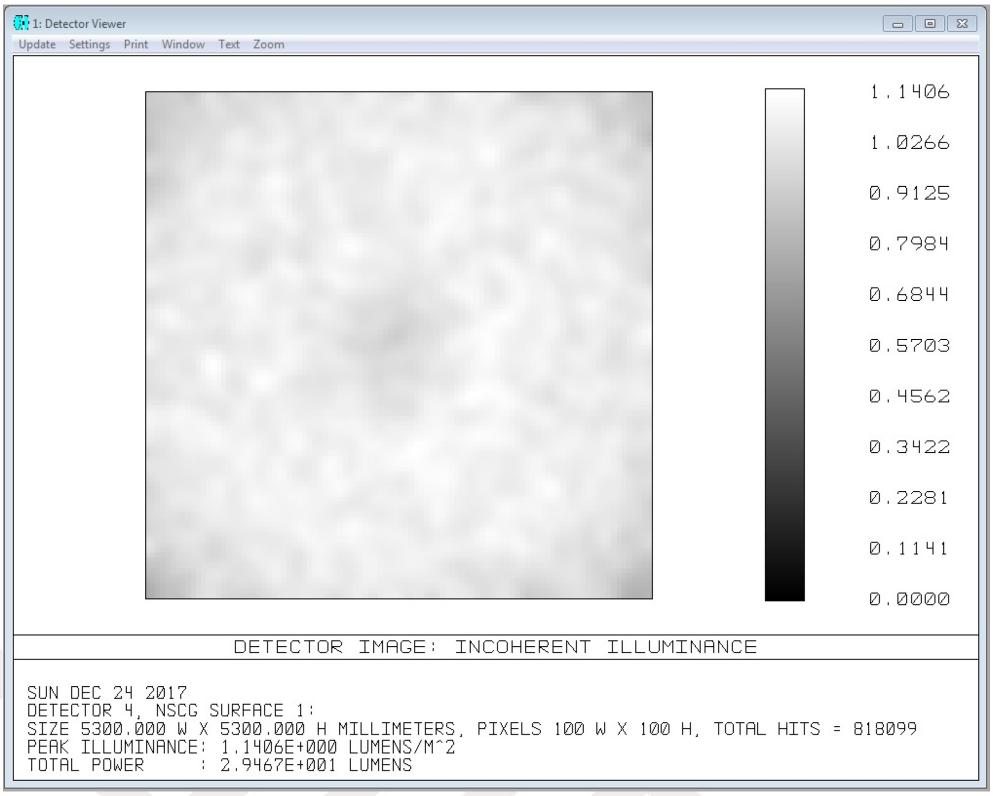

Figure C.20 Simulation result at 250 meter for PS lens.

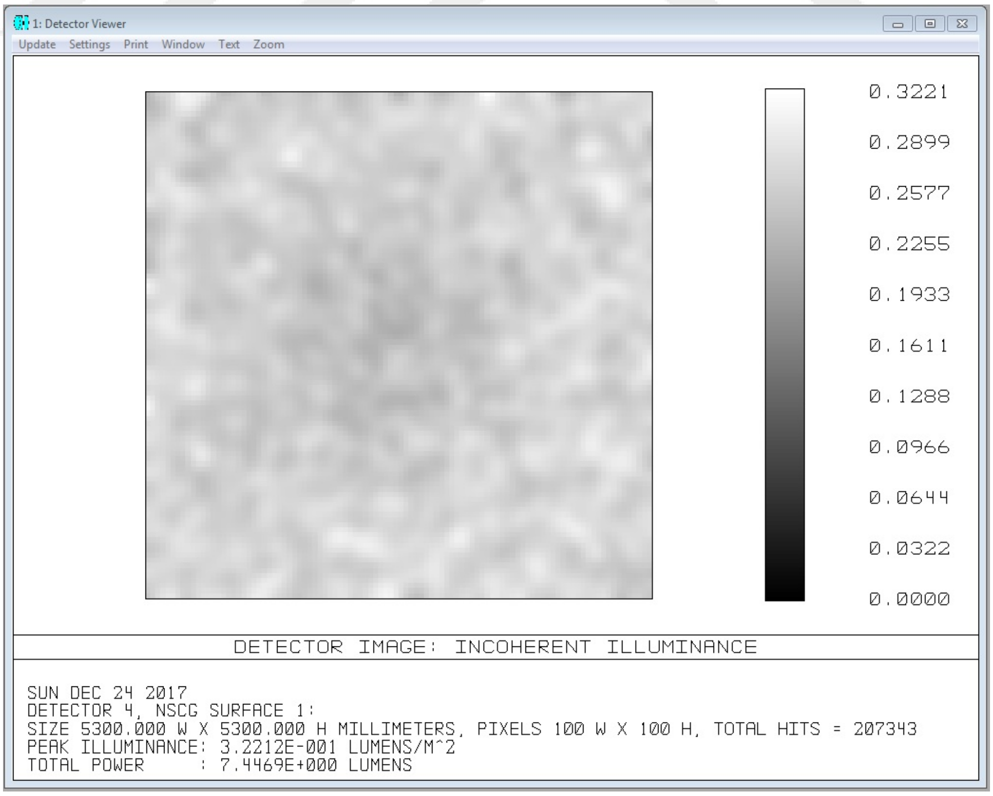

Figure C.21 Simulation result at 500 meter for PS lens.

APPENDIX D

SIMULATION RESULTS FOR DIFFERENT MATERIALS USING IR LED

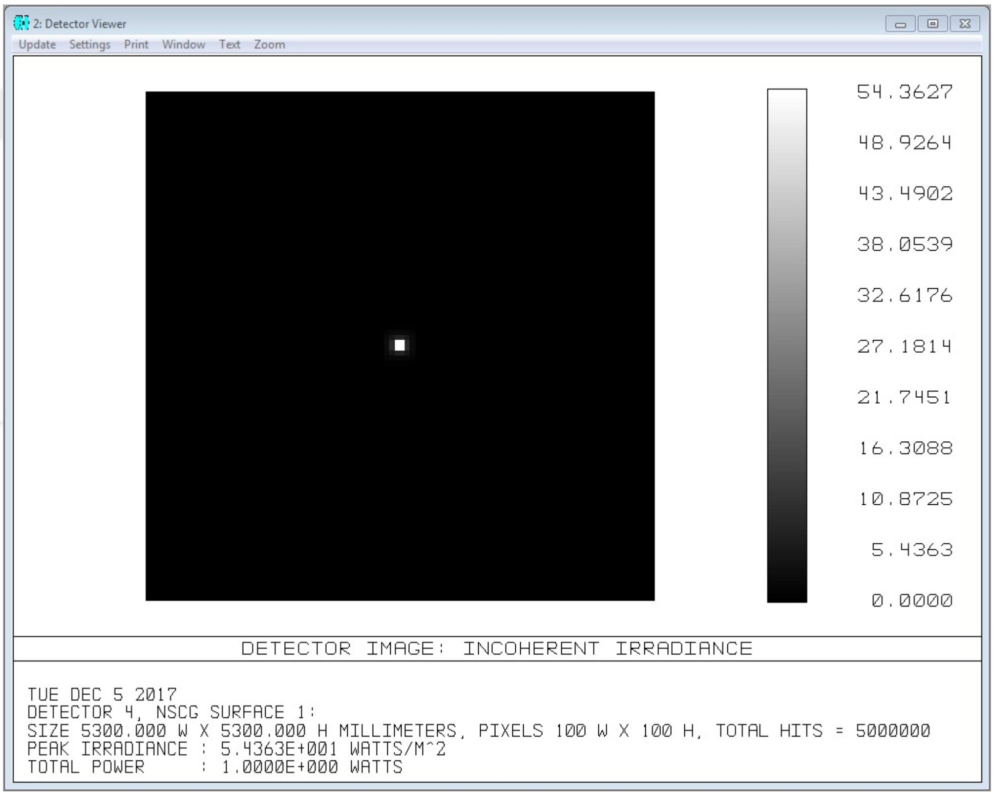

Figure D.1 Simulation result at 1 meter for PMMA lens.

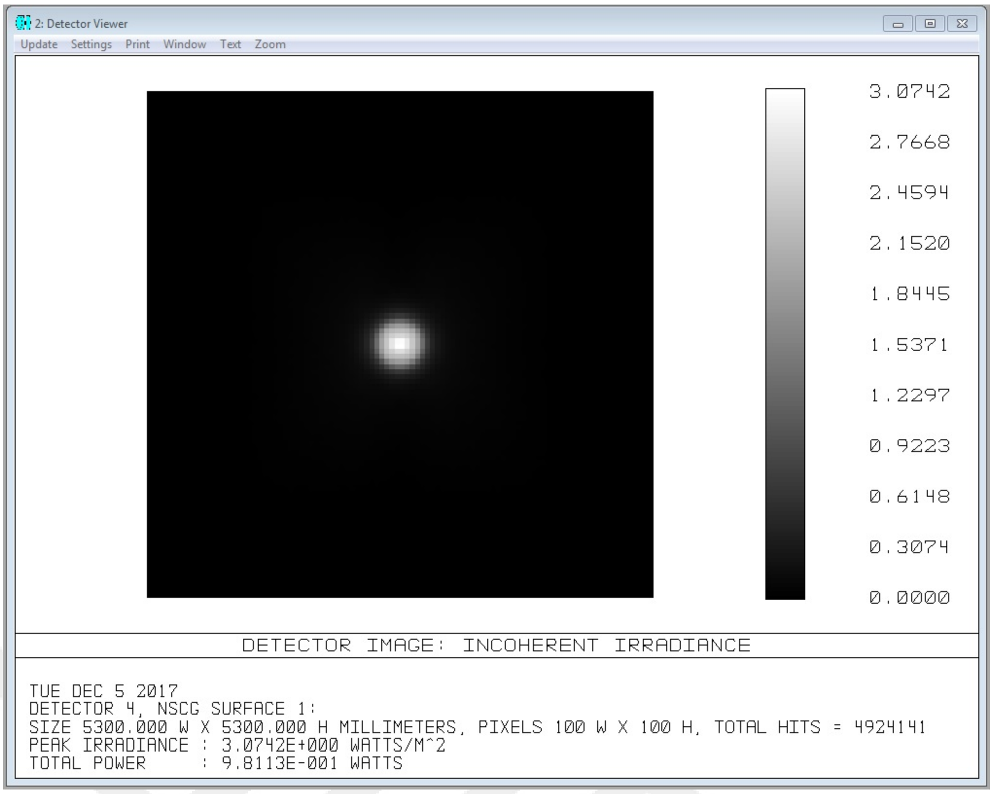

Figure D.2 Simulation result at 10 meter for PMMA lens.

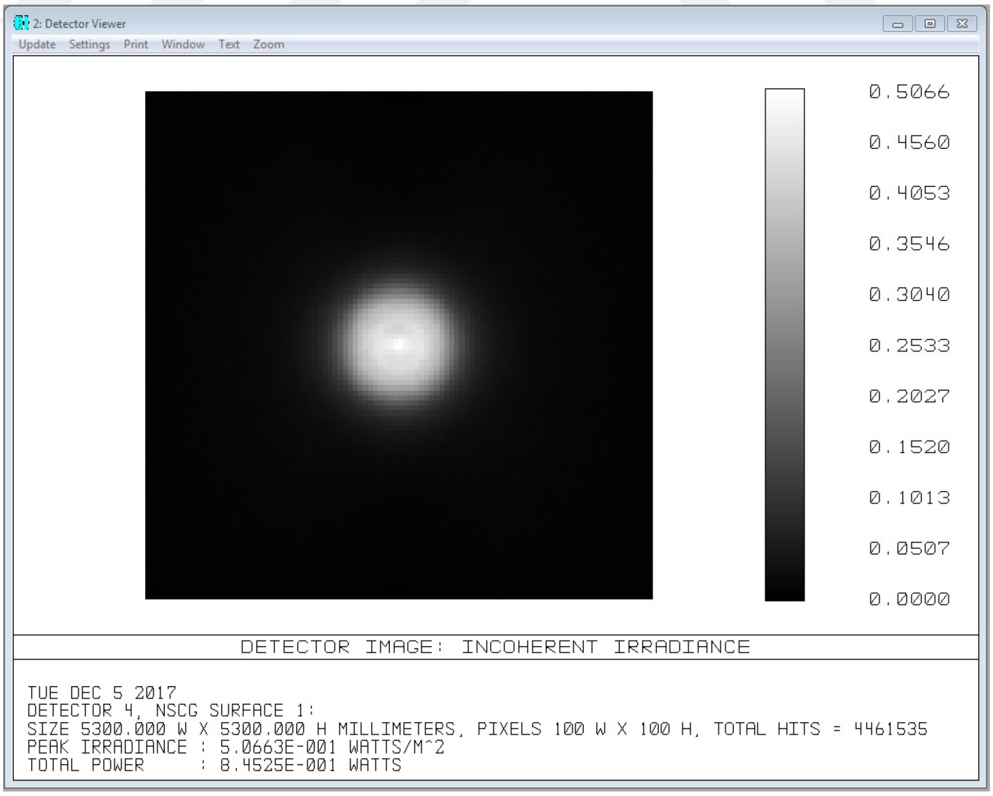

Figure D.3 Simulation result at 25 meter for PMMA lens.

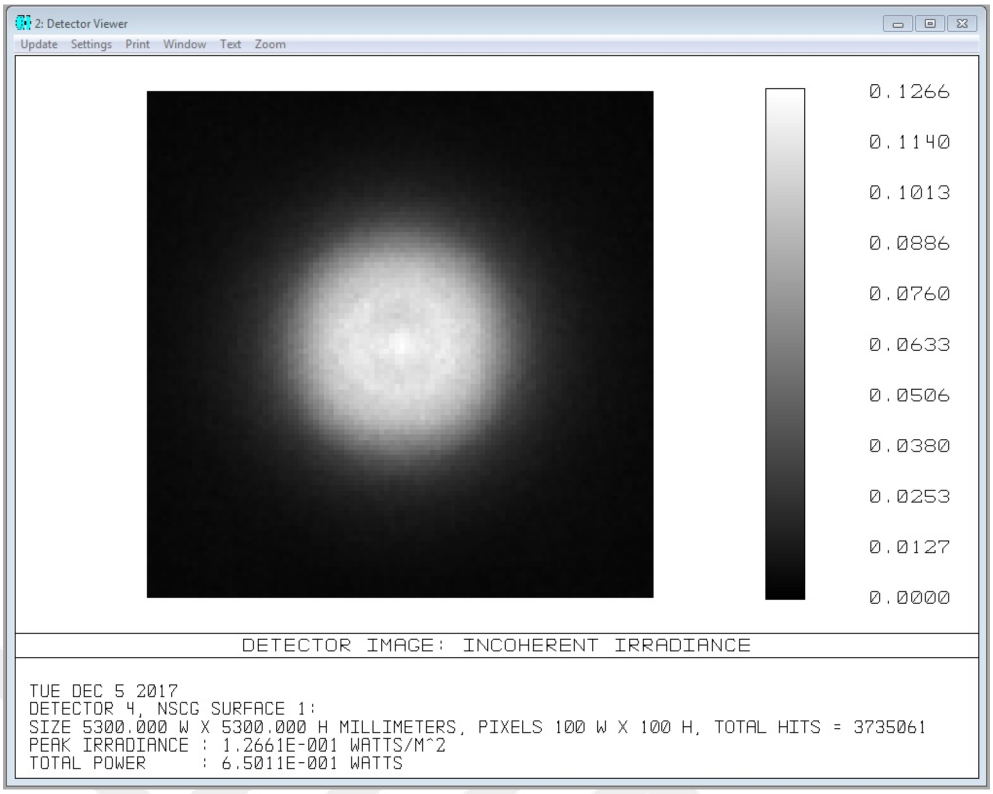

Figure D.4 Simulation result at 50 meter for PMMA lens.

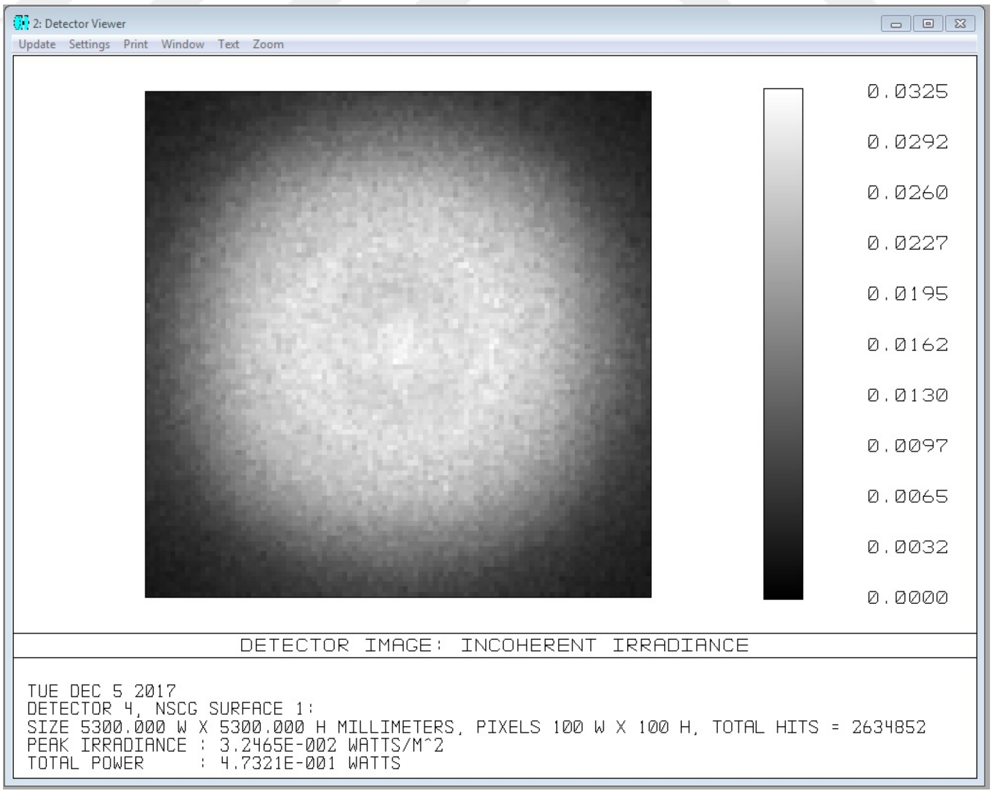

Figure D.5 Simulation result at 100 meter for PMMA lens.

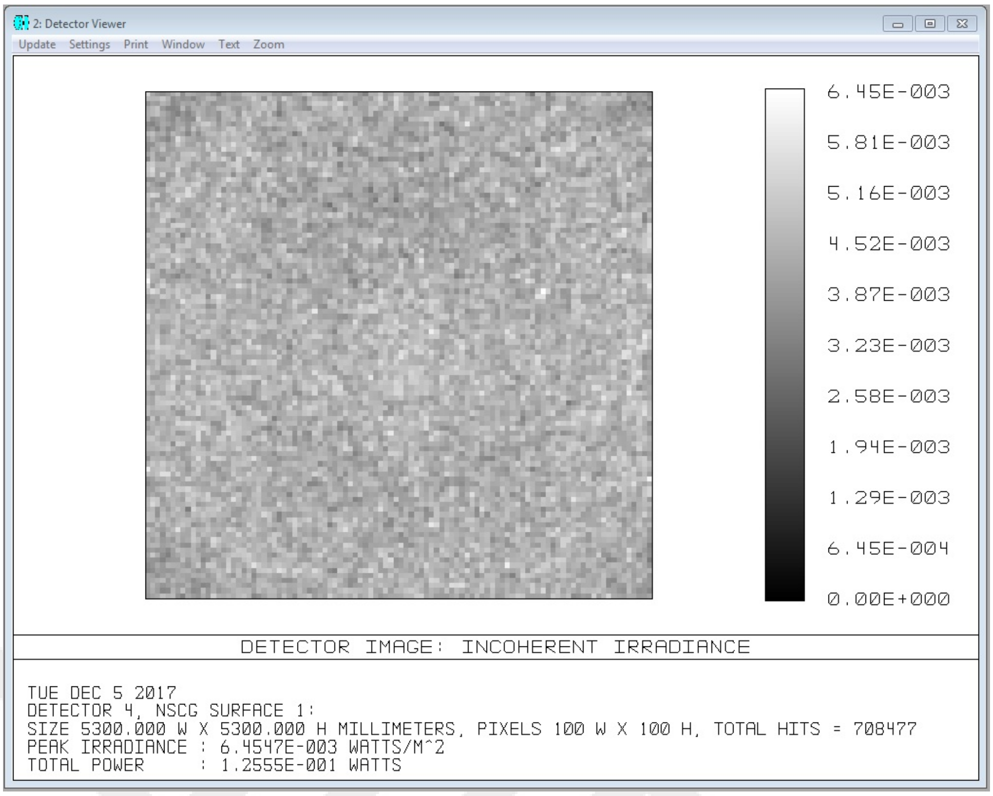

Figure D.6 Simulation result at 250 meter for PMMA lens.

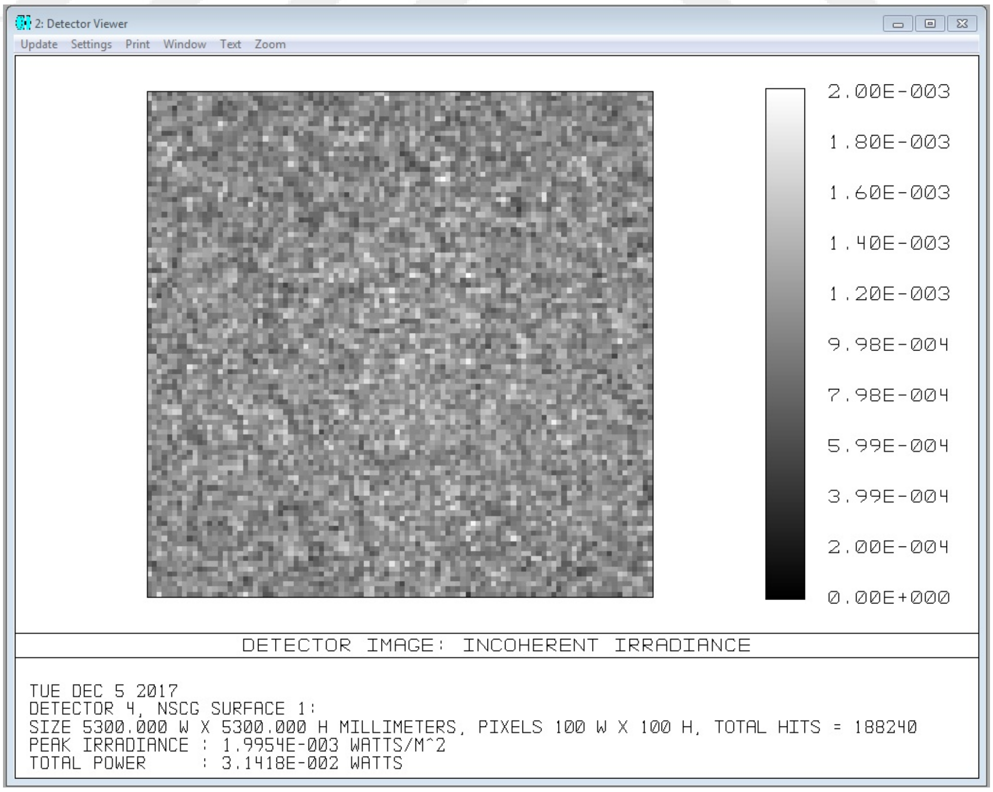

Figure D.7 Simulation result at 500 meter for PMMA lens.

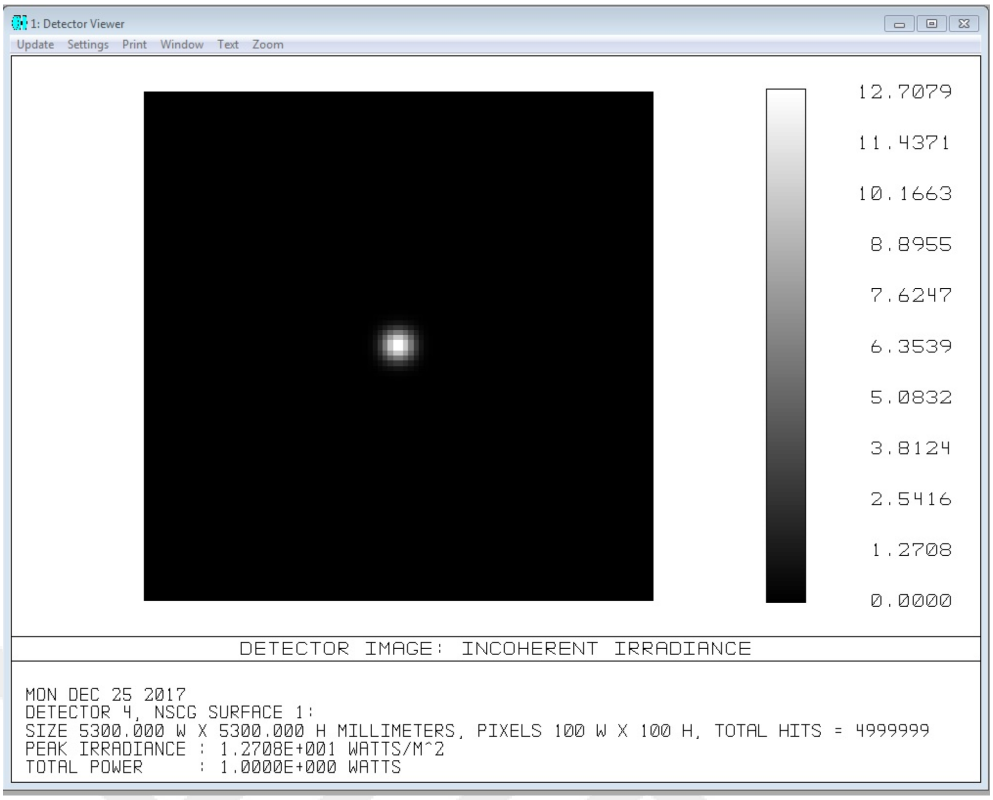

Figure D.8 Simulation result at 1 meter for PC lens.

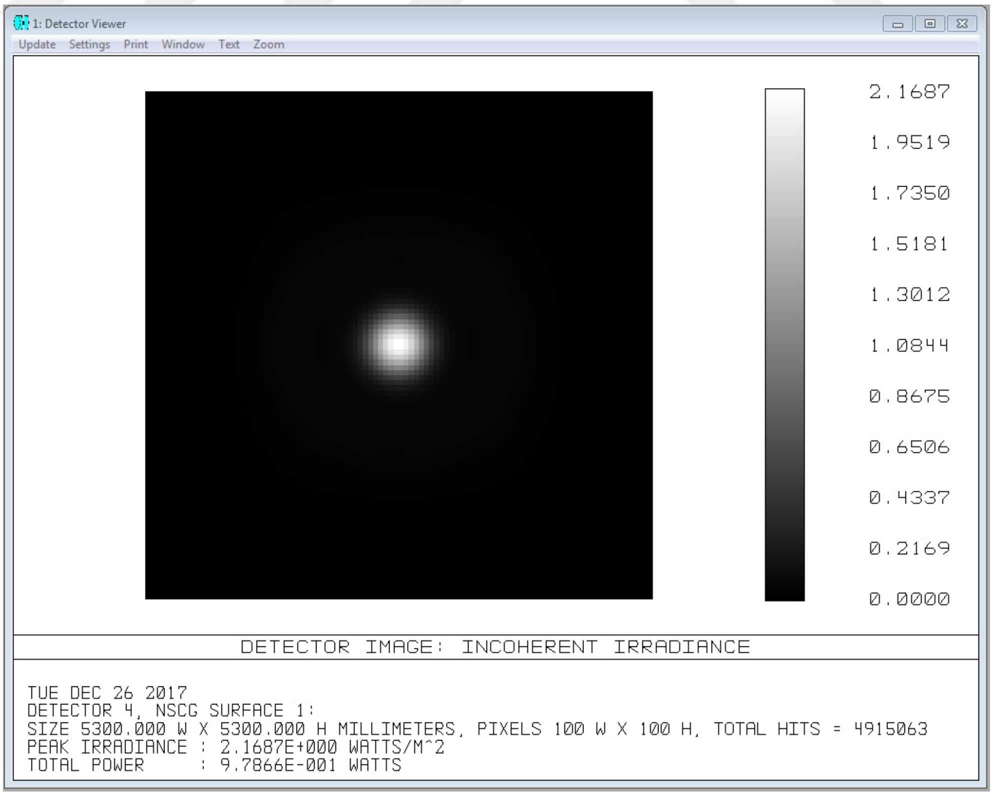

Figure D.9 Simulation result at 10 meter for PC lens.

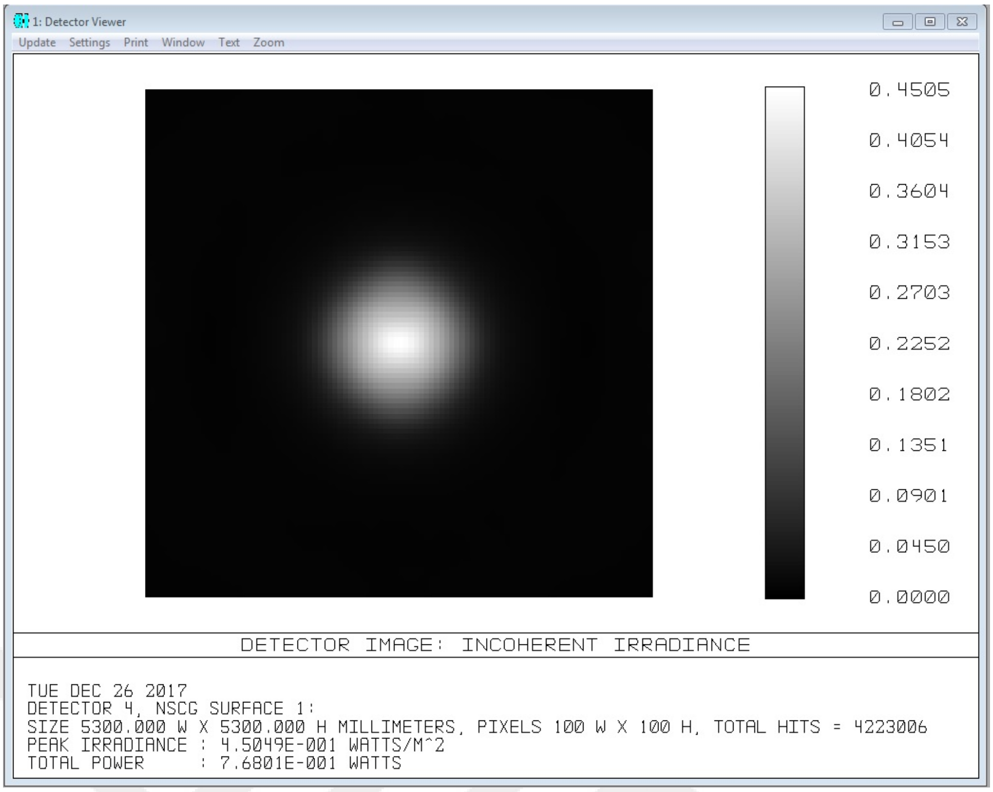

Figure D.10 Simulation result at 25 meter for PC lens.

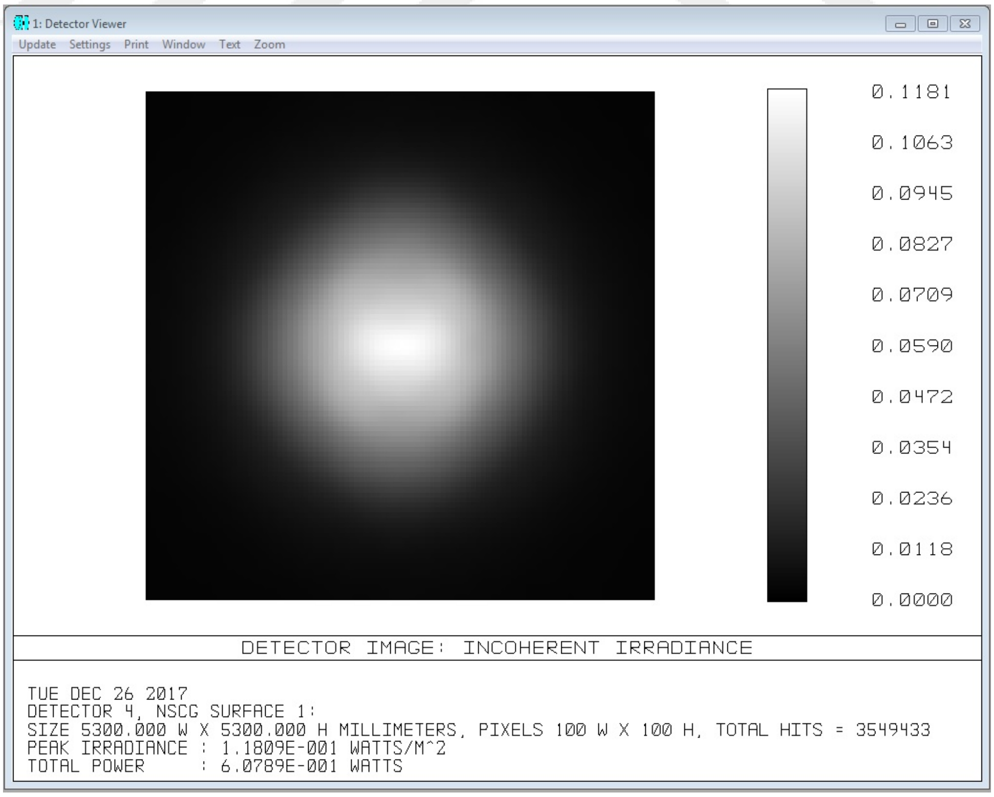

Figure D.11 Simulation result at 50 meter for PC lens.

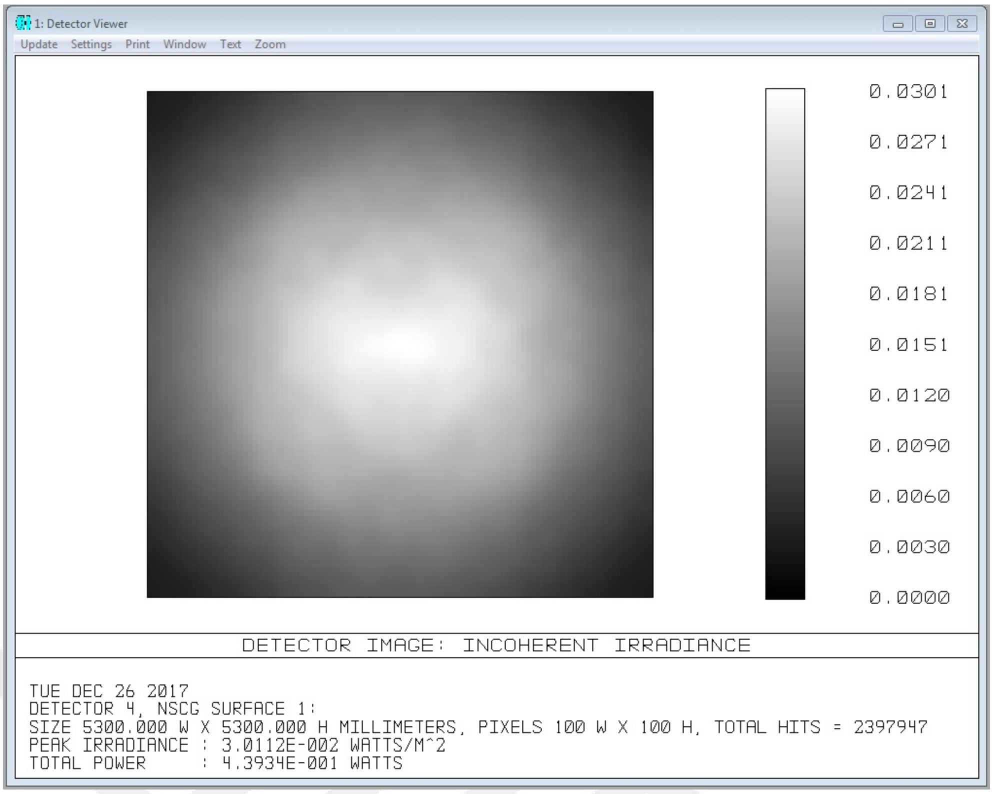

Figure D.12 Simulation result at 100 meter for PC lens.

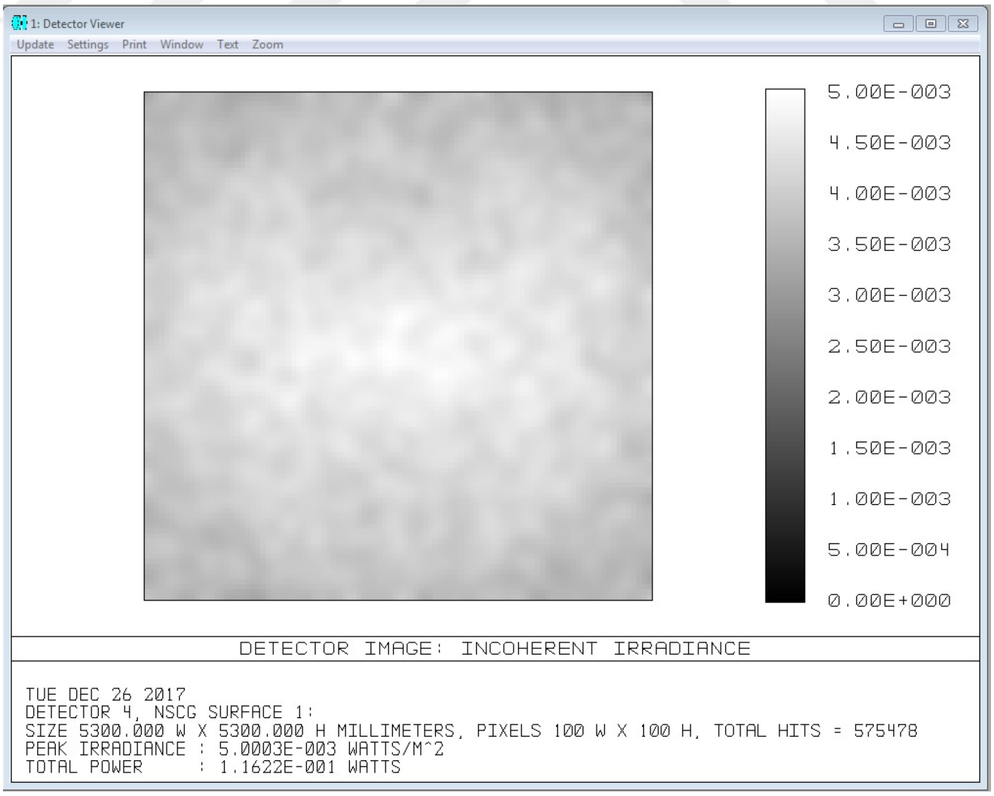

Figure D.13 Simulation result at 250 meter for PC lens.

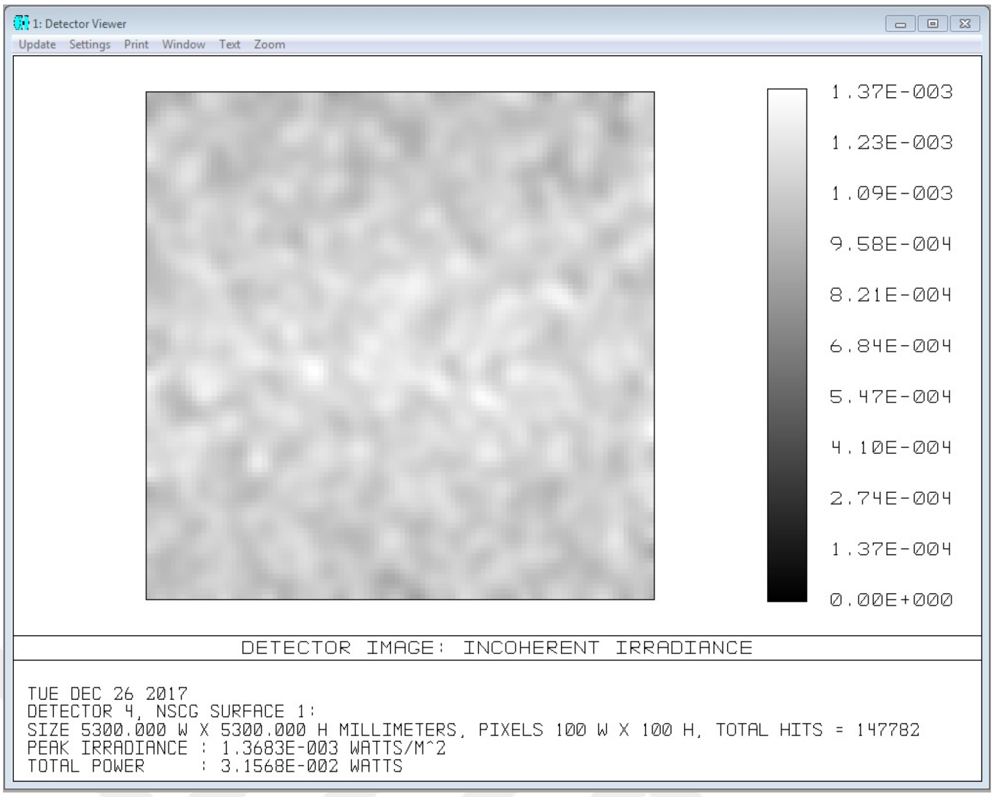

Figure D.14 Simulation result at 500 meter for PC lens.

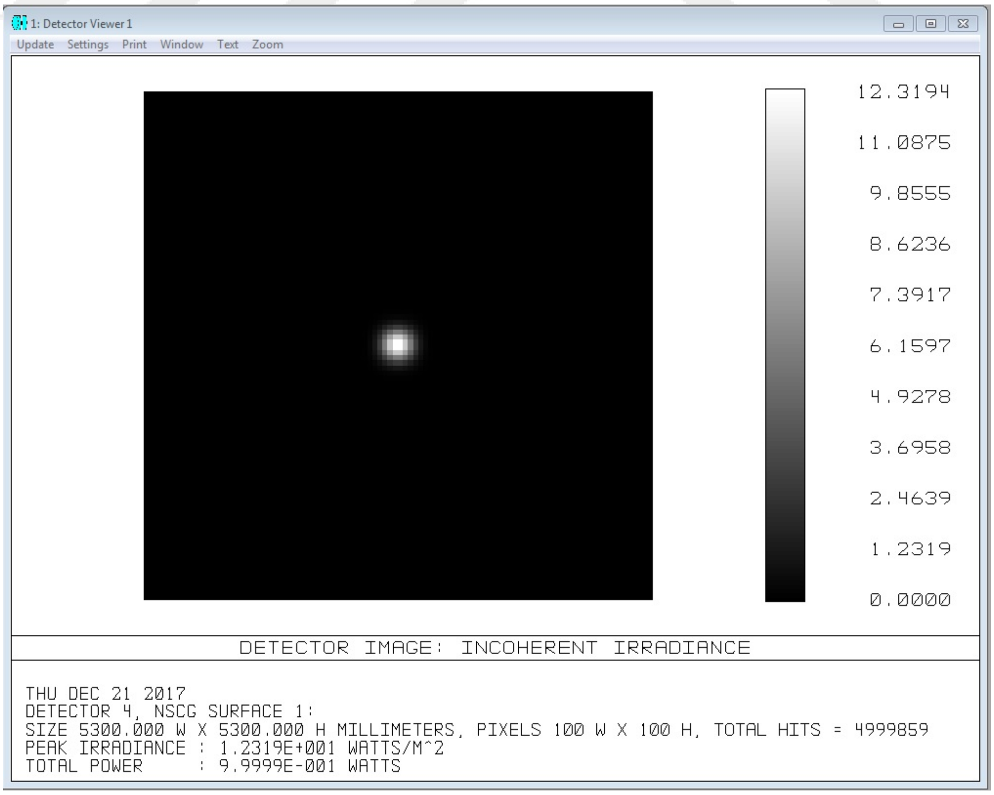

Figure D.15 Simulation result at 1 meter for PS lens.

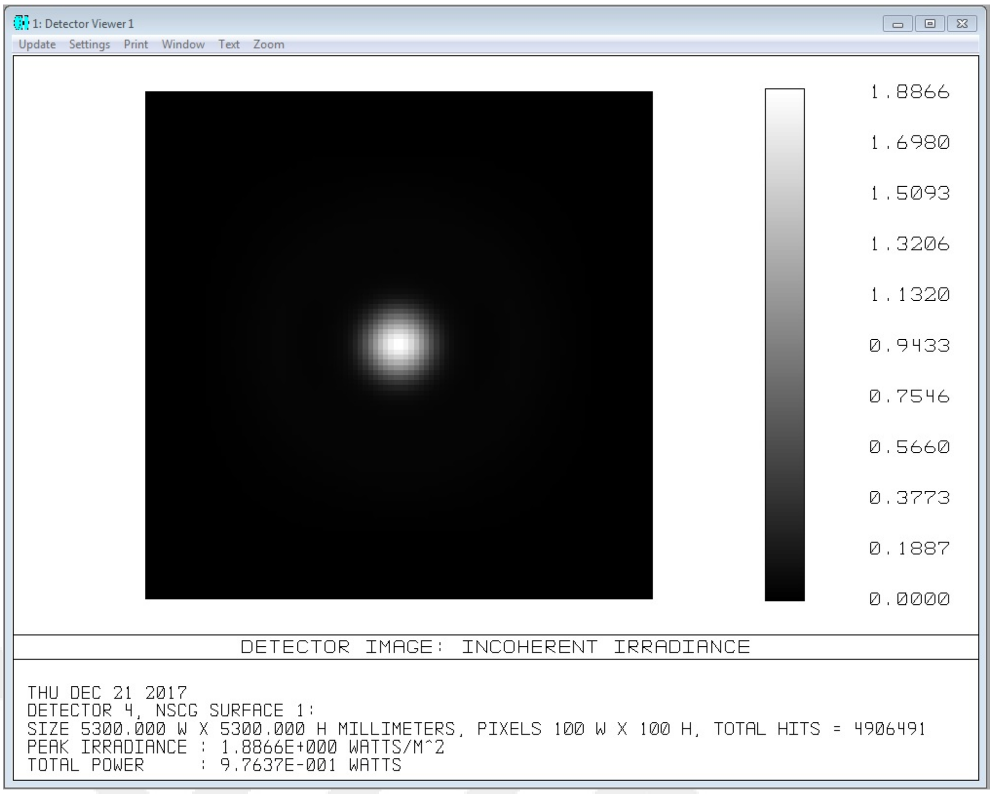

Figure D.16 Simulation result at 10 meter for PS lens.

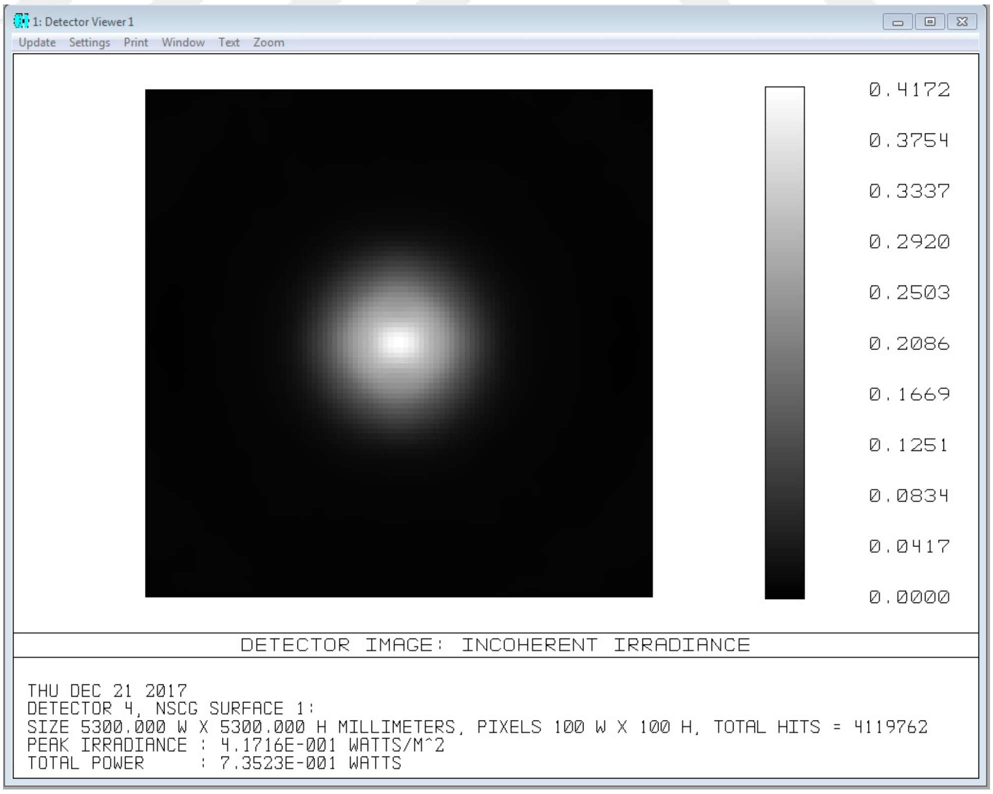

Figure D.17 Simulation result at 25 meter for PS lens.

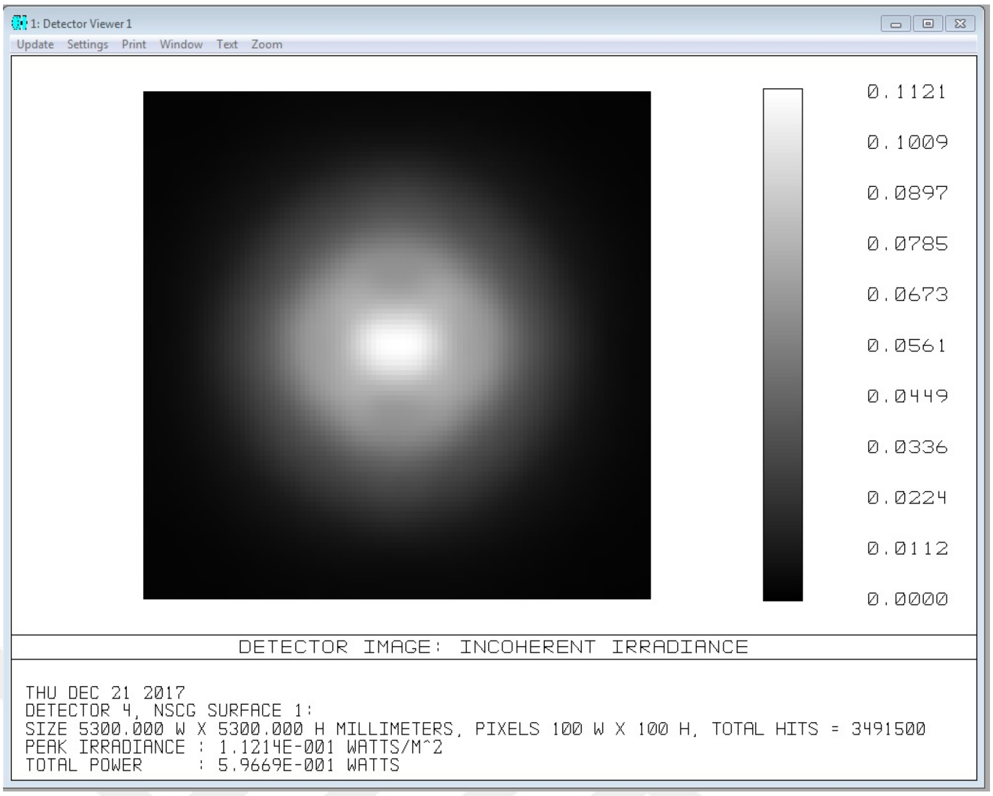

Figure D.18 Simulation result at 50 meter for PS lens.

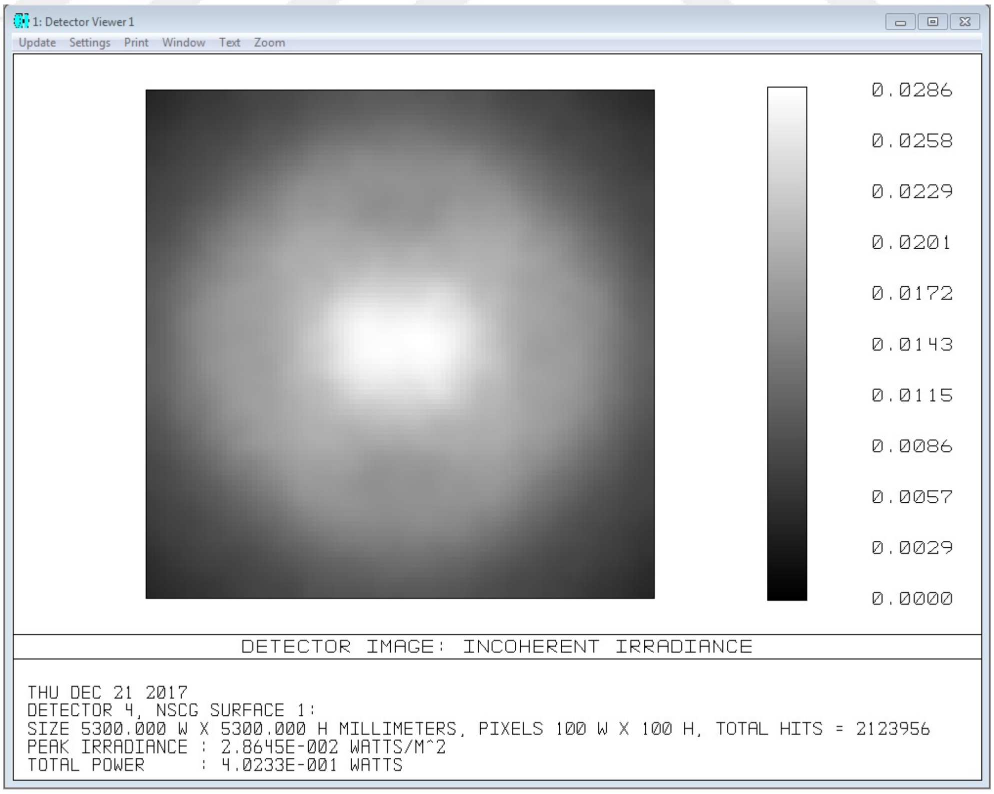

Figure D.19 Simulation result at 100 meter for PS lens.

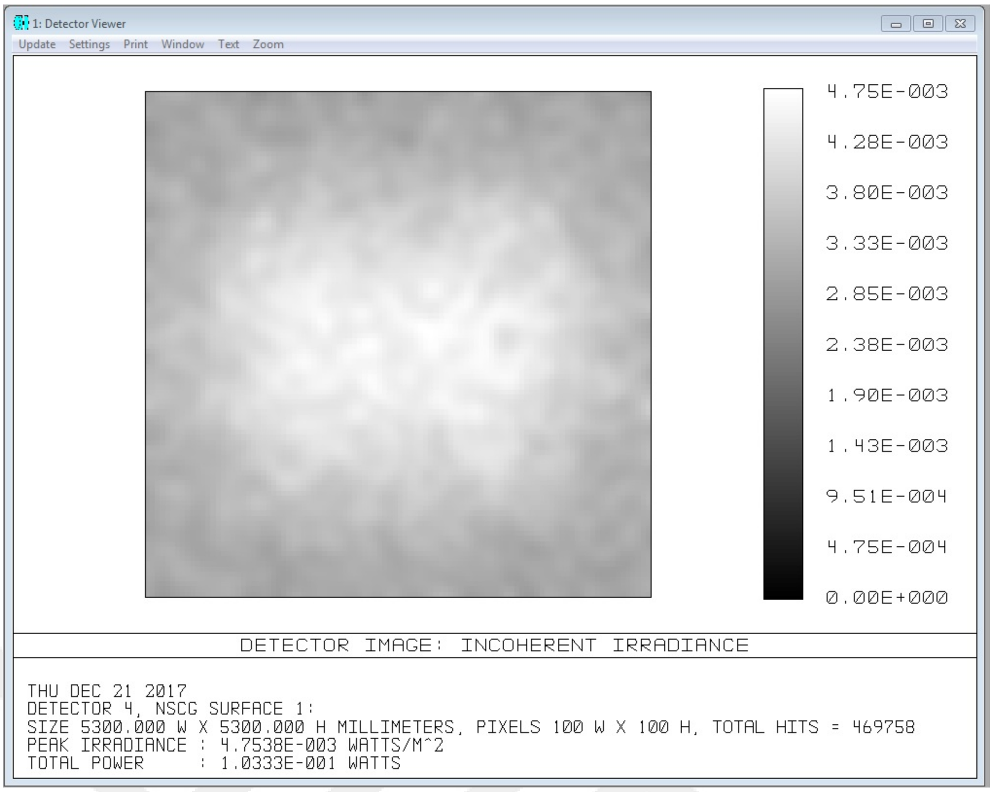

Figure D.20 Simulation result at 250 meter for PS lens.

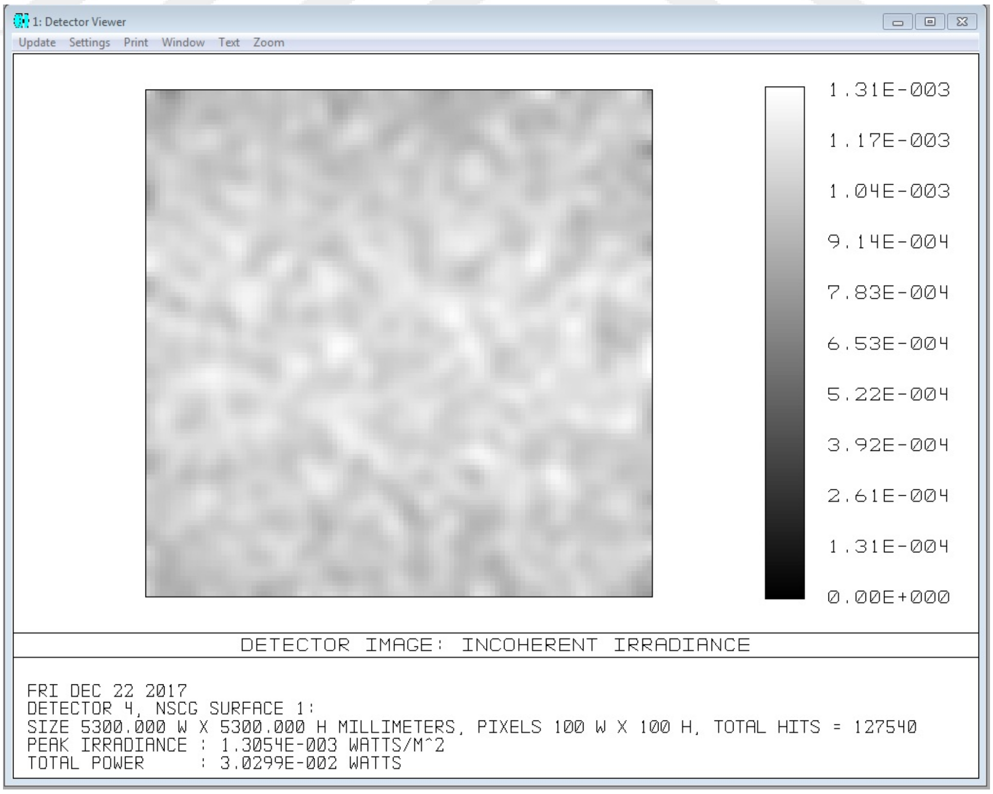

Figure D.21 Simulation result at 500 meter for PS lens.

APPENDIX E

MATLAB M-FILE FOR LENS DESIGN

```
%%%%%%%%%%%%%%%%%%%%%%%%%%%%%%%%%%%%%%%%%%%%%%%%%%%%%%%%%%%%%%%%%%%%%%%%%%%
% optikTasarim.m
% All units are in mm
% Version 1.0
% 27 Feb 2017
%%%%%%%%%%%%%%%%%%%%%%%%%%%%%%%%%%%%%%%%%%%%%%%%%%%%%%%%%%%%%%%%%%%%%%%%%%%
function optikTasarim
 clear; clc; tic;
 n = 1.4840; % index of refraction of PMMA at 850 nm
 N = 18;     % Number of rays
 tc = asind(1/n); % critical angle
 p = 4; % distance to closest point on the hyperbola
 R = 8; % radius of curvature of the circle
 xint = 0;
 yint = 0;
 xint = NRroot1(p,n,R);
 yint = f(xint, p, n);
 aint = atand(yint/xint);

 % draw parabola
 X=R:0.1:25;
 Y=(X.^2-R^2)/(2*R);
 plot(X,Y,'-k')
 hold on

 for i=1:N
  angle = i*90/N;
  x0 = 0;
  y0 = 0;
  alpha1 = angle*pi/180;
  m1 = tan(alpha1);
  x1 = R*(m1+sqrt(1+m1^2));
  y1 = m1*x1;

  if angle <= aint
   y2 = 500000; % constant!
   theta = atan(x1/R);
   alpha2 = 2*theta-alpha1;
   m2 = tan(alpha2);
   x2 = (y2-y1)/m2 + x1;
   xx = x1;
   yy = y1;
  else
```

```
    x1 = NRroot(m1, p, n);
    y1 = f(x1, p, n);
    theta = atan(turev(x1,p,n));
    beta = asin(sin(pi/2-alpha1+theta)/n);
    alpha2 = theta+pi/2-beta;
    m2 = tan(alpha2);
    x2 = (y2-y1)/m2 + x1;
  end

  % draw rays
  X=[x0 x1]; Y=[y0 y1]; line(X,Y,'LineWidth',0.5);
  X=[x1 x2]; Y=[y1 y2]; line(X,Y,'Color','r', 'LineWidth',0.5);
 end

 axis([0 100 0 100]);
 grid on;

 % draw top line
 line([0 xx], [yy yy],'Color','k');

 % draw arc
 x=R:-0.0001:xint;
 y=sqrt(R.^2-x.^2);
 plot(x,y,'-k')

 % draw aspherical surface
 x = 0:0.0001:xint;
 y = f(x,p,n);
 plot(x,y,'-k');

 % spline points
 x = 0:0.1:xint;
 y = f(x,p,n);
 s = [x' y']
 hold off

 dt = toc;
 fprintf('\n\n');
 fprintf('*** DESIGN REPORT (%s) ***\n',date);
 fprintf('Index of refraction of PMMA,      n = %f\n',n);
 fprintf('Critical angle for PMMA and air, tc = %f degrees\n',tc);
 fprintf('Parabola intersection point,      R = %f\n',R);
 fprintf('Equation of parabolic surface,    y = %f*x^2 - %f\n',0.5/R, R/2);
 fprintf('Calculation time,                dt = %f seconds\n',dt);
end % end of OptikTasarim

%%%%%%%%%%%%%%%%%%%%%%%%%%%%%%%%%%%%%%%%%%%%%%%%%%%%%%%%%%%%%%%%%%%%%%%%%%%
% hyperbola
function y = f(x, p, n)
 y = (p*(n-1)*n + sqrt(p^2*n^2*(n-1)^2-(n^2-1)*(p^2*(n-1)^2-x.*x) )) / (n^2-1);
end

% circle
function y1 = f1(x, p, n, R)
 y1 = f(x,p,n)-sqrt(R.^2-x.^2);
end

% numnerical derivative
function y = turev(x, p, n)
```

```
 h = 0.001;
 y = (f(x+h,p,n) - f(x-h,p,n))/(2*h);
end

% retuns the root
% m is the slope
function x = NRroot(m, p, n)
 x = 1;
 tol = 1.0e-4;
 while 1
  err = (f(x, p, n) - m*x) / (turev(x, p, n) - m);
  x = x - err;
 if abs(err) < tol
   break;
 end
 end
end

function y1 = turev1(x, p, n, R)
  h = 0.001;
  y1 = (f1(x+h,p,n,R) - f1(x-h,p,n,R))/(2*h);
end

% retuns the root
% m is the slope
function x = NRroot1(p, n, R)
 x = 2;
 tol = 1.0e-4;
 while 1
  err = f1(x, p, n, R) / turev1(x, p, n, R);
  x = x - err;
  if abs(err) < tol
   break;
  end
 end
end
```